CHARACTERIZATION OF CKIIA-I1
-A PUTATIVE ORTHOLOG OF INTELLECTUAL DISABILITY CANDIDATE GENE ZBTB11

by

Barış Can Mandacı

B.S., Biology, Middle East Technical University, 2018

Submitted to the Institute for Graduate Studies in

Science and Engineering in partial fulfillment of

the requirements for the degree of

Master of Science

Graduate Program in Molecular Biology and Genetics

Boğaziçi University

2022

ACKNOWLEDGEMENTS

First and foremost, I would like to offer my deepest esteem to my advisor Prof. Dr. Arzu Çelik Fuss for becoming a role model on scientific thinking and providing me the opportunities to expand my horizons by supporting me to study plentiful topics during my Master's study. I would like to acknowledge her for her supervision and guidance during my study. I'm thankful to Prof. Batu Erman and Prof. Münire Özlem Çevik for assigning their valuable time to evaluate my thesis and their critics during the study. I would like to acknowledge Prof. Ralf Stanewsky for his collaboration in the analysis of expression in clock cells and for his valuable suggestion.

I want to send my thanks to Dr. Anastasia Fokina and Dr. Farzaneh Larti for their theoretical and experimental critics that contributed to the progress of this research. Also, I would like to especially thank Dr. Fokina for her wonderful assistance and patience during revision of this thesis. It would be hard to keep motivated without Ayşe Kahraman's friendship. So, she deserves special thanks for being my guardian angel both in the lab and on paper works. Also, I want to acknowledge Gencay Kaan Polat and Yasemin Akın for being great working partners rather than interns, and their theoretical and experimental contributions. I would like to thank Eren Can Ekşi for his contribution during organization of this thesis. I am grateful to my interns Alper and Ayça for their work in this study. I want to thank our former undergrad students Çiğdem and Serhat for their friendship and contributions to this study. I also want to send my thanks to recent and current Celik's lab members who make me felt lucky to study in a peaceful work environment.

I am more than glad to my sincere friend Aysu for her unconditional love and support. I also want to thank my friends Davod, Efe, İlke, Elif D., Elif Ç., Emre, Şiran, Zeynep D., Mehmet Can, Yiğit, Ayşe C., Harun, and Ulduz who devoted their time to discuss my project. In addition, I want to thank all the people in Boğaziçi University MBG Department with whom I hung out and chill in between my experiments.

Finally, I want to thank my dear family who always supports me both psychologically and financially during my whole life.

This study was supported by the funds of TUBITAK project (119Z309).

ABSTRACT

CHARACTERIZATION OF CKIIA-I1 -A PUTATIVE ORTHOLOG OF INTELLECTUAL DISABILITY CANDIDATE GENE ZBTB11

Intellectual Disability (ID) is a heterogenic neurodevelopmental disorder seen in different spectrums in affected individuals. Resulting problems in the diagnosis of ID and limitations in its treatment constitutes a great emotional and financial burden to society. Therefore, identification of ID-causative genes and their functional characterization are important for the improvement of the current conditions. Two pathogenic variants of one of the ID-candidate genes ZBTB11 was identified and its early characterization was performed. In addition, knockdown of CkIIα-i1, a *Drosophila* ortholog of ZBTB11 showed deficiency in learning and memory center of *Drosophila*. The main aim of this study is the further investigate CkIIα-i1 and ZBTB11 in *Drosophila* in the pursuit of identifying their orthology. Since both CkIIα-i1 and ZBTB11 were understudied genes, transgenic and KO fly lines were generated and utilized in this study. In parallel, the expression of CkIIα-i1 was characterized in mushroom bodies (MB) and clock cells, which are learning- and circadian rhythm-related brain compartments, respectively. In addition, the role of CkIIα-i1 in MB development was analyzed by performing morphological analyses of the MB in CkIIα-i1 knockdown flies. For loss-of-function analysis, two RNA interference lines for the knockdown of CkIIα-i1 were utilized. Furthermore, two CkIIα-i1 KO lines were generated using CRISPR/Cas and used for morphological analysis. Both knockdown and KO of CkIIα-i1 resulted in shrinkage in the α lobe of the MB, with higher frequencies in KO lines. In contrast, the over-expression of CkIIα-i1 using the Gal4/UAS system did not result in any changes in MB morphology. Results of morphological analyses indicated that CkIIα-i1 could have a role in axonal guidance of α lobe axons. In order to investigate orthology between CkIIα-i1 and ZBTB11, wt and two identified variant ZBTB11 constructs were transgenically expressed in *Drosophila* and their expression was validated in the fly brain.

ÖZET

ZİHİNSEL ENGELLİLİK ADAY GENİ ZBTB11 ORTOLOĞU CKIIA-İ1'İN KARAKTERİZASYONU

Zihinsel Engellilik (ZE), farklı spektrumlarda görülen heterogenik nörogelişimsel bozukluktur. ZE'nin teşhisinde ortaya çıkan sorunlar ve tedavisindeki kısıtlamalar, toplum için büyük duygusal ve finansal yük oluşturmaktadır. Bu nedenle ZE'ye neden olan genlerin tanımlanması ve fonksiyonel karakterizasyonu, mevcut koşulların iyileştirilmesi için elzemdir. ZE adayı genlerinden biri olan ZBTB11'in iki patojenik varyantı tanımlanıp erken karakterizasyonu yapılmıştır. Ayrıca ZBTB11'in *Drosophila* ortoloğu olan CkIIα-i1'in susturulması sonucunda sineğin öğrenme ve hafıza merkezinde bozukluk olduğunu göstermiştir. Bu çalışmanın temel amacı, potansiyel ortolojilerini belirleme arayışı ile CkIIα-i1 ve ZBTB11'in sinek üzerinde daha fazla araştırılmasıdır. Hem CkIIα-i1 hem de ZBTB11 yeterince çalışılmamış genler olduğundan, bu çalışmada transgenik ve nakavt sinek hatları oluşturulmuş ve kullanılmıştır. Paralel olarak, CkIIα-i1'in ifadesi, sırasıyla öğrenme ve sirkadiyen ritimle ilgili beyin bölmeleri olan mantarsı gövde (mushroom body- MB) ve sirkadyen hücrelerinde karakterize edildi. Buna ek olarak, CkIIα-i1'in MB oluşumundaki işlevi, CkIIα-i1'ın susturulduğu sineklerde Morfolojik MB analizi ile karakterize edildi. CkIIα-i1'in fonksiyon kaybı için, RNA enterferansı kullanılarak iki CkIIα-i1 susturma hattı ve CRISPR/Cas kullanılarak iki CkIIα-i1 nakavt hattı oluşturuldu. CkIIα-i1'in hem susturulması hem de nakavtı, nakavt hatta daha yüksek frekansla görülen MB'nin α lobunda daralma ile sonuçlandı. Buna karşılık, Gal4/UAS sistemi ile CkIIα-i1'in aşırı ifadesi, MB morfolojisinde herhangi bir değişiklikle sonuçlanmadı. Fonksiyonel analizler CkIIα-i1'in MB'nin lob aksonlarının aksonal yönlendirmesinde rolü olabileceğine işaret etti. CkIIα-i1 ve ZBTB11 arasındaki ortolojiyi araştırmak için ZBTB11'in wt ve tanımlanmış iki varyant formu *Drosophila*'da transgenik olarak eksprese edildi ve ekspresyonları sinek beyni üzerinde doğrulandı.

TABLE OF CONTENTS

LIST OF FIGURES

LIST OF TABLES

LIST OF SYMBOLS

µg	Microgram
µl	Microliter
µm	Micrometer
bp	Base pair
g	Gram
kb	Kilobase
L	Liter
M	Molar
ml	Milliliter
mM	Millimolar
mm	Millimeter
n	Number of samples
ng	Nanogram
rpm	Revolutions per minute
^{o}C	Degree Celcius

LIST OF ACRONYMS/ABBREVIATIONS

CkIIα	Casein kinase II alpha subunit
CkIIα-i1	Casein kinase II alpha subunit interactor-1
CRISPR	Clustered regularly interspaced short palindromic repeats
DNA	Deoxyribonucleic acid
gDNA	Genomic DNA
GFP	Green fluorescent protein
gRNA	Guide RNA
HA	Human influenza hemagglutinin
HDR	Homology directed repair
NHEJ	Non-homologous end joining
nt	Nucleotide
PAM	Protospacer adjacent motif
PBS	Phosphate buffered saline
PBST	Phosphate buffered saline with Triton X-100
PCR	Polymerase chain reaction
PFA	Paraformaldehyde
pH	Power of hydrogen
RNA	Ribonucleic acid
RNAi	RNA interference
RT	Room temperature
TF	Transcription factor
UAS	Upstream activating sequence

1. INTRODUCTION

1.1. Intellectual Disability

Neurodevelopmental disorders, as the name implies, are primarily associated with disabilities observed in the development and functioning of the nervous system (Morris-Rosendahl and Crocq, 2020) and constitute a financial burden for low and middle-income countries (Bitta *et al.*, 2018). Symptoms emerge in childhood before the age of 18 years (Baio *et al.*, 2018). The major neurodevelopmental disorders are attention-deficit/hyperactivity disorder, cerebral palsy, distorted vision and hearing abilities, impaired language and speech, autism, and intellectual disability (ID) (Morris-Rosendahl and Crocq, 2020). Genetic and epigenetic factors are the initiative causes of neurodevelopmental disorders. However, the symptoms can be aggravated according to the environmental factors such as physical, chemical or psychological abuse, insufficient nourishment and socioeconomic factors exposed during prenatal stages and/or during adulthood (van Karnebeek and Stockler, 2012). Thus, the diagnosis of neurodevelopmental diseases can be tricky since some of these diseases like ID can emerge with a 70% frequency in individuals with autism (La Malfa *et al.*, 2004). In addition, different individuals with ID and autism are affected by the disorders with different levels. Thus, both ID and autism are accepted as spectrum disorders (APA, 2013). Although ID and autism have some shared molecular defects such as a pathogenic variant in FOXP2 (Hamdan *et al.*, 2010; Le Fevre *et al.*, 2013), thanks to comprehensive clinical and molecular research and advanced bioinformatic technology, today they can be distinguished by identification of potential causative genes via Next Generation Sequencing such as whole-exome sequencing (Sanders *et al.*, 2012; Aspromonte *et al.*, 2019; Chiurazzi *et al.*, 2020). While autism spectrum disorders mostly appear as oligogenic or polygenic cases in harmony with de novo and common inherited variants (Chaste *et al.*, 2017), ID often represents monogenic mutations, which could be sporadic de novo mutations or coalesced recessive mutations in consanguineous families (Arnett *et al.*, 2018). Although more than 1200 disease-associated ID genes were identified until now (Moser, 2004), characterization of their function is necessary for appropriate treatment.

According to the diagnostic and statistical manual of mental disorders published by the American Psychiatric Association, ID is characterized by deficits in both intellectual and adaptive functioning (APA, 2013). While intellectual malfunctioning in ID patients can be observed as a distortion in reasoning, planning, problem-solving and abstract thinking, their adaptive behaviors are presented insufficiency in self-management, practical knowledge acquisition and social skills such as communication and friendship abilities (APA, 2013). In addition to these criteria, accompanied by clinical judgment, individuals with an IQ score lower than 70 are regarded as individuals with an ID (APA, 2013). Depending on the severity of adaptive malfunctioning, ID is also classified as mild, moderate, severe, and profound ID (APA, 2013).

Current treatment by pharmaceuticals and professional therapy only alleviates the symptoms and covers only a small group of ID patients (van Karnebeek and Stockler, 2012). However, if the spatial and temporal function of impaired gene/protein was characterized, it could give rise to potential guided genetic or pharmaceutical therapies to restore the distorted function of the causative ID gene/protein. However, genetic heterogeneity of ID has been a noteworthy challenge for the comprehensive study of candidate genes. Therefore, *Drosophila melanogaster*, the fruit fly, is a well-established model organism for the functional characterization of a candidate ID-related gene in the nervous system from gene to behavior (Mariano *et al.*, 2020). Several studies showed that restoring the investigated ID-related phenotypes is possible by rescuing of impaired ID-causative proteins via genetic or pharmaceutical manipulations, even in adult animals (Guo *et al.*, 2000; McBride *et al.*, 2005; Guy *et al.*, 2007; Kramer *et al.*, 2011; Lee *et al.*, 2014).

1.2. Zbtb11

WES analysis performed in two Iranian consanguineous families having individuals with ID identified two highly pathogenic variants of Zinc Finger and BTB Domain Containing 11 (ZBTB11) (Fattahi *et al.*, 2018). As its name implies, a predicted transcription factor, ZBTB11 includes a bric-à-brac, tramtrack and broad complex transcription regulators (BTB) and 12 C2H2-type Zinc-Finger (ZNF) domains. Zbtb11 is located on the third chromosome and its pathogenic variants include two separate missense mutations in the coding sequence of Zbtb11 (NM_014415.3: c.2185C>T, and c.2640 T>G; Fattahi *et al.*, 2018). According to in silico analysis of ZBTB11 variants on the protein level these mutations were causing the substitution of one of the Histidines in the C2H2 ZNF domains 5 and 10 (NM_014415.3: p.H729Y, p.H880Q). These mutations affected the subcellular localization of ZBTB11 (Fattahi *et al.*, 2018). While wild-type (wt) ZBTB11 was localized to the nucleolus, which is engaged in ribosome biosynthesis within the nucleus, two mutant variants of ZBTB11 were dispersed in the nucleus (Fattahi *et al.*, 2018). In addition, to identify the ZBTB11 target genes and pathway, Chip-seq in three different cell types was performed and a GO enrichment analysis of Chip-seq revealed that ZBTB11 can have roles in protein translation, RNA synthesis, ribosomal assembly, RNA modification, mRNA biogenesis, RNA metabolism, protein translation and stress sensing (Wilson *et al.*, 2020). The localization of ZBTB11 in the nucleolus (Fattahi *et al.*, 2018) and the GO enrichment analysis (Wilson *et al.*, 2020) suggest that ZBTB11 is involved in ribosome biogenesis. In addition, it was shown that ZBTB11 has a regulatory role in the activation and repression of pro-differentiation genes by affecting polymerase II in embryonic stem cells (Garipler *et al.*, 2020). Also, the study in Zebrafish revealed a regulatory function of ZBTB11 in neuropil development and differentiation (Keightley *et al.*, 2017). Another study in mice demonstrated the high expression level of ZBTB11 in the developing retina (Brooks *et al.*, 2019). In addition, previous studies on ZBTB as a protein family emphasized their role in the development of diverse tissues or organs such as lymphocyte development and axon guidance (Ji and Jaffrey, 2014; Tonchev *et al.*, 2016; Zhu *et al.*, 2018; Cheng *et al.*, 2021). The common function of characterized ZBTB proteins and ZBTB11 are their role in both nervous and immune systems (Siggs and Beutler,

2012). Additionally, disturbance of ZBTB7A and ZBTB16 were shown to result in sleep deficiency (Wang *et al.*, 2010; Ohishi *et al.*, 2020). ZBTB11 was upregulated under sleep deprivation in mice (Gaine *et al.*, 2021). Therefore, ZBTB11 might have a role in the development of both the nervous and immune systems and defects in the function of ZBTB11 may be observed as distortions in both systems with a common symptom of sleep deficiency.

The two affected ZBTB11 patients displayed changes in the brain morphology including cerebellar atrophy and ventriculomegaly and also neuromuscular impairments such as facial hypotonia and ataxia (Fattahi *et al.*, 2018). In addition, when the expression of ZBTB11 was analyzed in 52 different healthy adult human tissues, the expression was highly dispersed in all organs, along with a high expression in the cerebellum (Wilson *et al.*, 2020). Therefore, ZBTB11 may have various functions in different tissues.

To conclude, in the light of previous studies, I speculate that ZBTB11, as a developmental TF protein controlling protein synthesis, might have a role in the regulation of sleep by functioning as a regulator in both the nervous and immune system.

1.3. Modeling Candidate ID-Causative Genes in *Drosophila*

Ever since the beginning of the 20$^{\text{th}}$ century, when Thomas H. Morgan identified the first mutation in the fruit fly, *Drosophila melanogaster* has been in the focus of biological research all around the world (Jennings, 2011). With the improvements in whole genome and exon sequencing, single cell genome and RNA sequencing, and connectomics techniques, *Drosophila melanogaster* became an important organism in modeling human diseases such as developmental disorders, neurological disorders, and cancer (Bier, 2005). Considering the heterogenic feature of ID, modeling in *Drosophila* provides a fast and cheap option compared to other model organisms.

While deciphering ID in *Drosophila*, after revealing possible disease-related genes in humans, the next step would be to decide if there are orthologues of those genes in the fly that will be used for disease modeling. Even though flies and humans diverged across different paths a long time ago, mechanisms at the molecular, cellular, synaptic and behavioral levels are highly conserved (Tian *et al.*, 2017). *Drosophila melanogaster* is an ideal model organism in this respect, as 75% of all human disease genes were found to have similar sequences in the fly genome (Bier, 2005). Additionally, flies carry orthologues of human genes and their investigation helps to understand various developmental and neurological disorders (Bier, 2005). Some of these orthologues include the HD gene to study Huntington disease (Marsh *et al*, 2003) and the parkin gene to study Parkinson disease (Haywood and Staveley, 2004).

One great advantage of modeling ID in *Drosophila* is that one can study the results of gene manipulation at the level of the whole organism via behavioral assays (van der Voet *et al.*, 2014). Various behavioral protocols are assessing both simple fly behaviors and also more complex behaviors like learning and memory (van der Voet *et al.*, 2014). Some of the human genes that have fly orthologues associated with learning and/or memory defects include FMR1 (Bolduc *et al.*, 2008), NSUN2 (Abbasi-Moheb *et al.*, 2012), CEP89 (van Bon *et al.*, 2013), and ANK3 (Iqbal *et al.*, 2013). It was also shown that the type of mutant allele used in these assays could affect the behavioral outcome. Furthermore, different types of behavioral assays can give different results when used with mutants of the same gene (van der Voet *et al.*, 2014). These points should be taken into consideration while modeling ID in *Drosophila* using behavioral assays. Combining genetic approaches and behavioral assays to understand the effects of ID-related genes offers a great opportunity to see the big picture behind small details.

Some ID-patients have alterations in their circadian clock and consequently problems in their sleep cycle (Maaskant *et al.*, 2013). *Drosophila* is a well-defined animal model to study circadian rhythm and sleep disorders, and discovery of molecular mechanism underlying circadian rhythm (including *Drosophila* research) were awarded with a Nobel prize in 2017. Although there are slight differences in individual proteins, the general mechanism of the molecular circadian clock pathway is conserved from fly to

human (Panda *et al.*, 2002). Also emphasizing this conservation, characterization of dFMRP, the *Drosophila* ortholog of the Fragile X Mental Retardation Protein (FMRP), revealed defects in circadian rhythm and memory consolidation resulting from unregulated synaptic proteins in the neural circuitries from clock cells to Kenyon cells, which control memory formation and consolidation (Gatto and Broadie, 2009).

Another opportunity *Drosophila* offers for ID modeling is that the organization of the brain and nervous system can be examined in detail. It was shown that a number of ID genes take part in neuronal development, specifically during the formation of synapses, dendrites, and axons (van der Voet *et al.*, 2014). *Drosophila* neuro-muscular junctions serve as an important synapse model for neurotransmitter release studies, synapse formation and physiology research (Broadie and Bate, 1995). Some researchers also use dendritic arborization (DA) neurons to study dendrite formation and physiology, which have an important role in ID (van der Voet*et al.*, 2014; Coll-Tane *et al.*, 2019). *Drosophila* neurons, as well as NMJ structures are further available in vivo instruments to measure neuronal activity via electrophysiology and calcium imaging (Coll-Tane *et al.*, 2019). In his review, in 2011, Hans van Bokhoven mentions various cellular functions and mechanisms affecting ID including synapse formation and plasticity, pathways related to presynaptic mechanisms, postsynaptic protein complexes, cytoskeleton dynamics, cellular signaling cascades, and epigenetic regulation of transcription (van Bokhoven, 2011). In addition, even though the anatomy of fly and mammalian brains is very different, mushroom bodies (MB) of *Drosophila* and mammalian hippocampus show a high degree of homology regarding gene expression, neural circuitry and behavioral output (Heisenberg, 1998). Consequently, MB was highly utilized to study ID-related genes to reveal the role of ID proteins in the development and circuit assembly of this learning and memory center (Kepa *et al.*, 2017; Lanore *et al.*, 2012).

1.4. Mushroom Bodies (MBs)

The MBs consist of ∼2500 Kenyon cell axons and a bilateral neuropil-rich center in the adult fly brain (Fahrbach, 2006). The anatomical structure of the MB formed by the cell bodies and axons of Kenyon cells resemble a pair of mushrooms (Anzi and Zinn, 2018). Several sensory system circuits relay their sensory inputs to Kenyon cells, such as visual, auditory, olfactory, and gustatory (Masek and Scott, 2010; Vogt *et al.*, 2014). These inputs are regulated by dopaminergic neurons, which are triggered by modulatory reward and punishment cues (Liu *et al.*, 2012). On the other hand, output neurons of MB are cholinergic, GABAergic or glutamatergic and the output neurons project their axons to divergent brain areas to respond to sensory inputs by associated behavior (Aso *et al.*, 2014). Therefore, associative learning has been highly studied in MB. However, other functional studies revealed that MBs are recruited in other behaviors such as olfactory learning (Dubnau *et al.*, 2001), sleep (Joiner *et al.*, 2006) and habituation (Glanzman, 2011).

Development of the MB begins at early third instar larval stages by activation of 4 collateral neuroblasts. Each neuroblast consecutively generates three types of Kenyon cells. First, γ-neurons form the larval MB structure until the mid-third instar larval stage. Second, α'/β'-neurons project their axons in parallel to γ-neurons until the mid-third instar larval stage. Finally, α/β-neurons project their axons in parallel to α'/β'-neurons during the pupal stage (Ito *et al.*, 1997; Zhu *et al.*, 2003; Yu and Lee, 2007). However, both branches of γ-neurons are pruned during the early pupal stage by glial cells (Hakim *et al.*, 2014) and reformed during the late pupal and adult stages. Medial extension of β/β' and γ-neurons are restricted only to the medial lobe (Lee *et al.*, 1999).

Axons of Kenyon cells create a large bundle called the peduncle and the distal tip of the peduncle bifurcates into two branches, one going through dorsal and the other medial side of brain (Yang *et al.*, 1995). While the dorsal branch consists of two parallel α (alpha) and α' lobes, the medial branch consists of three parallel β (beta), β' and γ (gamma) lobes (Lee *et al.*, 1999) (Figure 1.1.). (Figure 1.1. was adopted from Aso *et al.*, 2014 by permission of the terms of the Creative Commons Attribution License) All of the lobes were divided into 5 subdomains according to stereotypical synaptic connection with axons of MB-input neurons and dendrite of MB-output neuron. For instance, α/β-neurons are composed of α1, α2, α3, β1, β2 subdomains (Aso *et al.*, 2014).

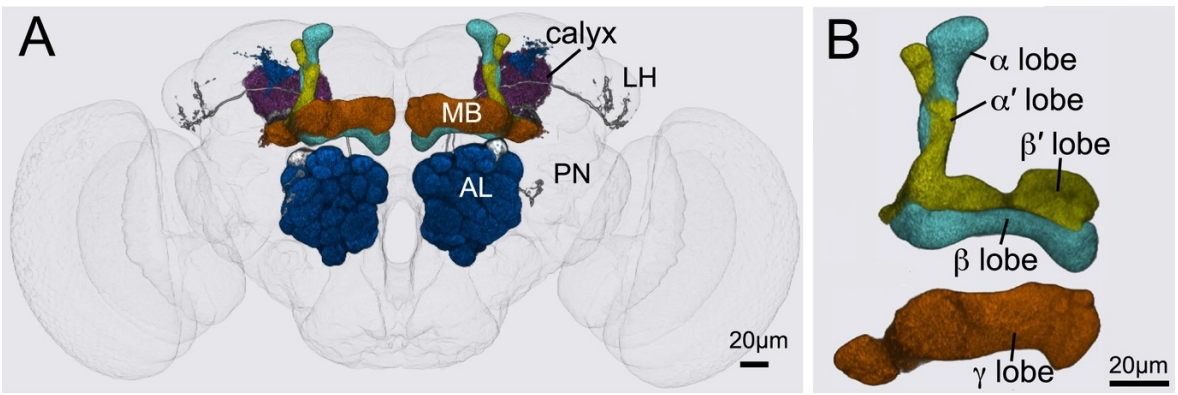

Figure 1.1. Scheme of mushroom bodies in adult brain. (Aso *et al.*, 2014). A. Position of MB in the adult fly brain and B. MB lobes.

Development of MB morphology is tightly controlled by neurodevelopmental genes (Crittenden *et al.*, 2018). Orthologs of ID-causative genes were tested in *Drosophila* by loss or gain-of-function studies and several morphological abnormalities such as fusion of β and γ lobes, α lobe misguidance due to defects in axon guidance (Michel, 2004; Chubak*et al.*, 2019; Kim *et al.*, 2021), and decrease or increase in axon volume due to defects in proliferation and differentiation of Kenyon cells neuroblast (Brown *et al.*, 2012; Crittenden *et al.*, 2018) were described in flies. In addition, MB-specific knockdown of CkIIα-i1 (ortholog of ZBTB11 in *Drosophila*) displayed abnormalities in MB morphology (Fattahi *et al.*, 2018).

1.5. CkIIα-i1

Casein Kinase II alpha interactor 1 (CkIIα-i1) was identified as a *Drosophila* ortholog of human ZBTB11 by the online tool PANTHER (Protein Analysis Through Evolutionary Relationships) depending on the GO enrichment analyses of both fly and human proteins (Mi *et al.*, 2021). The location of CkIIα-i1 (Flybase ID: FBgn0015025 and *Drosophila* symbol: CG6215 gene in the third chromosome is 3L:15.816.979-15.818.621. Its predicted molecular functions are protein kinase binding, DNA-binding, transcription factor activity, and RNA polymerase II cis-regulatory region sequence-specific DNA binding activities. It was predicted to have 4 C2H2-type ZNF domains and to localize to the nucleus (Larkin *et al.*, 2021). According to the results of GST pull-down assays, CkIIα-i1 is phosphorylated by Casein Kinase 2 alpha subunit (CkIIα) (Kalive *et al.*, 2001). In Yeast-two-hybrid assays, in addition to CkIIα, CkIIα-i1 was shown to interact with Antennepedia (Antp), Septin interactor protein-1 (Sip1) and Widerbrost (Wdb) (Giot *et al.*, 2014). Antp, as a Hox-protein, was shown to be involved in the development of body segment and differentiation of the imaginal disc (Kuert *et al.*, 2003). Recently, Sip1 was reported to play a regulatory role in neurogenesis in the early larval brain (Wei *et al.*, 2022). A protein complex STRIPAK, which consists of Wdb and CkIIα proteins regulates neural stem cell reactivation by Hippo and Insulin Receptor Signaling pathways in larvae (Gil-Ranedo *et al.*, 2019) and circadian rhythm in the adult fly (Andreazza *et al.*, 2015). In the developing larvae, regulation of neurogenesis appears to be the common function of interaction partners of CkIIα-i1 protein. Therefore, CkIIα-i1 may have a function in neurodevelopmental processes.

1.6. Sequence Conservation Between Functional Domains of ZBTB11 and CkIIα-i1

To understand the functional orthology between ZBTB11 and CkIIα-i1, I analyzed the protein sequence conservation of their functional protein domains in both PRALINE (Heringa , 1999) and NCBI/ protein BLAST online tools (Altschul *et al.*, 1990). BLAST showed 33% identity and 37% similarity between ZNF 9-12 of ZBTB11

and ZNF 1-4 of CkIIα-i1. Using PRALINE I found 20% identity and 47% similarity between the predicted BTB domain of ZBTB11 between amino acids 214 and 282. The first 38 amino acids of the N-terminus of CkIIα-i1 are not annotated(Figure 1.2.).

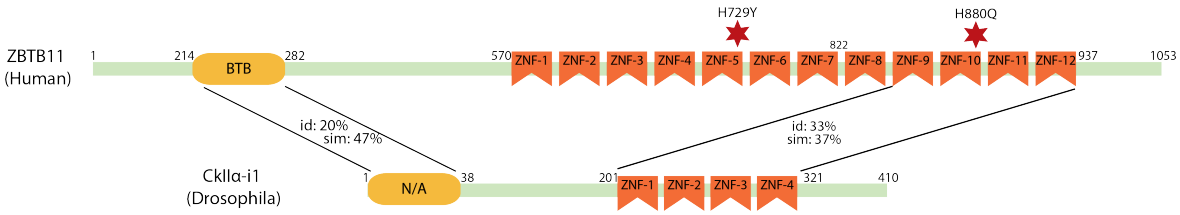

Figure 1.2. Protein sequence conservation of functional domains of CkIIα-i1 and ZBTB11. Red stars: Location of variants ZBTB11^{H729Y} and ZBTB11^{H880Q}.

1.7. The CRISPR/Cas System

Usage of P element, for modifying endogenous genomic sequences, is an indispensable method for genome engineering in *Drosophila* since the early 1980s (Spradling and Rubin, 1982). Even though it can induce double stranded breaks (DSB) at the excision location of DNA, it is not possible to guide P elements to specific sites in the genome. At the beginning of this century, engineered zinc finger nucleases (ZFNs) and transcription activator-like effector nuclease (TALENs) tools were favored among gene-editing strategies since they offered the ability to generate site-specific modifications (Bibikova *et al.*, 2002). Nevertheless, together with the establishment of CRISPR/Cas technology, they fell from grace because their working mechanisms require high labor-intensity, show unpredictable off-target activity and create technical challenges (Eid and Mahfouz, 2016). CRISPR/Cas system, clustered regularly interspaced short palindromic repeats (CRISPR) and CRISPR associated proteins (Cas), was discovered in bacteria and archaea and provides endogenous adaptive immunity toward invaders (Wiedenheft *et al.*, 2012). The CRISPR/Cas system represents a concise two-component system, a chimeric RNA (chiRNA) and Cas9 protein. After publication of the first findings, it was quickly utilized by several laboratories and verified as a novel gene-editing system. For instance, after only one year, the efficiency and feasibility of CRISPR/Cas was tested

in *Drosophila* for the first time (Gratz *et al.*, 2013). This highly revolutionary and versatile system was awarded the Nobel prize in Chemistry to Jennifer A. Doudna and Emmanuelle Charpentier in 2021(Jinek *et al.*, 2012). Although there are three types of CRISPR/Cas immune systems in bacteria, which can be distinguished according to the maturation of crRNA and interference mechanism, the type II CRISPR/Cas system that is based on a restrainable maturation process and includes the versatile member of Cas family protein, Cas9, was favored for gene-editing. Type II CRISPR/Cas works as follows: a single chimeric RNA (chiRNA) or guide RNA (gRNA) that consists of crRNA and tracrRNA is produced. While target-specific guidance is procured by crRNA, tracrRNA ensures the recruitment of Cas, by acting as a scaffold, and leads to maturation of crRNA and cleavage of the breaking site. Cas9 is used to introduce double-stranded (ds) breaks in the target DNA. At sites complementary to the crRNA-guide sequence, the Cas9 HNH nuclease domain cleaves the complementary strand, whereas the Cas9 RuvC-like domain cleaves the noncomplementary strand (Huai *et al.*, 2017).

Double-strand breaks (DSBs) can be repaired by two methods: non-homologous end joining (NHEJ) and homology-dependent repair (HDR). Both methods are accessible and are being used by almost every cell in an organism. Single guide RNAs (sgRNAs) that are designed for a specific region in the genome can introduce DSBs with the help of the Cas9-mediated CRISPR system. Cas9 mediated DSBs can cause one of the two repair responses NHEJ and HDR. Although NHEJ and HDR are caused by the same circumstance, DSBs, they have different ways to overcome discontinuous DNA strands. NHEJ can be used to introduce indels (insertions and deletions) in the region of interest, while HDR can be used to incorporate exogenous DNA strands.

NHEJ repair system mostly depends on the DNA Ligase mechanisms and occurs throughout the cell cycle (Panier and Boulton, 2013). NHEJ re-joins cut ends without using the guidance of homologue chromosomes or an external DNA strand. As NHEJ is known to be error-prone, it is associated with random indels at DSB sites, and it is being used for mutagenesis (Wang *et al.*, 2013). Thus, Cas9-mediated DSBs can result in small mutations, which can be frameshifting, silent or sense. In addition

to that, the use of multiple Cas9-mediated DSBs generally result in the loss of the region flanking the two DSBs, thus giving rise to larger indels. The application of the CRISPR/Cas9 system in *Drosophila* can be used to generate targeted mutations to investigate interregional or intermolecular interactions. Targeted mutagenesis is being used at protein-coding sequences, P-elements, and other regulatory regions on the genome, like transcription factor binding sites, and non-coding RNAs (Bassett and Liu, 2014).

The HDR system uses the help of another DNA strand, normally sister chromatid for repair of the DSB. In contrast to NHEJ, HDR is an error-free process and repairs the missing sequence of DNA using the template DNA. In *Drosophila*, the CRISPR/Cas9 system is both being used to generate targeted DSBs and insert genomic modifications. Since CRISPR/Cas9 system provides a homologous DNA template, desired and defined genomic changes can be introduced to the genome through the DSB site (Bassett and Liu, 2014). The success of HDR through exogenous template relies on the large excess of a homologous template that includes the desired modifications. The donor DNA can take two forms: single-stranded DNA (ssDNA) which is used to insert DNA up to 200 nucleotides long and double-stranded DNA (dsDNA) that is used to insert hundreds and thousands of nucleotides. In flies, when the DSBs occur, NHEJ is the primary system that is activated, and this is not a desired situation if the aim is to introduce a genetic modification through HDR. It has been shown that mutation in DNA Ligase IV creates a bias towards HDR since it has a crucial role in the NHEJ system (Beumer *et al.*, 2008, 2013; Bassett *et al.*, 2014). Using ssDNA as a template in HDR is important and preferred in the addition of short genomic regions like antibody tags for proteins to establish localization and interaction, and site-specific recombinase sites that allow integration of various modifications into the same region easily. dsDNA-associated HDR allows for the integration of longer sequences, tags, and regulatory regions. For example, fluorescent protein GFP is being tagged to proteins via dsDNA, or GAL4 transcriptional reporter is being introduced to the desired gene to determine its role in the genome through overexpression or knock-down essays.

1.8. The RNA Interference (RNAi) System

Discovered by Andrew Z. Fire, Craig C. Mello, and their colleagues in 1998, using C. elegans (Fire *et al.*, 1998), RNAi proved to be a powerful tool to study gene function by downregulation of gene expression through mRNA degradation. The mechanism is originally believed to be evolved as an innate response to viral infection and has been discovered in all kinds of eukaryotes (Taxman *et al.*, 2010). The process starts with the introduction of double-stranded RNA (dsRNA) to cells. When an exogenous or endogenous dsRNA is introduced to cells, a type III ribonuclease called Dicer 2 generate the short/small interfering RNA (siRNA) by cleaving the dsRNA. Then, siRNA is loaded to Argonaute 2 (Ago2) and along with other associated proteins, the RNA-induced silencing complex (RISC) is assembled. After the sense strand of the siRNA is degraded in the RISC, the antisense strand guides the cleavage of complementary mRNA molecule by Ago2 of the RISC (Zhu and Palli, 2020). Finally, other endogenous nucleases further degrade the cleaved mRNA (Taxman *et al.*, 2010). There are also other alternative RNAi pathways that use microRNA (miRNA) or piwi-interacting RNA (piRNA) for the suppression of gene expression (Zhu and Palli, 2020).

In *Drosophila*, RNAi can be induced exogenously by microinjection of dsRNA into embryos, or endogenously by creating transgenic fly lines that express a long double-stranded hairpin RNA, which can be expressed in a tissue specific manner by using the UAS-GAL4 system (Czech and Hannon 2011). However, long hairpins are observed to be ineffective for gene silencing in the female germline (Ni *et al.*, 2011). An alternative to long hairpins is the small hairpin RNA (shRNA), which is an artificial miRNA. Similar to miRNA, shRNAs are proccessed by the Drosha-Pasha protein complex and Dicer 1 upon loading onto Ago1. Differently, processed shRNA can be also loaded into Ago2, which is the major RNAi organizer in *Drosophila*, giving a remarkable silencing potency. Additionally, shRNA is also shown to work efficiently during oogenesis, and provides an alternative to long hairpins (Ni *et al.*, 2011).

1.9. *trans* -Tango

trans- Tango is a general and flexible technique for anterograde transsynaptic labelling. It uses an exogenous ligand (human glucagon)-receptor pair, and pan-neuronally expressed core components of the signaling pathway. Expressed by the binary UAS-GAL4 system, the ligand appears as a fusion protein of glucagon that is attached to cytosolic and transmembrane domains of Neurexin1 via a flexible linker. When the ligand binds to the receptor, that has the transcriptional activator QF at its cytoplasmic tail via a linker that contains a cleavage site, the receptor recruits a pan-neuronally expressed fusion protein that cuts the linker between the cytoplasmic tail and QF. Then the QF binds to the QUAS of the reporter gene to mark postsynaptic neurons. The cell-type specifically expressed GAL4 binds in addition to the UAS of a reporter gene to mark the presynaptic neuron. In the end, presynaptic neurons are marked only in the Gal4 expressing neurons, and postsynaptic neurons are only marked only in the QUAS-activated neurons. Because, the signaling pathway components are expressed pan-neuronally, all neurons become a potential postsynaptic neuron, while only the Gal4 expressing neurons remain as a presynaptic neuron. Also, unlike the other labelling techniques, the ligand doesn't diffuse away because it is tethered to a synaptic protein (Talay *et al.*, 2017).

2. AIM OF THE STUDY

Previously, two pathologic variants of Zbtb11, a candidate ID-causative gene, were identified in two consanguineous families (Fattahi *et al.*, 2018). One of the predicted *Drosophila* orthologues of ZBTB11, CkIIα-i1, was analyzed in MB by MB-specific knockdown of CkIIα-i1. It was shown that disruption of CkIIα-i1 resulted in a promising phenotype in the MB (Fattahi *et al.*, 2018). The main purpose of this study is the further characterization of CkIIα-i1 for the better understanding of its function and experimental validation of the orthology between CkIIα-i1 and ZBTB11.

In order to understand the function of CkIIα-i1, first, I analyzed the expression pattern and localization of CkIIα-i1 in the fly brain using a CkIIα-i1-Gal4 reporter line and a CkIIα-i1 tagged BAC line. Also, for the better understanding of endogenous expression, I attempted to generate an endogenously tagged CkIIα-i1 trangenic line. Second, the effects of misexpression and overexpression of CkIIα-i1 on MB morphology was analyzed to understand the involvement of CkIIα-i1 in development of the MB. For this purpose, two separate CkIIα-i1 mutants were generated by CRISPR/Cas and were molecularly characterized.

To validate the orthology between ZBTB11 and CkIIα-i1, wild-type and two pathogenic variants ZBTB11-expressing transgenic fly lines were generated and validated. Finally, their expression was characterized in the fly brain.

3. MATERIALS AND METHODS

3.1. Biological Material

Drosophila melanogaster cultures were maintained at 25°C and 70% humidity with a 12:12 light and dark cycle. Genesee Scientific Nutri-Fly™ Bloomington formula fly food was prepared according to company's manual and used for rearing flies within culture vials. Stock fly cultures were transferred into fresh fly food vials monthly. Fly lines which were generated for this study are listed in Table 3.1. Fly lines which were utilized in this study are listed in Table 3.2.

Table 3.1. List of generated fly lines.

Name	**Chr. No.**	**Description**
CkII-i1-Gal4 Pr-1	2	Expresses Gal4 protein under the control of the promoter sequence of C*kII-i1*
CkII-i1-Gal4 Pr-2	2	Expresses Gal4 protein under the control of the promoter and first exonic sequence of C*kII-i1*
UAS-ZBTB11-HA^{wt}	2	Expresses HA-tagged ZBTB11 under the control of UAS sequences
UAS-ZBTB11-HA^{H729Y}	2	Expresses HA-tagged the H729Y variant of ZBTB11 under the control of UAS sequences
UAS-ZBTB11-HA^{H880Q}	2	Expresses HA-tagged the H880Q variant of ZBTB11 under the control of UAS sequences

Table 3.2. List of utilized fly lines.

Name	**Chr. No.**	**Description**
Elav-gal4	1	Expresses Gal4 in post-mitotic neurons under the control of *elav* promoter
Actin-Gal4	3	Expresses Gal4 protein under the control of an *actin* promoter
OK107-Gal4	4	Expresses Gal4 protein in mushroom bodies
UAS-CkII-i1-HA	2	Expresses HA-tagged CkII-i1 under the control of UAS sequences
UAS-CkII-i1-RNAi-1	2	Expresses dsRNA for RNAi of CkIIalpha-i1 under the control of UAS sequences (Bl #53025)
UAS-CkII-i1-RNAi-2	2	Expresses dsRNA for RNAi of CkIIalpha-i1 under the control of UAS sequences (Bl #60102)
UAS-mCD8::GFP	3	Expresses mCD8-tagged GFP under the control of UAS sequences
UAS-LacZnZ	3	Expresses nuclearly localized beta-galactosidase under the control of UAS sequences
nos-cas9	1	Expresses germ line specific Cas9 protein
Canton-s		Wild type flies
w^{1118}	1	Flies carrying a deletion mutation in their w genes
CkII-i1::GFP-FPTB	3	Expresses GFP and FLAG tagged CkIIalpha-i1 protein
trans-Tango	2	Expresses trans-Tango components
ywQB	1,2,3	Multichromosome balancer

3.2. Chemicals and Equipment

3.2.1. Chemicals

Chemicals used in this study are listed in Table 3.3.

Table 3.3. List of chemicals.

Chemical	**Manufacturer**
1 kb marker	NEB, USA (N3232L)
100 kb marker	NEB, USA
Agarose	GeneOn, USA (604,001)
Ampicilin	Sigma-Aldrich, USA (59349)
Bovine Serum Albumin	Sigma-Aldrich, USA (A9647)
EDTA	Sigma-Aldrich, USA (59417C)
Ethidium Bromide	Sigma Life Sciences, USA (E1510)
Isopropanol	Sigma-Aldrich (W292907)
KCl	Sigma-Aldrich (29676)
KOAc	Sigma-Aldrich (P1190)
LiCl	Sigma-Aldrich (L9650)
NaCl	Sigma-Aldrich, USA (S7653)
Paraformaldehyde	Sigma-Aldrich, USA (P6148)
Phenol:chloroform:Isoamyl alcohol	Sigma-Aldrich, USA (P2069)
Proteinase K	Roche, Germany (139963000)
Tris	Sigma-Aldrich, USA (T6066)
Triton-X 100	AppliChem, USA (A4975)
Tween 20	Roche, USA (11332465001)

3.2.2. Buffers and Solutions

Buffers and solutions used in this study are listed in Table 3.4.

Table 3.4. List of buffers and solutions.

Buffer/Solution	**Substances**
Formaldehyde Solution (4%)	160 g/l PFA, pH 7.4
	1M NaOH until solution becomes transparent
PAXD	50 g BSA
	3 g Sodium Dexoycholate
	0.3% Triton X-100 In PBS
PBS (1X)	137 mM NaCl
	2.7 mM KCl
	10 mM Na2HPO4
	1.8 mM KH2PO4
PBST	PBS (1x)
	0.3% Triton X-100
TAE Buffer (1X)	40 mM Tris-Cl
	1 mM EDTA
	0.1% Acetic acid
Squish Buffer	10 mM Tris, pH 8.0
	1 mM EDTA
	25 mM NaCl
Buffer A	100 mM Tris, pH 7.5
	100 mM EDTA
	100 mM NaCl
	0.5% SDS

3.2.3. Primers

Primers used in this study are listed in Table 3.5.

Table 3.5. List of primers.

Name	**Sequence (5'>3')**
CkIIa-i1-A1	AGCAAAATGACAGAAGCGGA
CkIIa-i1-A2	CAGGCTGATGAACTCTCCT
CkIIa-i1-15-RP-1	GGCGGGGTTTACAAGAATGC
CkIIa-i1-CDS-FP	ATGACAGAAGCGGAAATTTGC
CkIIai1_Bl_gRNA_RP	TGGGTTTCTTTGCATTTGAC
CkIIa-i1_HDR _RP_2	CGTTTCCAGCCTCAGACAA
UAS-zbtb11F3	GGGGACAAGTTTGTACAAAAAAGCAGGCT ATGTCAAGCGAGGAAAGCTAC
UAS-zbtb11R3	GGGGACCACTTTGTACAAGAAAGCTGGGT TTCTCCTCCTGAAATATGTGC
pDONOR-FP	TAACGCTAGCATGGATCTC
zbtb11-2028_294-FP	AATGAAGCATCGGGAACATC
pDONR207 RP	AACATCAGAGATTTTGAGACACG
zbtb11_930_F	GTAAGGCCAGCTTCCTTCCT
zbtb11_1905_F	TGCACAAACTGAAACATGAAAGA
pUASt-HA- FP	GCAACTACTGAAATCTGCCAAG
pUASt- HA- RP	CCCGCATAGTCAGGAACATC

3.2.4. Antibodies and dyes

Antibodies and dyes used in this study are listed in Table 3.6.

Table 3.6. List of antibodies and dyes.

Primary Antibodies				
Name	**Antigen**	**Host**	**Dilution**	**Source**
Anti-Elav	Elav	Rat	1:20	DSHB
Anti-GFP	GFP	Rabbit	1:1000	Torrey Pines
Anti-FasII	Fasciclin II	Mouse	1:20	DSHB
Anti-B-gal	b-galactosidase	Rabbit	1:5000	Cell Signaling
Anti-Dach	Dachshund	Mouse	1:10	DSHB
Anti-HA	HA	Rabbit	1:100	Roche
Anti-FLAG	FLAG	Rat	1:200	Cell Signaling
Anti-PDF	PDF	Mouse	1:500	DSHB
Secondary Antibodies				
Alexa 488	Rat	Goat	1:800	Invitrogen
Alexa 488	Rabbit	Goat	1:800	Invitrogen
Alexa 555	Rat	Goat	1:800	Invitrogen
Alexa 647	Mouse	Goat	1:800	Invitrogen
Alexa 647	Rat	Goat	1:800	Invitrogen
Cy5	Mouse	Goat	1:800	Invitrogen
Other Dyes				
Alexa Fluor 647 Phalloidin	F-actin		1:1000	Thermo-fisher
TOTO-3 Iodide	Nucleic Acids		1:1000	Thermo-fisher

3.2.5. Embedding Media

Vectashield Embedding Medium was used for tissue mounting (Vector Laboratories, Inc).

3.2.6. Disposable Labware

Disposable equipment is listed in Table 3.7.

Table 3.7. List of disposable equipment.

Material	**Manufacturer**
Micropipette Tips	Greiner Bio-One, Belgium
PCR tubes (200 µl)	Bio-Rad, USA
Pipette Tips (10 - 200 - 1000 µl)	VWR, USA
Plastic Pasteur pipettes	TPP Techno Plastic Products AG, Switzerland
Syringe (1cc)	Becton, Dickinson and Company, USA
Test Tubes, (0.5 - 1 - 1,5 - 2 ml)	Citotest Labware Manufacturing, China
Test Tubes, (15 - 50) ml	Becton, Dickinson and Company, USA
Culture tubes (14 ml)	Greiner Bio-One, Belgium
Filter Tips	Greiner Bio-One, Belgium
Petri Dishes, 60 x 15 mm	TPP Techno Plastic Products AG, Switzerland
PVDF membrane	Roche Life Science
Microscope cover glass	Fisher Scientific, UK
Microscope slides	Fisher Scientific, UK

3.2.7. Equipment

Laboratory equipment is listed in Table 3.8.

Table 3.8. List of equipment.

Material	**Manufacturer**
Autoclave	Astell Scientific Ltd., UK
Centrifuges	Eppendorf, Germany (Centrifuge 5424, 5417R)
Confocal Microscope	Leica Microsystems, USA (TCS SP5)
Electrophoresis Equipment	Bio-Rad Labs, USA
Fluorescence Stereomicroscope	Leica Microsystems, USA (MZ16FA)
Freezers	Arçelik, Turkey
Gel Documentation System	Bio-Rad Labs, USA (Gel Doc XR)
Heating Block	Fisher Scientific, France
Heating Magnetic Stirrer	IKA, China (RCT Basic)
Incubator	Weiss Gallenkamp, USA (Incubator Plus Series)
Laboratory Bottles	Isolab, Germany
Micropipettes	Eppendorf, Germany
Microwave oven	Vestel, Turkey
Mini-PROTEAN Tetra Cell	Bio-Rad Labs, USA
pH meter	WTW, Germany (Ph330i)
Refrigerators	Arçelik, Turkey
Stereo Microscope	Olympus, USA (SZ61)
Thermal Cycler	Bio-Rad Labs, USA (C1000 Thermal Cycler)
Cold Room	Birikim Elektrik Soğutma
Vortes Mixer	Scientific Industries, USA (Vortex Genie2)

3.3. Molecular Biology Techniques

3.3.1. DNA Amplification by PCR

Two DNA polymerases were used for PCR protocols in this project: Q5 High-Fidelity DNA polymerase and OneTaq DNA polymerase. Protocols for both of the polymerases were applied as the manufacturer's recommendations. Melting temperatures (TM) of each primer pair were calculated separately with regards to the polymerase used. A reaction with Q5 High-Fidelity DNA polymerase contains 1X Q5 Reaction Buffer, 10 mM dNTPs, 10 μM forward primer, 10 μM reverse primer, 0.02 U/μl Q5 High-Fidelity DNA polymerase, various concentrations of template DNA, and nuclease-free water (ddH2O) up to final concentration, which depends on the further experiments to be carried on. In necessary situations, 1X Q5 High GC Enhancer was also added to the reactions. Standard cycling conditions were as follow: an initial denaturation step at 98°C for 30 seconds, a total of 25-35 cycles of 98°C for 10 seconds, annealing temperature depending on the TMs of primer pairs for 30 seconds and 72°C for 30 seconds per kilobase to be amplified, and lastly a final extension step at 72°C for 2 minutes.

A reaction with OneTaq DNA polymerase contains 1X OneTaq Standard Reaction Buffer, 10 mM dNTPs, 10 μM forward primer, 10 μM reverse primer, 0.025 U/μl OneTaq DNA polymerase, various concentrations of template DNA, and ddH2O up to a final concentration depending on the further experiments. Standard cycling conditions include an initial denaturation step at 94°C for 30 seconds, a total of 30 cycles of 94°C for 30 seconds, annealing temperature depending on the TMs of primer pairs for 1 minute and 68°C for 1 minute per kilobase to be amplified, and a final extension step at 68°C for 5 minutes.

3.3.2. Agarose Gel Preparation

Agarose was dissolved in 1X TAE buffer with a final concentration of 1% unless otherwise stated. Microwave was used for heating the mixture and after cooling down, 50ng/mL ethidium bromide (EtBr) was added. Then this mixture was poured to an appropriate tray with a comb and let to get firm. After the gel got solidified, the comb was removed and the gel was placed into an electrophoresis tank with tray.

3.3.3. Agarose Gel Electrophoresis

DNA samples were prepared by adding of DNA loading dye to a final concentration of 1X. The dye and samples were mixed thoroughly. Then the samples were loaded to the wells as well as a DNA ladder to compare band sizes. 1kb or 100bp DNA ladder was used according to the expected band sizes. The electrophoresis tank was filled with 1X TAE buffer. The samples were run at 90-110V for 50-60 minutes. Visualization was performed under a transilluminator (Bio-Rad, USA).

3.3.4. DNA Extraction from Agarose Gel

DNA fragments of interest were cut from the gel on a UV box with a clean scalpel and transferred into 1.5 mL Eppendorf tubes. QIAEX II Gel Extraction Kit (QIAGEN, cat. nos. 20021 and 20051) was used for the extraction. The protocol was adapted from the manufacturer's suggested protocol. Firstly, 300 μL QX1 buffer (Solubilization Buffer) and 200 μL ddH2O were added to the tubes for each 100 mg of gel slice. 3 μL QIAEX II Suspension was also added to the tubes and vortexed for 30 seconds for resuspension. Then the tubes were incubated at 50°C for 15 minutes for agarose solubilization and DNA binding. Tubes were vortexed every 2 minute to keep the QIAEX II solution in suspension. The samples were centrifuged for 30 seconds and the supernatant was removed. The pellet was washed with 0.75X QX1 buffer for two times. During washing, 300 μL buffer was added to the tubes, the pellet was resuspended by vortexing, centrifuged for 30 seconds, and the supernatant was removed. Next, the pellet was washed with Buffer PE for three times. This washing steps were the same as

before: 300 μL buffer was added to the tubes, the pellet was resuspended by vortexing, the samples were centrifuged for 30 seconds, and the supernatant was discarded. After the last washing step, the pellet was air-dried at 37°C for 10-15 minutes until it becomes white. For DNA elution, 15 μL ddH2O was added to the dried pellet and vortexed until the pellet was resuspended. The tubes were incubated at 55-60°C for 10-15 minutes and centrifuged for 30 seconds. The DNA containing supernatant was transferred into a clean tube. To increase the yield efficiency, the elution step could be repeated for a second time. Extracted DNA was stored at -20°C for further purposes.

3.3.5. DNA Extraction from *Drosophila*

Genomic DNA extraction from a single fly and wings: Selected fly was placed in a 200 μL PCR tube and frozen at -20°C until the fly becomes inactive. For each tube, a mixture of 50 μL Squish Buffer and 0.5 μL freshly added Proteinase K (20mg/mL) was prepared. Using yellow tips, this newly prepared solution was pipetted and the fly was mechanically smashed with the same tip. While homogenization, the buffer was released into the tube and mixed slowly. The tubes were then incubated at 37°C for 30 minutes and at 95°C for 3 minutes in a thermocycler. After incubation, the samples were centrifuged with a mini centrifuge for 2 minutes and the supernatant was transferred to a clean tube. Extracted genomic DNA was stored at -20°C for further use.

For the protocol of genomic DNA extraction, two wings of the fly were dissected and put into a 200 μL PCR tube. For each tube, 1 μL Proteinase K (20mg/mL) was freshly mixed with 49 μL of Squish Buffer. The wings were not homogenized but rather the buffer was carefully placed into the tube to prevent the wings' floating on the buffer. The tubes were then incubated at 37°C for 60 minutes and at 95°C for 3 minutes in a thermocycler. After incubation, the tubes were stored at -20°C for further use.

Genomic DNA extraction from whole flies (isopropanol extraction): Fifteen selected flies were placed into a 1.5 mL Eppendorf tube and the flies were frozen at -20°C. Then, 200 μL Buffer A was added into the tubes and the flies were homogenized thoroughly with a homogenizer in this buffer. The samples were then incubated at 65°C for 30 minutes. After incubation, they were cooled down to the room temperature. When the samples reached the room temperature, 114 μL 5M KOAc and 286 μL 6M LiCl were added to the tubes, mixed roughly, and incubated on ice for at least 10 minutes. Then, the tubes were centrifuged at room temperature for 15 minutes at 13000 RPM. The supernatant was transferred into a clean tube, while avoiding the pieces of the flies. The DNA was extracted by adding 1 volume of phenol-chloroform (600 μL) onto the supernatant. When the phenol-chloroform was added onto the supernatant, two phases could be seen clearly. The floating phase was transferred into a new tube and the extraction step was repeated with an equal proportion of phenol-chloroform. Next, the DNA was precipitated by adding isopropanol with a volume of 0.7. The tubes were then centrifuged at room temperature for 15 minutes at 13000 RPM. The supernatant was discarded and the pellet was washed with 400 μL of 70% EtOH by vortexing. The samples were again centrifuged at room temperature for 10 minutes. The supernatant was discarded and the remaining pellet was air-dried at 37°C until the pellet becomes white. And lastly, dried pellet was dissolved in 75 μL ddH2O and stored at -20°C for further use.

Most of the genomic DNAs used in this project were extracted from single flies or wings but in some necessary occasions, when a purer DNA is needed, this protocol was used.

3.3.6. Gateway Cloning

Both BP and LR cloning were performed according to manufacturer's suggestions (Catalog Numbers 12535-019 and 12535-027).

3.3.7. DpnI Digestion

DpnI restriction enzyme was used to remove the methylated DNA. 1 μL of DpnI was added to 50 μL of PCR products to be restricted. They were mixed by pipetting shortly. The mixture was then incubated at 37°C for 3 hours.

3.3.8. Restriction Digestion

For all DNA digestion protocols, manufacturer's suggestions were followed. In a total volume of 50 μL reaction solution, 1 μg of DNA was digested with 1 μL (20U) restriction enzyme in 5 μL (with a final concentration of 1X) of 10X appropriate buffer. The reaction solution was incubated at 37°C for at least 1 hour.

3.3.9. Transformation

Previously prepared competent bacteria (DH5α strain of Escherichia coli) were transformed with target plasmid by heat-shock. 50 μL competent bacteria were let to thaw on ice. 1ng DNA was added on the competent bacteria slowly and they were incubated on ice for 30 minutes. Then a 42°C heat-shock was applied on the samples for 1 minute. After heat-shock, the samples were quickly put back on ice and incubated on ice for 5 minutes. 500 μL LB was added on the cells next to a Bunsen Burner, mixed gently and the samples were incubated at 37°C for 1 hour on a shaker at 250 RPM. 100 μL of this liquid culture was spread on LB agar plates which also had appropriate antibiotics. The plates were incubated at 37°C overnight and fitting colonies were selected the next day for further applications.

3.3.10. Plasmid isolation

Miniprep: For small scale plasmid DNA isolation, QIAGEN QIAprep Miniprep Kit was used and protocol was carried on as manufacturer's suggestions. Single colonies were selected from agar plates and inoculated in 3 mL LB medium containing appropriate antibiotic. The samples were incubated at 37°C for 12-16 hours on a shaker at

250 RPM. After incubation, bacterial cells were centrifuged at room temperature for 3 minutes at 8000 RPM in a tabletop centrifuge. Supernatant was discarded after centrifugation. All further steps from this point were carried on at room temperature. The pelleted bacterial cells were resuspended in 250 μL RNase A-added Buffer P1. Then 250 μL of Buffer P2 was added and mixed thoroughly by inverting the tube 4-5 times. The samples were incubated for 3 minutes. Next, 350 μL of Buffer N3 was added and mixed immediately by inverting the tubes for 4-6 times. The samples were centrifuged for 10 minutes at 13000 RPM in a tabletop centrifuge. 800 μL of the supernatant containing plasmid DNA was transferred to QIAprep spin columns and centrifuged for 1 minutes at 13000 RPM. The flow through was discarded. The columns were washed with 750 μL Buffer PE and centrifuged for 1 minute at 13000 RPM, the flow thorough was discarded. After repeating this washing step once more, the columns were centrifuged without an addition of any solution to remove remaining of washing buffer. Then the columns were placed into a clean 1.5 mL Eppendorf tubes. 50 μL of Buffer EB was added to the columns carefully and the samples were incubated for 3 minutes. Lastly, they were centrifuged for 1 minute at 13000 RPM. The DNA containing Flow through was collected and stored at -20.

Midiprep: For medium scale plasmid DNA isolation, QIAGEN Plasmid Plus Midi Kit was used and manufacturer's suggestions were followed for isolation protocol. Bacterial cultures in 50 mL LB were harvested by centrifuging at 6000 x g for 15 minutes at 4°C. the supernatant was discarded and the bacterial pellet was resuspended in 2 mL RNase A-added Buffer P1. Then 2 mL of Buffer P2 was added, mixed gently by inverting and the samples were incubated at room temperature for 5 minutes. Next, 2 mL Buffer P3 was added and mixed immediately by inverting for 5-6 times. The samples were centrifuged at a minimum of 20000 x g for 30 minutes at 4°C. while the samples were centrifuging, a QIAGEN-tip was equilibrated with 4 mL Buffer QBT by gravity flow. After centrifugation, the supernatant was applied to the equilibrated QIAGEN-tip and allowed to enter the resin by gravity flow. Next, 10 mL Buffer QC was added and let to run through the QIAGEN-tip via gravity flow. This step was repeated for two times. The DNA elution was performed by 5 mL Buffer QF into a 15 mL falcon tube. For DNA precipitation, 3.5 mL isopropanol was added to the samples,

carefully mixed and centrifuged at a minimum of 15000 x g for 30 minutes at 4°C. The supernatant was discarded carefully. Next, the pellet was washed with 2 mL of 70% EtOH and centrifuged at a minimum of 15000 x g for 10 minutes at room temperature. EtOH was discarded and the pellet was air-dried for 10-15 minutes. Finally, the DNA was eluted with a minimum of 100 μL of ddH2O.

3.4. Histological Techniques

3.4.1. Immunohistochemistry for Adult Brain

Adult fly brains were dissected in PBS (1X) in 40 minutes and brains were put into an Eppendorf tube. After dissection, brains were fixed in 4% PFA for 30 minutes and washed with 0.03% PBS-T for four times, 3 minutes at first and then 20 minutes for each washing. After fixation and washing treatments, blocking was made with PAXD for 30 minutes at room temperature. Following the blocking step, primary antibodies with appropriate dilutions were prepared in blocking solution. Adult brains were incubated with primary antibody solution for two over-nights at 4°C. After primary antibody incubation, adult brains were washed with 0.03% PBS-T four times for 15 minutes at room temperature. Following the washing steps, secondary antibodies with appropriate dilutions were prepared in blocking solution. Brains were incubated with secondary antibody solution for two overnights at 4°C. After incubation with secondary antibodies, brains were washed with 0.3% PBST four times for 15 minutes and then they were washed with PBS (1X) two times for 15 minutes at room temperature. After the washing process, brains were mounted on a slide using Vectasield mounting medium.

4. RESULTS

4.1. Examination of the Expression Pattern of CkIIα-i1

Identification of the expression pattern of a gene is important to understand its function. The expression of a particular gene or its protein product can be analyzed using different techniques. To get an understanding of the expression and localization of CkIIα-i1, I investigated the activity of cis-regulatory elements and fusion proteins: CkIIα-i1-Gal4 reporter lines were used to understand the activity of cis-regulatory elements of CkIIα-i1. In addition, in order to investigate the protein expression pattern of CkIIα-i1, I aimed to generate an endogenously tagged CkIIα-i1 and I utilized a BAC transgenic fly line expressing tagged CkIIα-i1.

4.1.1. Generation and Selection of Gal4-Expressing CkIIα-i1 Reporter Lines

Cis-regulatory elements (CREs) are non-coding DNA sequences which regulate the transcription of neighboring genes. Promoters and enhancers are the most studied CREs (Markstein *et al.*, 2008). While promoter regions are approximately 35 bp upstream and downstream of the transcription initiation site, enhancer regions can be located in various places, mostly however 1500 bp upstream of the transcription initiation site as well as within the first intron (Berendzen *et al.*, 2006).

To analyze the expression of CkIIα-i1 two putative CRE regions were investigated. The first region included 626 bp of intergenic region located between the genes CkIIα-i1 and Flower (Pr-1, 640 bp; Figure 4.1.). The second region included the first exon and first intron of CkIIα-i1 in addition to the intergenic region (Pr-2, 820 bp; Figure 4.1.). These CRE regions were PCR amplified from genomic DNA, cloned into the P-element Gal4 plasmid pBPGUw (Addgene 17575) and integrated into the second chromosome of the fly genome to express Gal4 under the control of these CREs (constructs were prepared by Cigdem Soysal) (Figure 4.1.).

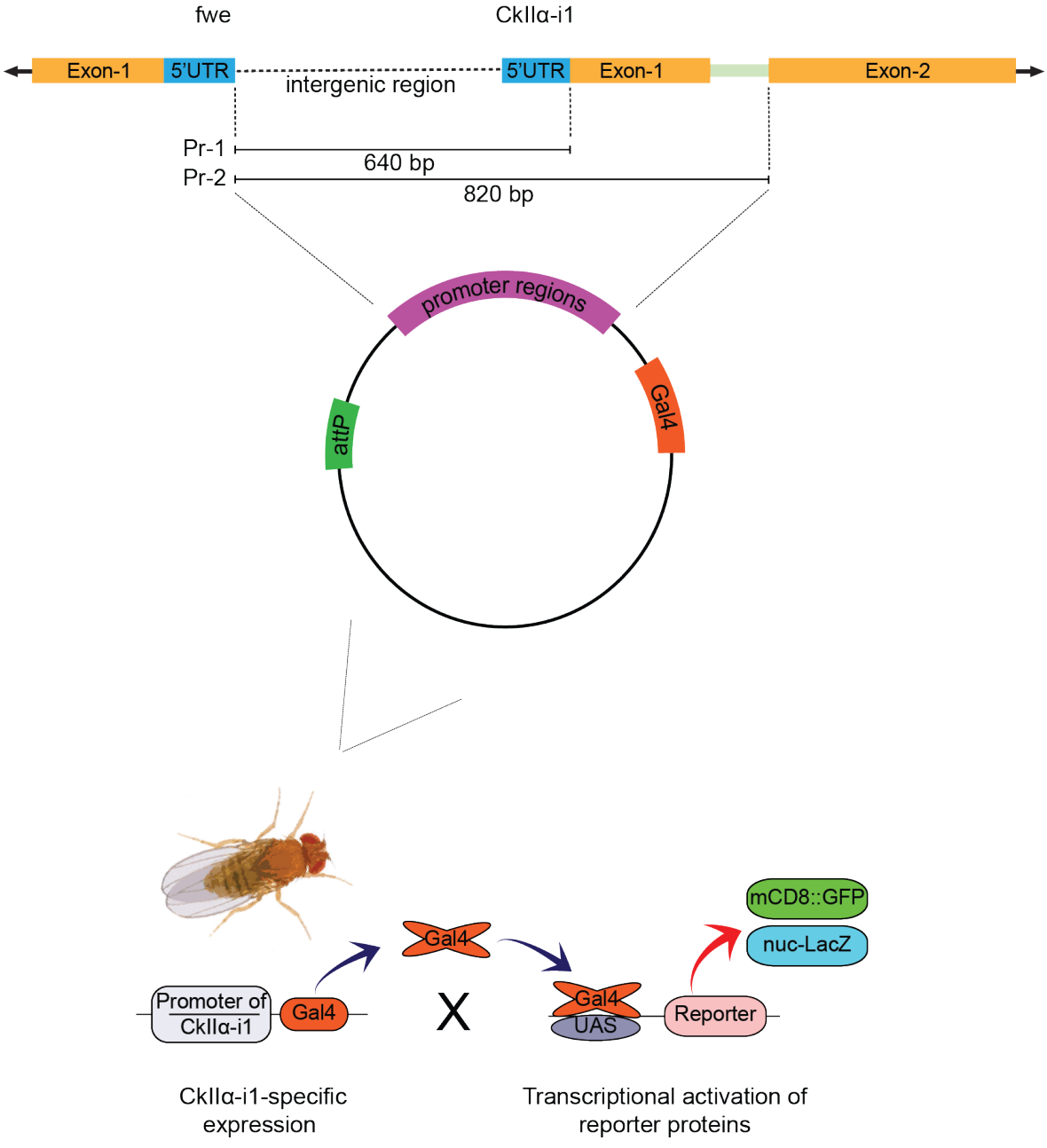

Figure 4.1. Generation and crossing scheme of Gal4 lines. Cloning of putative CRE regions between *fwe* and *CkIIα-i1*: Pr-1 and PR-2 in Gal4-expressing vector (up and middle). Crossing of CkIIα-i1- Gal4 lines with UAS reporter lines.

Transgenic flies carrying the Gal4 constructs were crossed with two UAS reporter lines. The use of the UAS-mCD8::GFP reporter allows the localization of GFP to the membrane and thus visualization of the morphology of the cells, whereas the UAS-nLacZ localizes β -Galactosidase to the nucleus and allows co-localization with cell type-specific markers and thus identification of the identity of labeled cells. The two Gal4 lines were tested for differences in expression pattern including possible sex-dependent differences. Furthermore, co-expression of CkIIα-i1-expressing cells with mushroom body neurons (Kenyon cells) or their projections as well as pacemaker cells was analyzed. Finally, post-synaptic partners of CkIIα-i1-expressing cells were determined using the *trans*-Tango method.

The brains of 5 male and 5 female flies from Pr1-Gal4 and 4 male and 5 female flies from Pr-2-Gal4 lines were stained against GFP and visualized using confocal microscopy (Figure 4.2.). The area of the brain corresponding to the MB was analyzed with particular emphasis, however no GFP-expressing cells close to the MB could be identified. A common expression pattern was detected in all brains, which includes a collateral group of 1-2 dorsal neurons and a group of 3-5 lateral neurons that projected their axons to the dorsal side of the brain (arrowheads in Figure 4.2.). The analysis showed that they were not expressed close to the MB and their expression patterns were similar in both sexes. Therefore, in the following experiments the Pr-2 CkIIα-i1-Gal4 line was used.

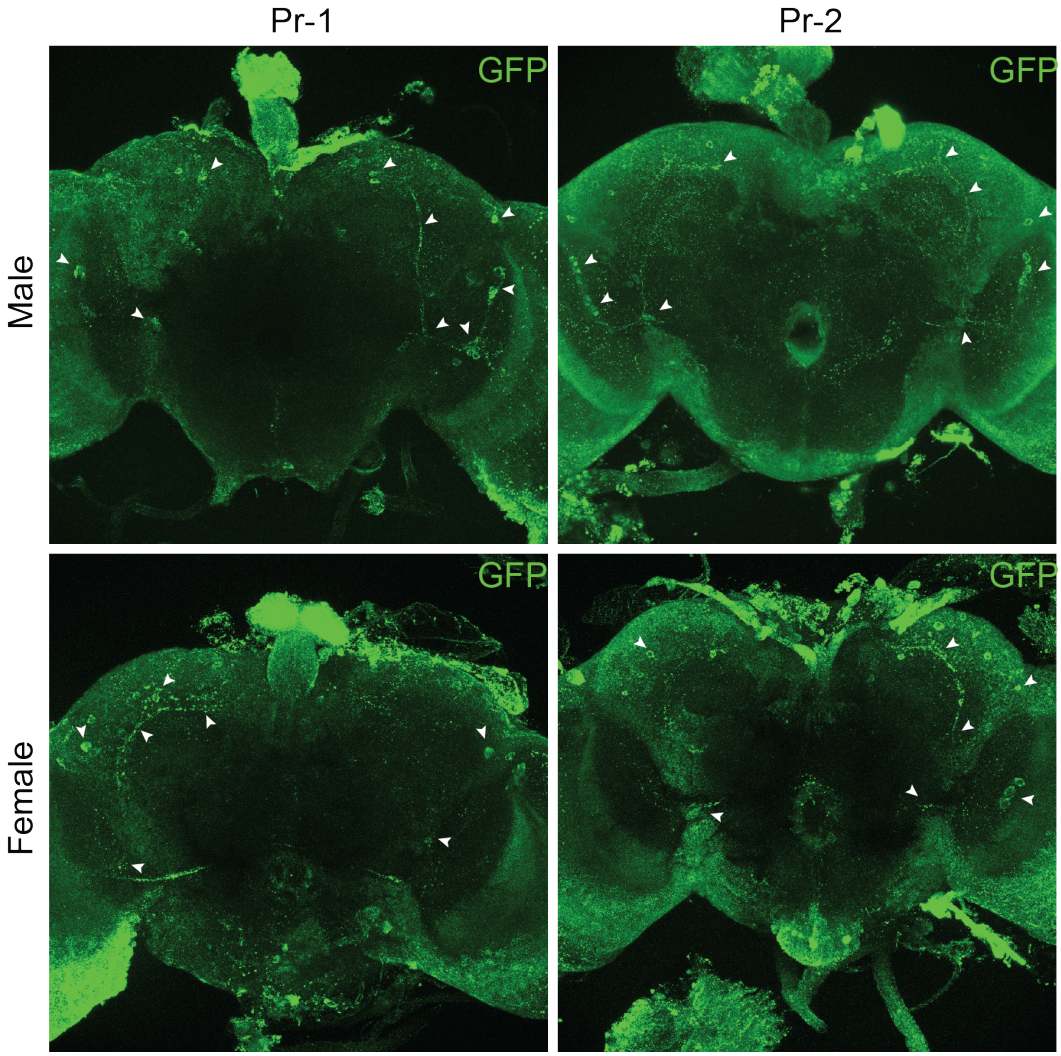

Figure 4.2. Analysis of Pr-1 and Pr-2 CkIIα-i1-Gal4 lines. Immunohistochemistry in CkIIα-i1-Gal4>UAS-mCD8::GFP expressing male and female adult fly brains

Thanks to establishment of single cell RNA sequencing (scRNAseq) technology identification of the expression level of almost all of the genes in each individual cell of investigated tissues, organs or even in the whole organism is possible. The Aerts lab has published scRNAseq data of the adult fly (Li *et al.*, 2021) and provided an online tool SCope (scope.aertslab.org). Depending on the expression profile of every single cell, they were clustered. The clustered cells were annotated according to previously identified cell groups (Davie *et al.*, 2018). SCope allows the analysis of the expression of a gene-of-interest in single cell level and their annotations. The expression of CkIIα-i1 was analyzed by SCope and it was found that CkIIα-i1 is expressed in almost every

annotated cluster. However, only a few cells in the clusters displayed expression of CkIIα-i1 with an expression unit lower than 1.5 rpm. Unfortunately, in SCope, it was not possible to receive a list, which shows the percentage of CkIIα-i1 expressing cells in the annotated clusters. The percentage of CkIIα-i1-expressing cells in the a/b Kenyon cell cluster that consists of approximately 1700 cells was analyzed in more detail. CkIIα-i1 was expressed in only 15 cells within 1700 cells with 0.9%, which is consistent with expression of the Gal4 line co-staining with Kenyon cells.

4.1.2. Expression Pattern of CkIIα-i1 in Mushroom Bodies

MBs are important centers for learning and memory. To examine the expression of CkIIα-i1-Gal4 specifically in the MB their cell bodies (Kenyon cells) and neuropils (α/β lobes) were co-stained in adult brains. The co-localization of CkIIα-i1-Gal4 in Kenyon cells was examined in CkIIα-i1-Gal4>UAS-nLacZ flies. The nuclear marker Dachshund was used to label the Kenyon cells, and anti-β gal antibody to label CKIIα-i1-expressing cells. Dachshund is a transcription factor expressed in Kenyon cells, but also other cells in the dorsal part of the brain. Four brains were visualized by using confocal microscopy. A group of cells co-expressing Dachshund and CkIIα-i1 was identified in the middle-dorsal part of the brain as shown by the white circle in Figure 4.3.A, however no co-localization was observed in the Kenyon cell region.

In addition, the expression of CkIIα-i1 in a subgroup of MB compartments (α/β lobes) was analyzed in CkIIα-i1-Gal4>UAS-mCD8::GFP flies. While anti-FasII antibody was used to label α/β lobes of MB, anti-GFP was used to stain CkIIα-i1-expressing cells. Nine brains were immuno-labeled and visualized by confocal microscopy. While no co-localization of FasII and GFP was observed a few GFP-positive cells were detected in the dorsal part of the α lobes (arrowheads in Figure 4.3.B).

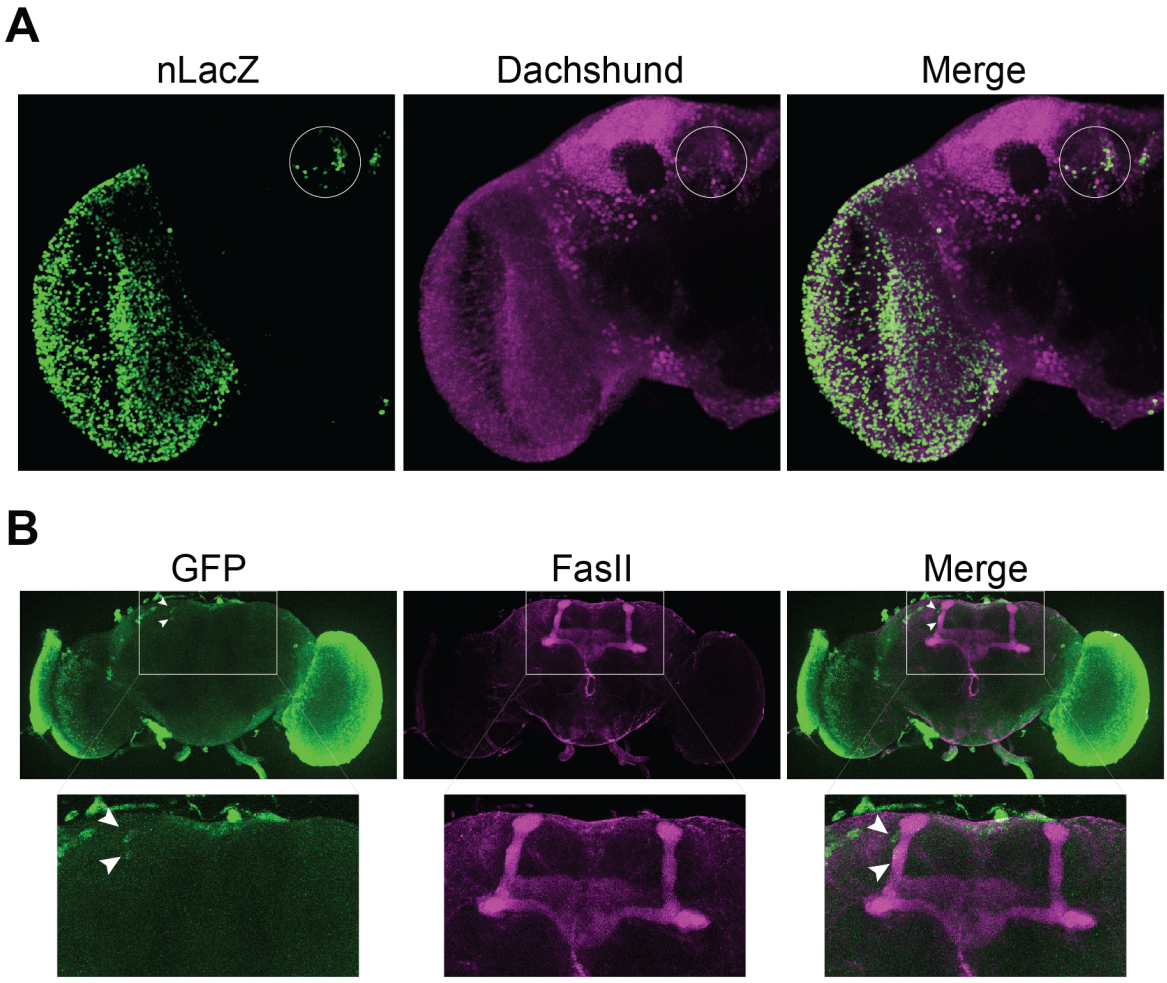

Figure 4.3. Expression of CkIIα-i1 in mushroom bodies. A. Immunohistochemistry in CkIIα-i1-Gal4>UAS-nLacZ expressing fly brain. B. Immunohistochemistry in CkIIα-i1-Gal4>UAS-mCD8::GFP expressing fly brain.

4.1.3. Expression Pattern of CkIIα-i1-Gal4 in Pacemaker Cells

The analysis of CkIIα-i1-expressing cells in Pr-1 and Pr-2-CkIIα-i1-Gal4 lines (Figure 4.2.), showed prominent expression in clock cells, which regulate the inner circadian clock of the fly (Sheeba *et al.*, 2008). It is known that cells related to the circadian rhythm regulate memory formation and consolidation in both human and flies (Dubowy and Sehgal, 2017).

In order to verify this co-expression, an anti-PDF antibody (pigment dispersing factor) which is a prominent marker of clock cells marker was used to label the pace-maker cells and anti-GFP antibody to label CkIIα-i1-expressing cells in CkIIα-i1-Gal4 >UAS-mCD8::GFP flies. Eight brains were imaged by confocal microscopy (Figure 4.4.). The experiment revealed that co-expression occurs in small and large lateral neurons (sLNvs and lLNvs) (circles in Figure 4.4.).

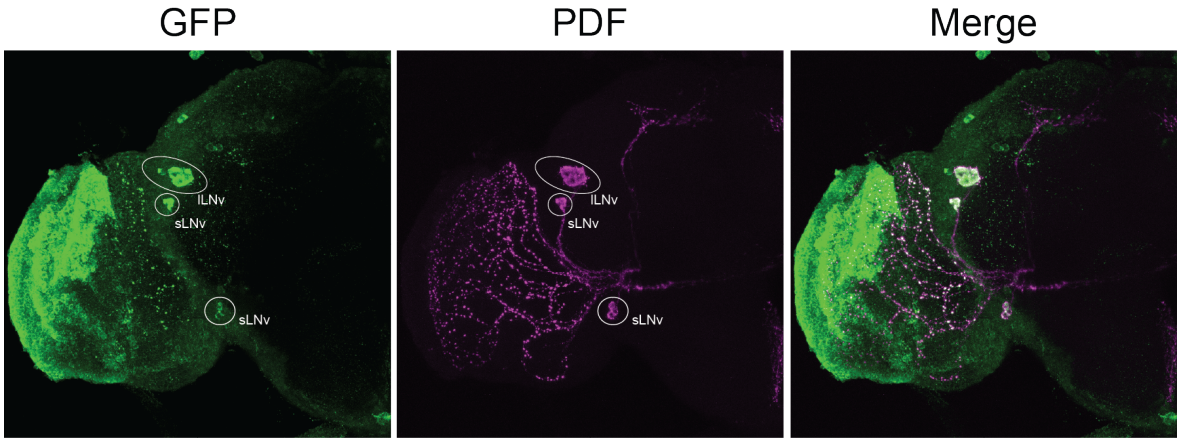

Figure 4.4. Expression of CkIIα-i1 in clock cells. Immunohistochemistry against GFP (green), PDF (magenta) in CkIIα-i1-Gal4>UAS-mCD8::GFP expressing fly brain.

4.1.4. Investigation of Postsynaptic Partners of CkIIα-i1-Gal4 Expressing Neurons by *trans*-Tango

We hypothesized that CkIIα-i1 expressing cells could have a role in learning and memory by post-synaptic interaction. Therefore, I used the *trans*-Tango system to reveal post-synaptic partners. The CkIIα-i1-Gal4 flies were crossed with flies that carry pre-synaptic and post-synaptic reporters together with *trans*-Tango transgenic elements. Pre-synaptic CkIIα-i1-expressing cells were labeled by anti-GFP antibody and an anti-HA antibody was used to stain post-synaptic cells. Additionally, anti-FasII antibody was used to label α/β lobes of the MB. Nine brains were imaged and analyzed.

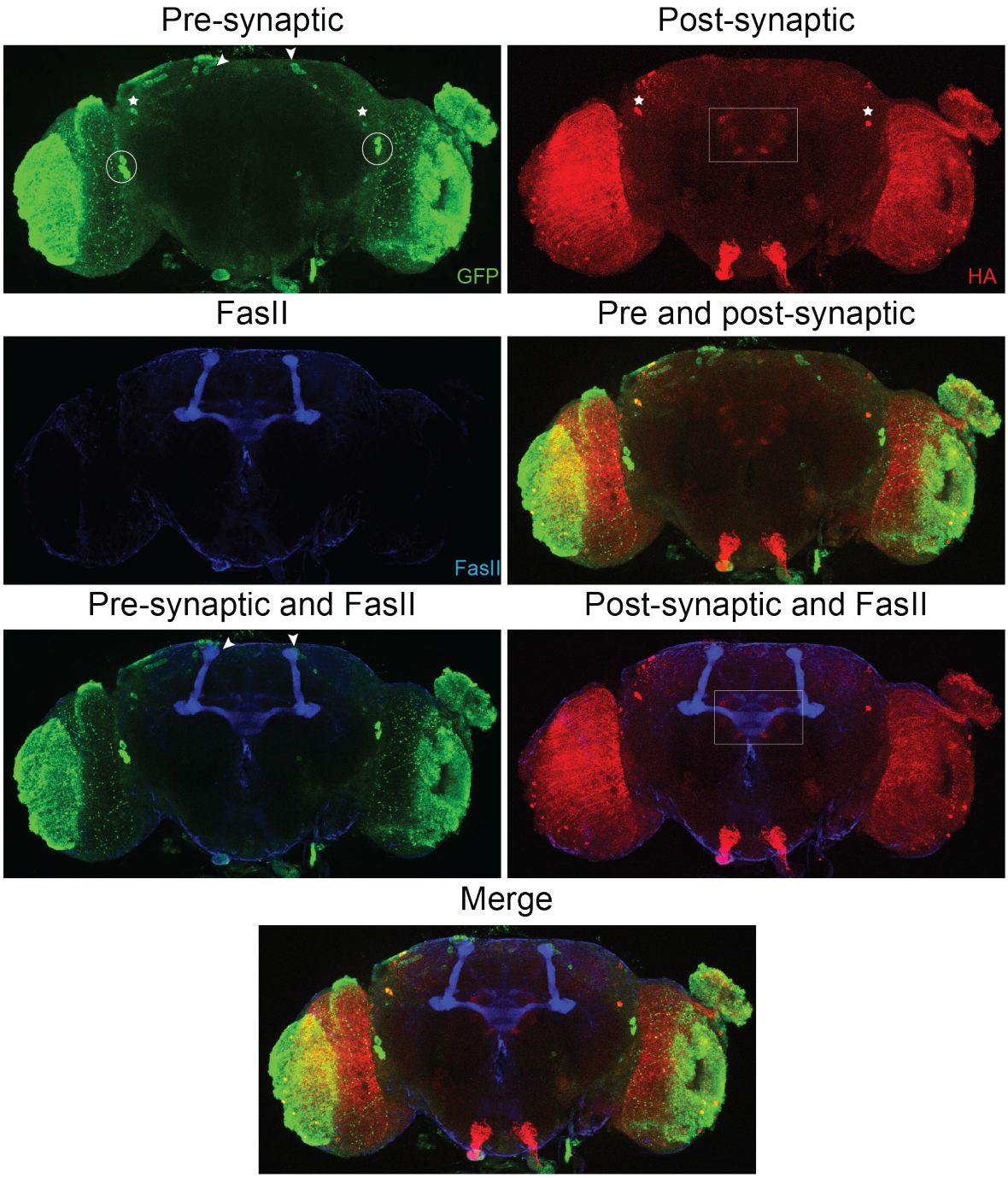

Figure 4.5. Characterization of pre- and post-synaptic CkIIα-i1 expressing neurons in the adult brain by *trans*-Tango. Immunohistochemistry in CkIIα-i1-Gal4>*trans*-Tango, UAS-mCD8::GFP, QUAS-mtdTomato-3xHA expressing fly brain.

Co-localization of FasII with either the pre- or post-synaptic cells was not detected (Figure 4.5.). However, a group of pre-synaptic dorsal cells close to the α3 lobes of the MB were clearly observed (see arrow heads). In addition, labeling of post-synaptic cells was observed in the fan-shaped body (rectangle in Figure 4.5.), which is part of the central complex and regulates sleep and learning behaviors (Liu *et al.*, 2012; Sakai *et al.*, 2012). In addition, two lateral dorsal neurons were pre- and post-synaptically labelled (indicated by stars in Figure 4.5.).

In conclusion, neither CkIIα-i1-Gal4 expressing cells nor their post-synaptic partners were found to localize to the MB. However, co-staining was observed with sLNvs and fan-shaped body neurons. Therefore, it could be suggested that CkIIα-i1 expressing cells might have a role in circadian rhythm, sleep and innate behaviors.

4.1.5. Generation of Endogenously Tagged CkIIα-i1

Gal4 lines are useful to get an understanding of the expression pattern of a gene if no other tool (e.g., antibody) is available. However, as critical enhancer/suppressor regions that lie far away from the gene of interest can be missed Gal4 lines are only meaningful, if their expression pattern can be confirmed using other tools. Thus, in order to get a better understanding of the endogenous expression of CkIIα-i1 and investigate its protein localization I aimed to endogenously tag CkIIα-i1 with a small tag (V5) using the CRISPR/Cas system and homology directed repair (HDR). The V5 (Parainfluenza virus 5 V/P tag) tag was preferred in order to prevent an effect on the three-dimensional structure of the resulting protein and the availability of antibodies against V5 that work well in immunohistochemistry. To tag CkIIα-i1 from the C-terminus a guide RNA close to the 3' end was selected and cloned into the pCFD5 plasmid to generate pCDF5_CkIIα-i1_gRNA_HDR (Table 4.1.; Figure 4.7.).

Table 4.1. Selected gRNA, its location in the genome and its off-targets.

Name	**Target locus**	**Selected sequence**	**Off-target**
CkIIa-i1_gRNA_HDR	3L: 15,817,256- 15,817,275 (+)	TGCATTTGCGAGCC-CTGCTT	None

The aim was to repair the Cas9-induced double-stranded break using the targeting construct "720921-1". The targeting construct was designed to include the sequence of the V5 tag and 1 kb homology arms upstream and downstream of the intended double-stranded break. Furthermore, the sequence corresponding to the guide RNA target site in the targeting construct was mutated without changing the predicted protein sequence of CkIIα-i1 to prevent recognition of the targeting construct by the guide RNA and its cleavage by Cas9.

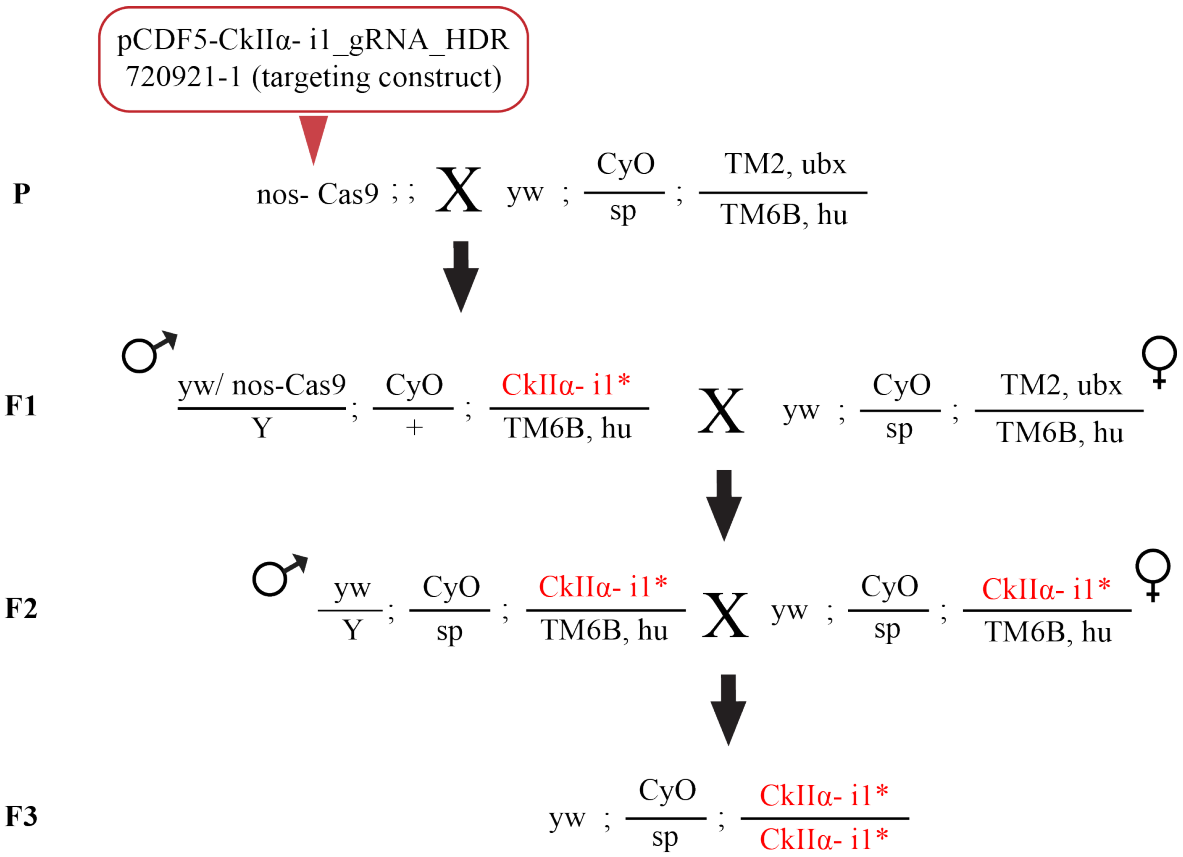

Figure 4.6. Crossing scheme of generation of V5-tagged CkIIα-i1.

The previously generated gRNA-expression vector and the targeting vector were injected into fly embryos expressing a germ cell-active Cas9 (nanos-Cas9) by the GenetiVision company. While 450 embryos were injected, only 7 of the embryos hatched. When flies reached adulthood, they were crossed twice to ywQB balancer flies to stabilize the intended genetic modification and to genetically remove nos-Cas9. F1 progenies of the injected flies (30 flies from each of the 7 injected flies, thus a total of 210 flies) were crossed with ywQB balancer flies. From these crosses only 60 were successful in producing F2 progeny. The other flies were lost during the maintenance process. The F2 progeny flies were heterozygous for the modification in CkIIα-i1. To obtain homozygous flies, these were inbred and their F3 progeny was screened by a PCR-based method (Figure 4.6.).

Genomic DNA was extracted from the F3 flies and primers CkIIα-i1-A1 and CkIIα-i1_HDR_RP_2 flanking the homology arms were used to amplify the sequence containing the intended modification (Table 3.5.; Figure 4.7.). The primers were expected to amplify 2519 bp in flies carrying the wild-type (unmodified) sequence or 2561 bp if the intended modification was obtained. Since the size of the amplified fragments was too close to detect the modification in agarose gels, I decided to analyze the amplified fragment by restriction digestion. Analysis of the amplified sequence in Snapgene showed that the restriction enzyme *HaeIII* is able to differentially digest the fragments due to an additional restriction site within the V5 sequence. The expected sizes of restriction products of the wild-type PCR fragment were 23, 193, 296, 429, and 1370 bp, while the expected sizes of restriction products of the modified fragment were 23, 193, 294, 296, 429, and 1118 bp. The 1370 bp and 1118 bp fragments were used to differentiate between the sequences of wild-type and modified fragments (Figure 4.7.A). The amplified fragments were digested with *HaeIII* and analyzed in a 1% agarose gel (Figure 4.7.B). All 60 fly lines were analyzed, however from the restriction patterns no pattern representing the modified version of CkIIα-i1 was detected.

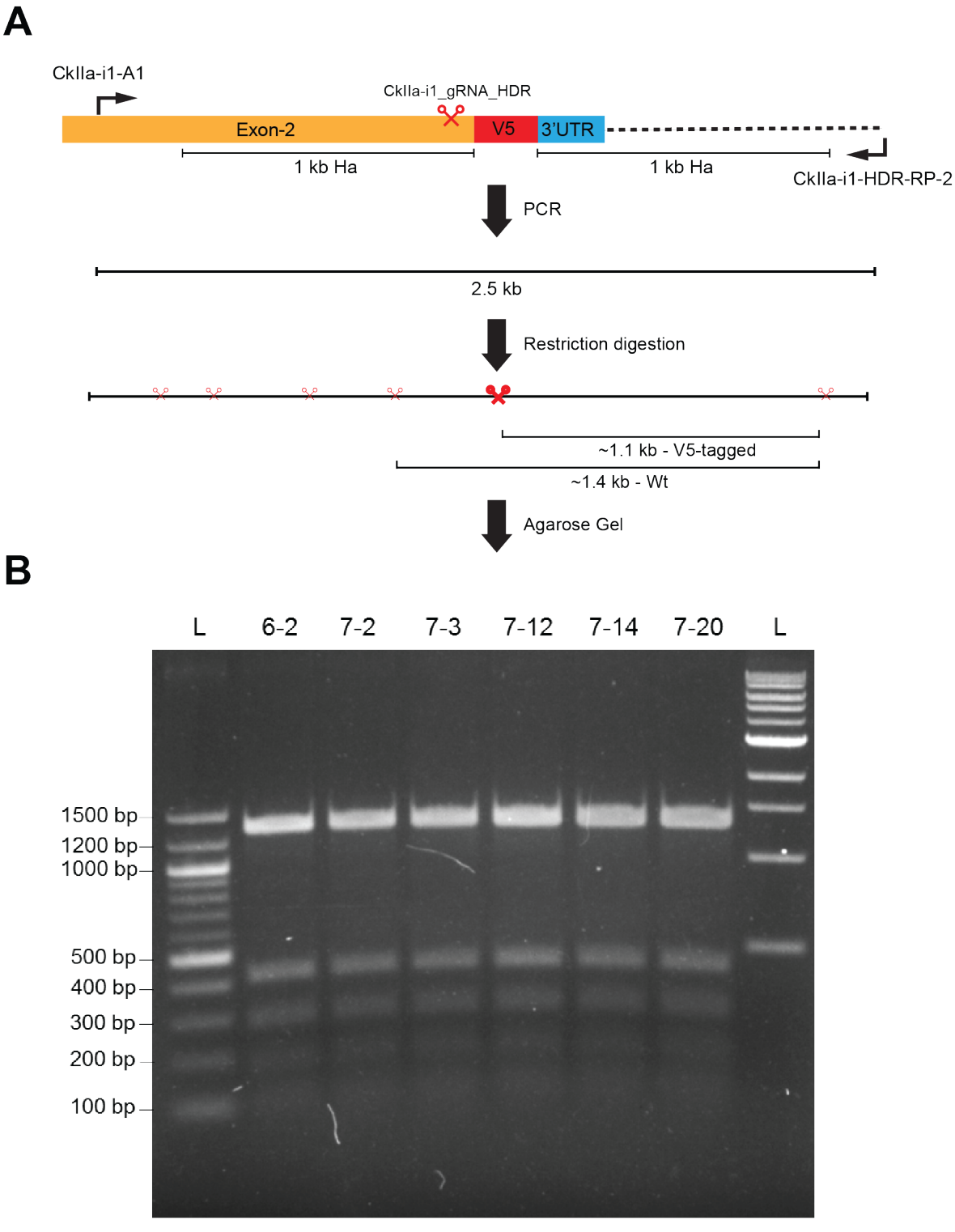

Figure 4.7. Scheme and a electropherogram of molecular screening of V5 tag insertion. A. The scheme shows amplified primers, analysis of restriction digestion, and expected band sizes. B. a electropherogram of restriction digestion products.

4.1.6. Investigation of Tagged CkIIα-i1 BAC Line in MB and Pacemaker Cells

Bacterial artificial chromosomes (BAC) allow the investigation of a gene–of–interest together with its regulatory sites after modification in bacteria and subsequent insertion into the genome. A BAC clone of CkIIα-i1 including intergenic regions, 5' and 3' UTRs and its CDS (CH322-72N9) was generated previously (Venken *et al.*, 2009). Later, a sfGFP-Tag:FLAG-Tag:CS(PSP)-Tag:CS(TEVp)-Tag:BLRP tag cassette was introduced to the 3' end of CkIIα-i1 by another group and the tagged BAC clone was integrated into the second chromosome (Kudron *et al.*, 2017). This fly line was recently made available through the Bloomington *Drosophila* Stock Center (BL 92307). The fly line was ordered and used for investigation of the expression pattern of CkIIα-i1 protein in the fly brain.

The brains of flies homozygous for the BAC construct were dissected and stained with anti-FLAG antibody. Localization of CkIIα-i1 was analyzed in the MB and pacemaker neurons by utilizing anti-FasII or anti-PDF antibodies (Figure 4.8.A and B). Four brains were analyzed for each experiment.

The co-localization analysis showed that CkIIα-i1 was co-localized around the MB. It even looked like there is co-localization within the MB. Individual analysis of Z-stacks revealed that CkIIα-i1 localized nearby MB and appeared to cover the α lobes and peduncles of the MB.

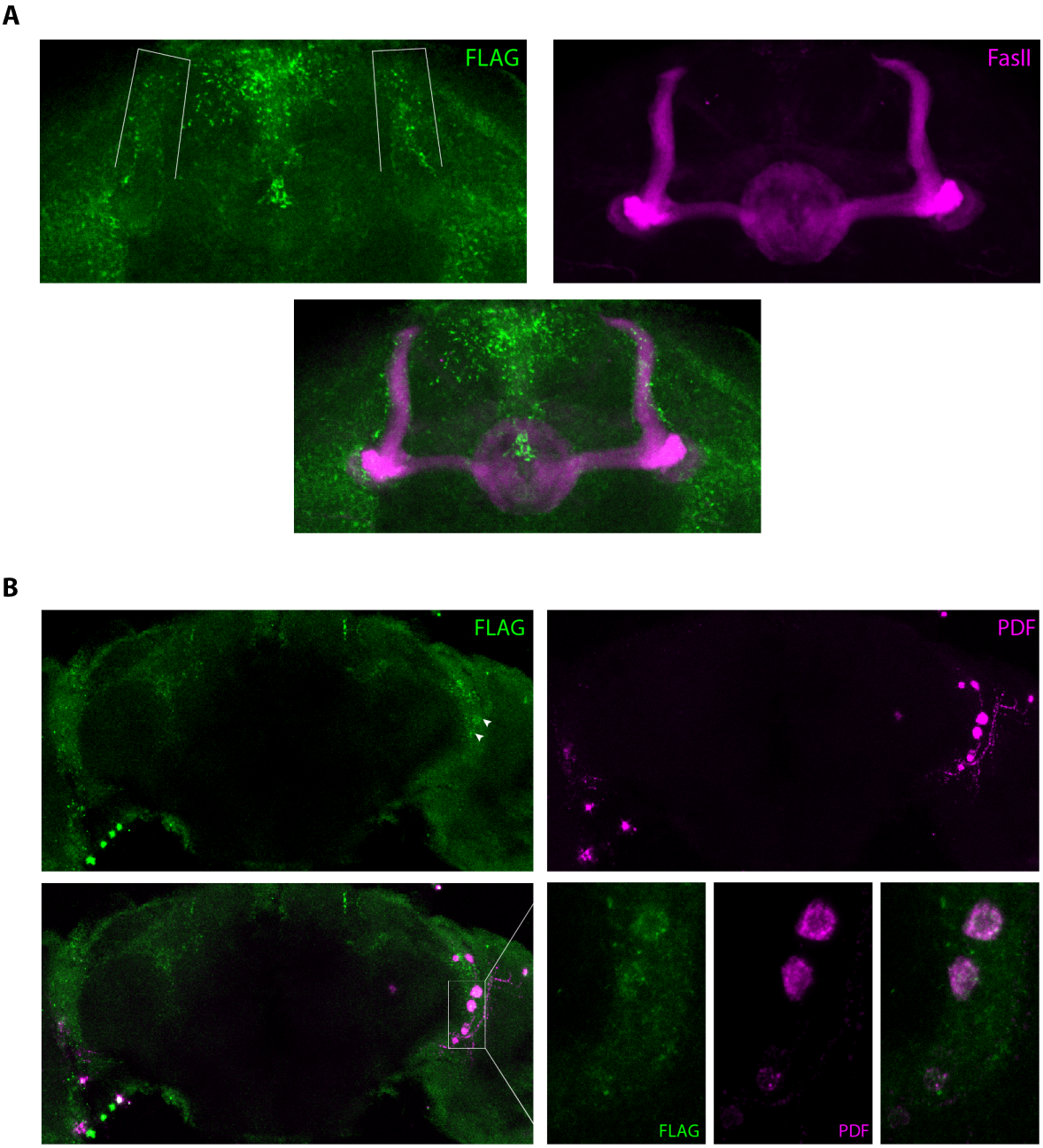

Figure 4.8. Localization pattern of CkIIα-i1 in MB and in LNvs. A. Immunohistochemistry against FLAG (green), FasII (magenta). B. Immunohistochemistry against FLAG (green), PDF (magenta).

4.2. Loss-of-Function Analysis of Knockdown of CkIIα-i1 in Morphological Changes of MB

During the examination of the expression and localization of CkIIα-i1, a group of Kenyon cells was found to be expressing CkIIα-i1 (see result 4.1.3). This suggested that CkIIα-i1 might really have a role in the MB. Therefore, in order to evaluate the function of CkIIα-i1 in MB, the effect of CkIIα-i1 knockdown in MB on the morphology of MB was analyzed. OK107-Gal4 is a previously established MB-specific Gal4 line which drives the expression in α/α', β and γ lobes and in their corresponding cell referred as Kenyon cells (Lee *et al.*, 1999). OK107-Gal4 lines were crossed with UAS-mCD8::GFP reporter flies to make the expression observable in fly brains.

OK107-Gal4, UAS-mCD8-GFP line was crossed with two transgenic CkIIα-i1 RNA interference (RNAi) lines: UAS- CkIIα-i1^{53025} (BL 53025) and UAS- CkIIα-i1^{60102} (BL 60102), which target different regions in the mRNA of CkIIα-i1 by short hairpin RNAs. Two separate RNAi lines were utilized because of diminishing effects of off-targets during analyzing function of CkIIα-i1. The w^{1118} line was crossed with OK107-Gal4, UAS-mCD8-GFP and used as a control. Both the control and the experimental flies were heterozygous for all of the constructs. Their brains were dissected and stained with anti-GFP and anti-FasII antibodies. While the OK107-Gal4 line drives expression of mCD8-GFP in α/α', β and γ lobes, labelling of FasII covers α, β and γ lobes in the MB. Therefore, differentially stained α' lobes could be identified by comparing the GFP and FasII labeling. For the analysis, 19 and 16 brains for UAS-CkIIα-i1^{53025} and UAS-CkIIα-i1^{60102} lines were analyzed, respectively. As a control, the wild-type w^{1118} line was used and 51 brains were imaged by confocal microscopy (Figure 4.9.).

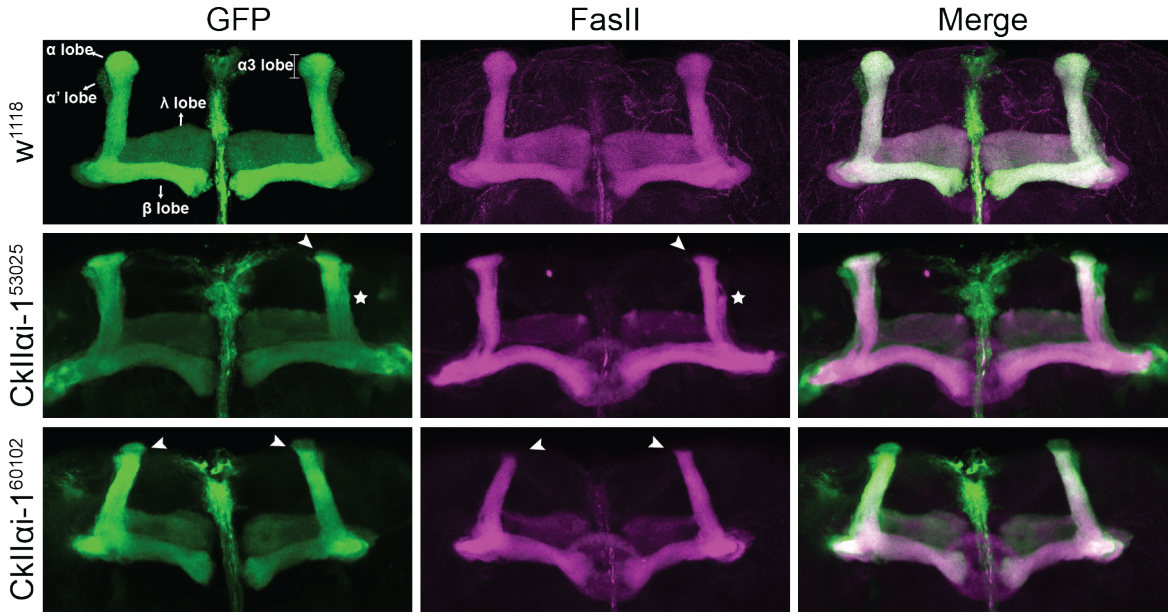

Figure 4.9. MB-specific knockdown of CkIIα-i1 by RNAi. Immunohistochemistry in OK-107-Gal4>UAS-CkIIα-i1^{53025} and UAS-CkIIα-i1^{60102} expressing fly brains.

Down-regulation of CkIIα-i1 by RNAi using two different lines caused shortening of the most distal part of the α lobe, the α3 lobe. In case of the CkIIα-i1^{53025} line 44% of analyzed α3 lobes, whereas 37% of all α3 lobes from the CkIIα-i1^{60102} line displayed this phenotype. The severity of the shortening was similar to the representative images shown in Figure 4.9, where the shortening of α3 lobes is indicated by arrow-heads. In addition, α' lobes were analyzed by comparison of the GFP and FasII images and it was shown that a ventral section of α' lobe was stained by anti-FasII in the CkIIα-i1^{53025} line with 15% frequency. This could be a result of misguidance of a group of α lobe axons or/and ectopic expression of FasII in α' lobes (indicated by a star in Figure 4.9.).

To sum up, the phenotype of shortened α3 lobes was shared with different frequencies in both RNAi lines tested. The differences in penetrance of the two lines could cause differences of the phenotypes. In order to better understand loss-of-function phenotypes of CkIIα-i1, I generated and utilized genomic CkIIα-i1 KO mutants.

4.3. Molecular and Functional Characterization of CkIIα-i1 KO Mutants

4.3.1. Generation of CkIIα-i1 KO Mutants by using CRISPR/Cas Genome Editing Technology.

In order to deplete the function of CkIIα-i1, I chose to disrupt the genomic sequence by creating a frame-shift mutation using the CRISPR/Cas system. While exogenous administration of gRNA and Cas9 both in the DNA and RNA form is possible, I decided to transgenically express gRNAs and Cas9 in order to increase their stability and efficiency (Gratz *et al.*, 2014). A germ cell-active Cas9-expressing transgenic fly line (nos-Cas9) is available at the Bloomington *Drosophila* Stock Center and was ordered for this experiment. To generate a gRNA-expressing transgenic fly line two gRNAs targeting CkIIα-i1 were selected by the CRISPR Optimal Target Finder tool (targetfinder.flycrispr.neuro.brown.edu/). Among fifty-one candidate gRNA-target sequences, two gRNAs were chosen according to their off-target score, location and feasibility for molecular identification of targeted events by a PCR-based analysis. gRNA1 and gRNA2 were located in the second exon of CkIIα-i1 (Table 4.2; Figure 4.10.A).

Table 4.2. Selected gRNA, its location in the genome and its off-targets.

Name	**Target locus**	**Selected sequence**	**Off-target**
gRNA1	3L: 15,817,256-15,817,275 (+)	TGCATTTGCGAGCCCT-GCTT	None
gRNA2	3L: 15,817,697-15,817,716 (-)	CGGCAATAGTAGACCG-GATT	None
Bl_gRNA	3L: 15,817,133-15,817,152 (-)	AAGTCTTTGCAGCAGTT-TAT	None

Two guide RNAs were chosen in order to increase the probability of having double-stranded breaks. Selected gRNAs were cloned by PCR into pCFD4 vector (by Anastasia Fokina), a expression vector designed to concomitantly express double gRNAs using two subtypes of the ubiquitous U6 snRNA promoters (Port *et al.*, 2014).

The pCFD4 vector carrying the two guide RNAs was injected into 250 fly embryos and integrated into the VK1 landing site on the second chromosome by the GenetiVision company. Three transgenic lines were generated and delivered to us.

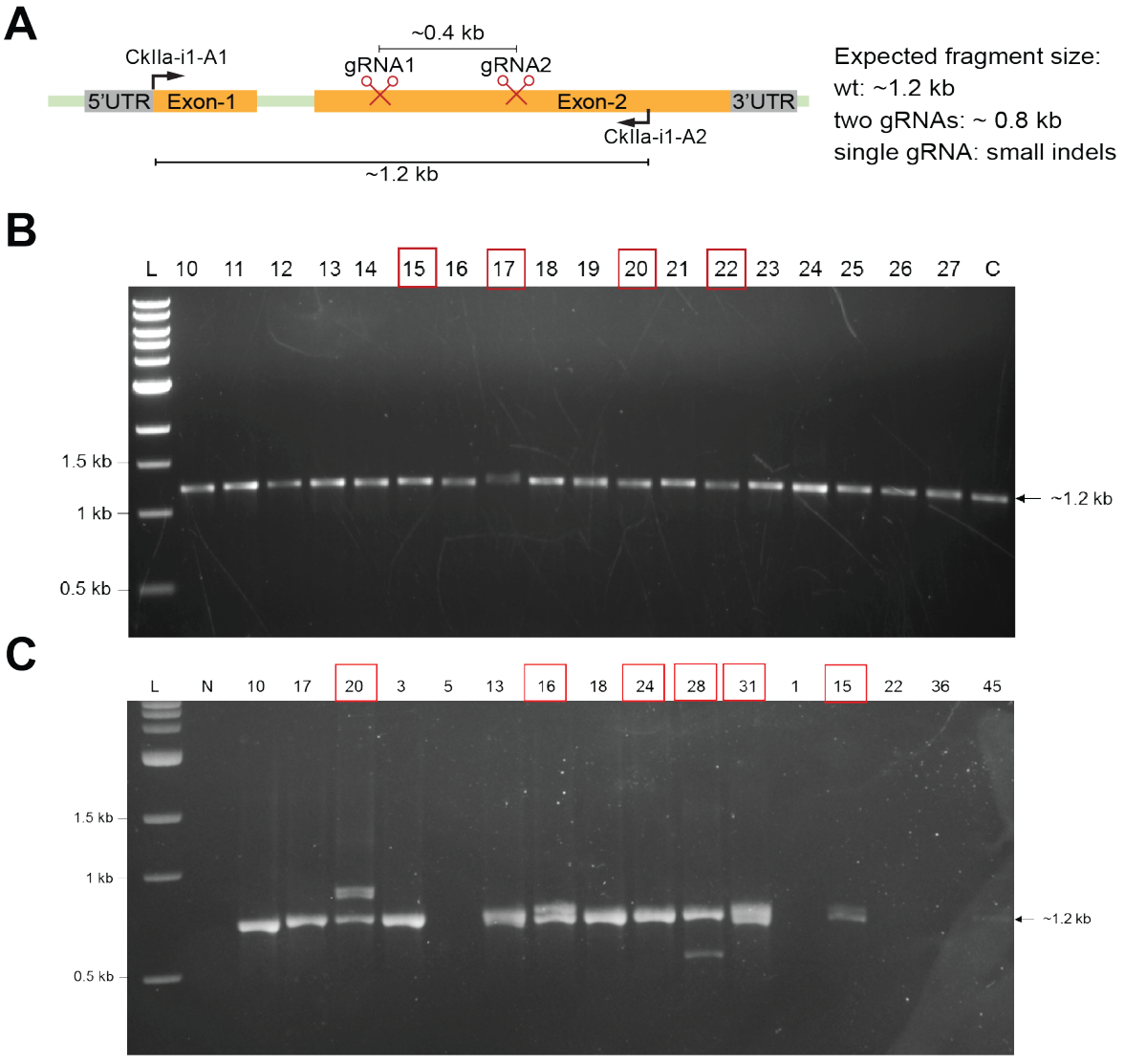

Figure 4.10. Scheme and a electropherogram of F2 and F3 generation screening of the CkIIα-i1 KO mutants generated by the gRNAs expressing line. A. The scheme shows steps of the screening B. a electropherogram belongs F2 and C. F3 generations.

Then, the generated gRNAs-expressing male flies were crossed with female flies that transgenically express Cas9 in their germ cells (nos-Cas9, BL #54591). Potential mutations are expected in the germ cells of the F1 generation expressing both the two gRNAs and Cas9. However, the putative mutation should be stabilized since DSBs might result in mosaic mutation and repair of DSBs in both alleles might result in different modifications (biallelic mutation). In addition, transgenic gRNAs and Cas9 expression might cause undesired toxic effects in the next generations. Thus, in order to both maintain the stability and remove the transgenic constructs, 76 single males from F1 generation were crossed with female flies with the ywQB fly line.

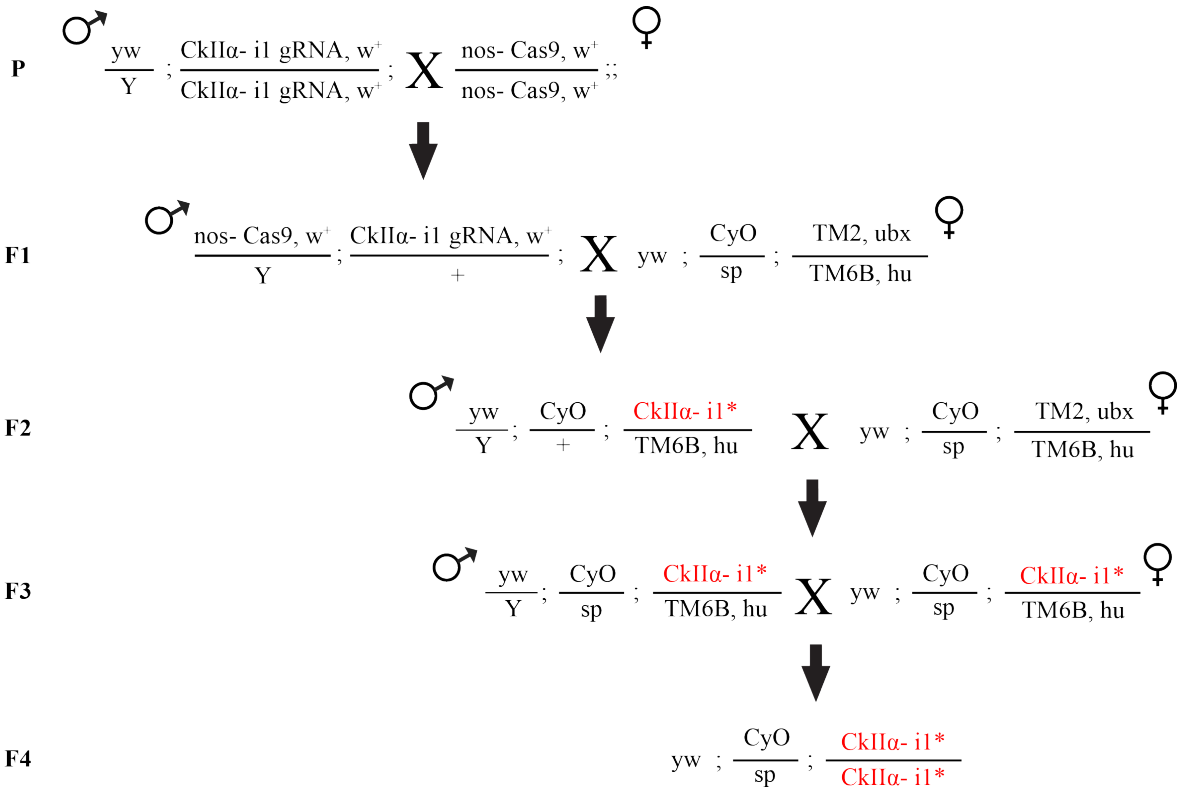

Figure 4.11. Crossing scheme of the CkIIα-i1 mutants generation.

While the white marker was used to identify removal of the transgenic constructs, TM6b balancer was used to maintain the putative stable mutation in ywQB fly line. TM6b balancer carries the humeral marker that can be identified by additional bristles on the humeral part of adult flies.

Each 76 different F2 generation fly lines a single male fly was selected if they had additional humeral bristles and counter-selected to w^+ eye color (Figure 4.11.). The selected single male flies were crossed with female ywQB flies for expansion of the fly lines.

DNA samples from F2 flies carrying putative mutant CkIIα-i1 alleles were screened using PCR (Figure 4.11.). The primers CkIIα-i1-A1 and CkIIα-i1-A2 used in this analysis were designed to amplify the region of the potential mutation (Figure 4.10.A). The amplified DNA fragments were analyzed in 1% agarose-gels (Figure 4.10.B). Since the F2 flies should be heterozygous and carry both wild-type and altered alleles, it was expected to observe two bands of different size. If the intended deletion occurred as a result of repair of two DSBs, it was expected to observe two bands: $\sim$ 1.2 kb band corresponding to the wild type allele and $\sim$ 0.8 kb band corresponding to the altered allele. In case only one of the intended DSBs occurred, small indel mutations were expected to happen, which would appear as a band close to the size of the wild-type allele band. Because no band around $\sim$ 0.8 kb was observed, we assumed that the two simultaneous DSBs did not occur. However, smear-like bands were observed in 16 candidate mutant lines 4 of which were labelled with red squares in Figure 4.10.B. Since detection of the small indel mutations in 1% agarose-gels was difficult, the PCR products were resolved in a 2% agarose gel and 6 candidate mutants were selected (red squares, Figure 4.10.C). The PCR products of 6 lines were sequenced with the same primers as were used for analysis (Table 3.5). Chromatograms obtained after sequencing contained heterozygous (double) peaks in the region of the mutation and the Inference of CRISPR Edits Analysis tool (ice.synthego.com) was used to predict altered nucleotides by comparing the chromatogram from the potential mutants with the chromatogram from the wild-type fly. According to the analysis, 6 candidate mutants were predicted to have frame-shift mutations. The F3 generation of 6 candidate frame-shift mutant lines were inbred and their progeny was selected against the humeral marker. Only one of the 6 candidate mutant lines was homozygous viable and the amplified fragment of the homozygous mutant allele was sequenced. Analysis of the sequencing results revealed that the mutant had 5 nucleotides deletion and 147 nucleotides insertion close to gRNA1-induced DSB site.

The deletion and insertion was analyzed in silico in Snapgene, a frame-shift mutation was predicted to result in an early stop codon which is at amino acid 110th, p.(Pro55LeufsTer110). The line was named as CkIIα-i1^{M20} mutant (Figure 4.12.).

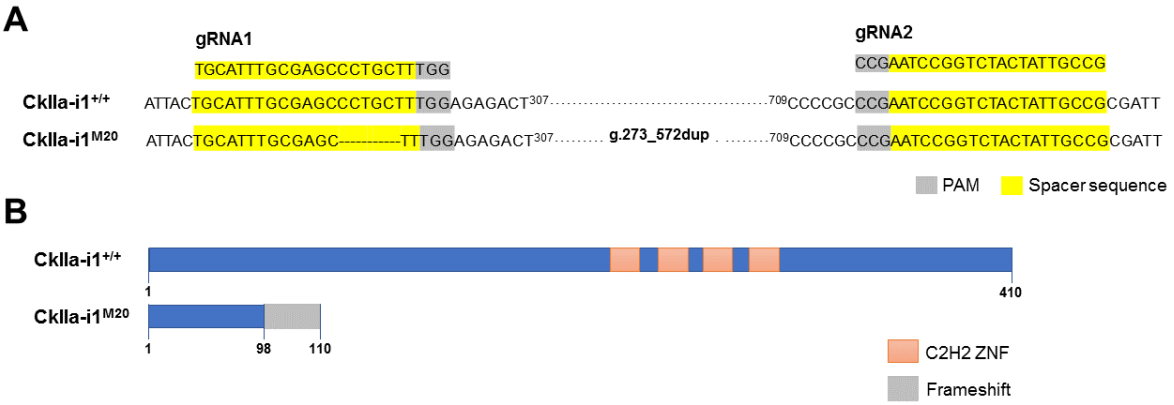

Figure 4.12. Scheme of genomic and protein level representation of CkIIα-i1^{M20} line. A. Genomic level and B. Protein level comparison of CkIIα-i1.

As previously mentioned, when gRNAs were designed, no off-target activity was predicted. Even though the prediction of off-targets gave reliable results in several studies, CRISPR/Cas system is known to create unpredicted off-targets (Iseli *et al.*, 2007). Therefore, comparing the phenotypes of mutant fly lines which were generated with different gRNAs targeting different sites of the same gene would be helpful to determine whether the observed phenotype was a result of the disruption of the intended locus or an off-target activity. While we were generating CkIIα-i1 mutant lines using the transgenic gRNAs-expressing line which was generated in our lab, another transgenic gRNA-expressing fly line which targets the first exon of CkIIα-i1 was generated by another research group (Kudron *et al.*, 2018) and became available in the Bloomington Stock Center (BL 83949). We named this line as BL_gRNA. No off-target activity was predicted for the gRNA from this line (Table 4.2). Therefore, we decided to generate a mutation in the first exon of CkIIα-i1 using the BL_gRNA line.

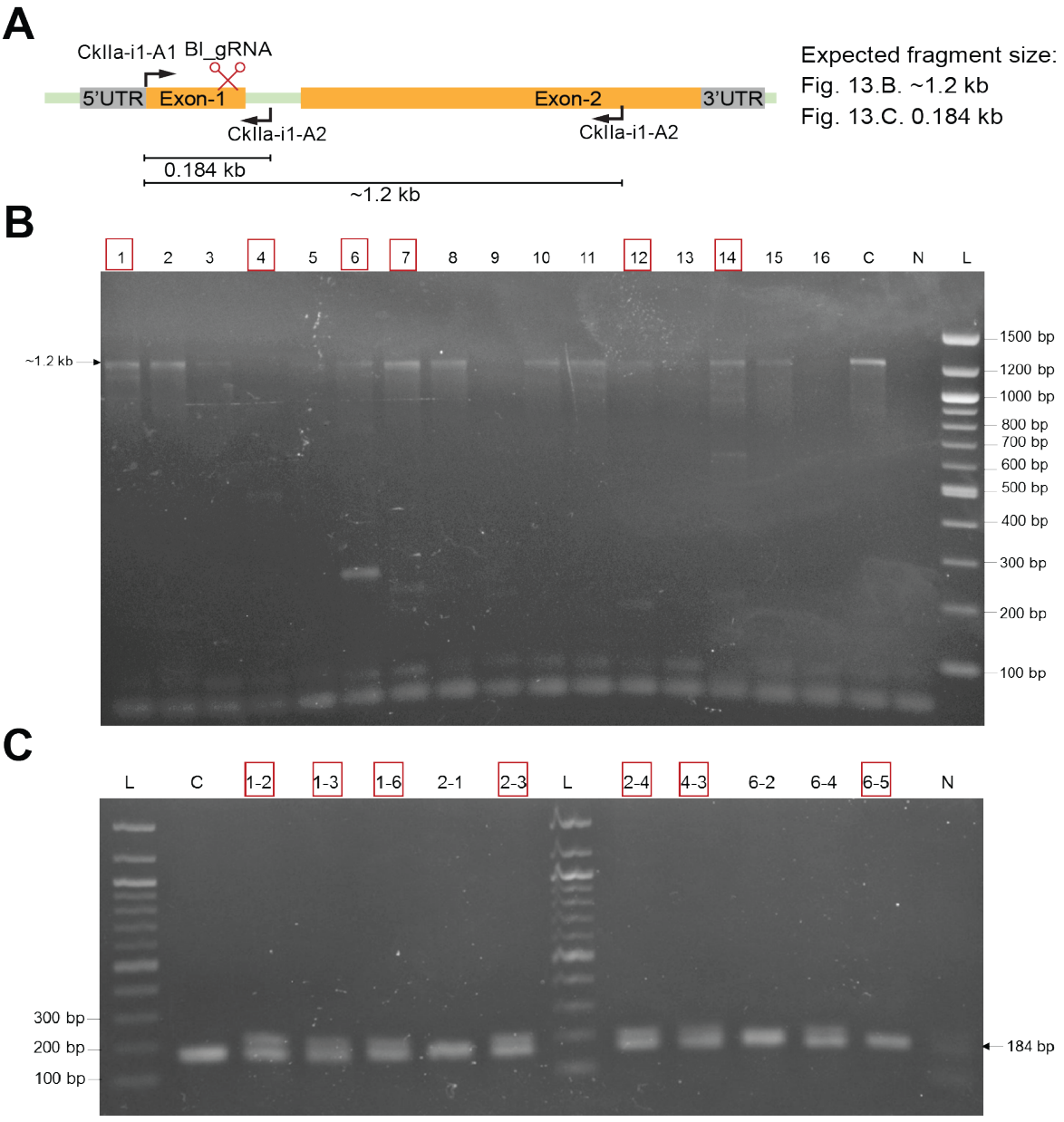

Figure 4.13. Scheme and a electropherogram of F2 and F3 generation screening of the CkIIα-i1 KO mutants generated by the BL_gRNA expressing line. A. The scheme shows steps of the screening B. a electropherogram belongs F2 and C. F3 generations.

It has been shown that NHEJ can create biallelic mutations in the intended locus of the F1 generation flies (Port *et al.*, 2014). In order to examine these putative mutations, F1 generation flies were screened (Figure 4.11). I decided to screen for the putative mutation in flies of the F1 generation using DNA from their wings in order to use the same flies for the generation of the F2 generation. Therefore, wings of 16

single males from the F1 generation were dissected and the wings were used to extract DNA.

Two primers, CkIIα-i1-CDS-FP and CkIIα-i1-A2, flanking the site of the putative mutation were used in the PCR-based screening (Table 3. 5; Figure 4.13.A). The amplified DNA fragments were analyzed in 2% agarose gels (Figure 4.13.B). Since heterozygous flies should carry both wild-type and altered alleles, small indel mutations were expected to be observed close to the wild-type band. PCR products of different size than the corresponding wild-type band were observed in 6 candidate mutant lines (Figure 4.13.B). Therefore, the 6 candidate mutant males were crossed with ywQB females. However, among these 6 candidates BL_M6, BL_M7 and BL_M14 lines showed more than two bands, which indicates the existence of mosaic mutations since independent mutation can be created in the cells which divided from different pluripotent stem cells in the eggs. In order not to lose these possible biallelic and/or mosaic mutations, 6 single F2 generation male flies generated from each of the 6 candidate mutant lines were selected and crossed with ywQB females. The F3 generation of the 36 candidate mutant lines were inbred and homozygous viable mutant lines were selected against humeral marker. 21 candidate mutant lines were screened by a PCR-based analysis (Figure 4.13.C). CkIIα-i1-CDS-FP and CkIIαi1_Bl_gRNA_RP primers were used to narrow down to the intended mutation site (Table 3.5; Figure 4.13.A.). 14 out of 21 lines have been found to be heterozygous for the mutation (Figure 4.13.C). The mutant alleles of five out of the 14 lines were subjected to sequencing. Analysis of sequencing results revealed that one of the five lines had a 13-nucleotide deletion close to BL_RNA-induced DSB site. In silico analysis of this sequence on Snapgene predicted a frame-shift mutation that results in an early stop codon at amino acid 58 (p.Asn29LysfsTer58). This candidate mutant was named CkIIα-i1^{M16} (Figure 4.14).

Canonically, a premature stop codon results in the degradation of the mRNA via nonsense-mediated mRNA decay (Hentze and Kulozik, 1999). However, Due to absence of a specific antibody for CkIIα-i1, we could not analyze the presence of CkIIα-i1. The CkIIα-i1^{M20} and CkIIα-i1^{M16} mutant lines were subjected to further examination.

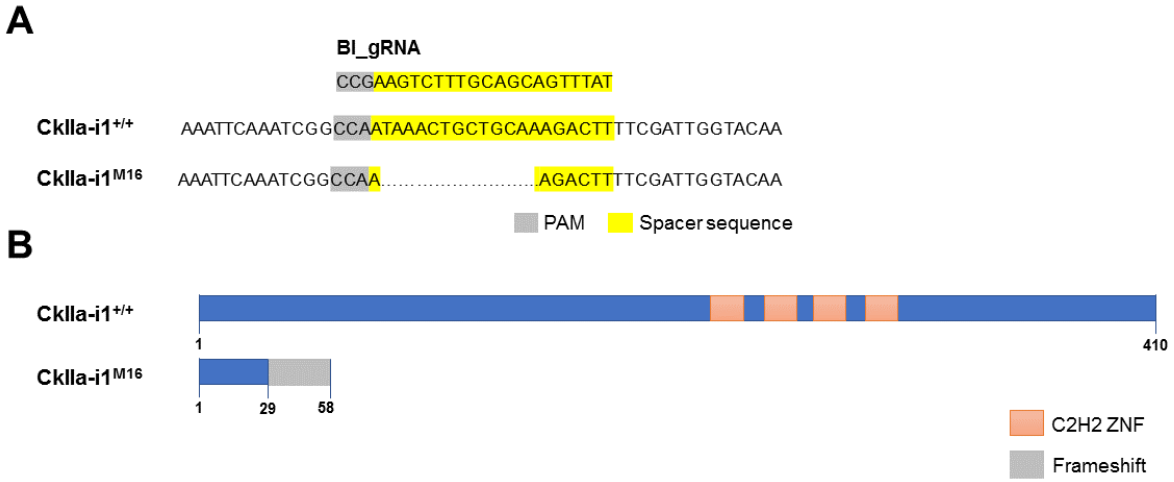

Figure 4.14. Scheme of genomic and protein level representation of CkIIα-i1^{M16} line. A. Genomic level and B. Protein level comparison of CkIIα-i1

In order to decrease mutation-independent phenotypes which could be observed in the tested different genomic background control and experimental flies (Kammenga, 2017), the mutant lines CkIIα-i1^{M20} and CkIIα-i1^{M16} were crossed twice with a balancer line (BL 24640) to isogenize the X and second chromosomes. The balancer line which was isogenic with w^{1118} (BL 5905) for X, and second chromosomes. Both the balancer line and w^{1118} was tested for common morphological and behavioral analyses.

4.3.2. Investigation of Functional Role of CkIIα-i1 by Morphological Analyses in MB.

The morphology of MB of homozygous mutant alleles of CkIIα-i1^{M20} and CkIIα-i1^{M16} was analyzed by FasII staining in the adult *Drosophila* brain. For the CkIIα-i1^{M20} line, both larval and adult brains were stained to observe whether the morphological alteration in MB has occurred during development from larvae to adult or already established during early development.

13 larval brains from each the w^{1118} (wild-type) and CkIIα-i1^{M20} lines were analyzed (Figure 4.15.). Mushroom bodies consist of axonal extensions of γ, α' and β' Kenyon cells in the late third instar larvae and when the mushroom body morphology of the larvae was analyzed, it was no morphological changes in the MB were observed.

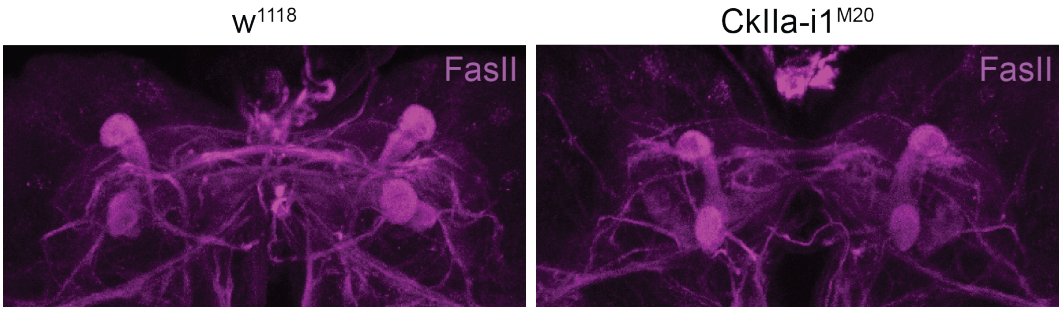

Figure 4.15. Larval mushroom bodies of CkIIα-i1^{M20} and wild-type lines. Immunohistochemistry against FasII (magenta) in CkIIα-i1M20 mutant brains.

Female and male adult brains of adult flies from CkIIα-i1^{M20} and CkIIα-i1^{M16} lines were stained and analyzed separately to follow possible sex-specific effects. In case of the CkIIα-i1^{M20} line 25 female and 34 male brains, and in case of the CkIIα-i1^{M16} line 18 female and 17 male brains were imaged by confocal microscopy and analyzed. 12 female and 52 male brains from the wild-type w^{1118} control line were used were subjected to the same analysis.

The morphology of the MB regarding the length, width, and guidance of α/β lobes was analyzed. I could not observe any significant phenotype both in CkIIα-i1^{M16} male and females. There was only a mild β lobe fusion phenotype in both sexes. However, the mild β lobe fusion was also observed in the control brains with a similar frequency. Several types of morphological changes were observed in both sexes in the MB of the adult CkIIα-i1^{M20}; however, their frequency was higher in males. Morphological changes included shrinkage and misguidance of α3 part of alpha lobe, shortage and skewing of α lobe, missing of α lobe and missing of α/β lobes. Representative examples of the observed phenotypes are shown in Figure 4.16.

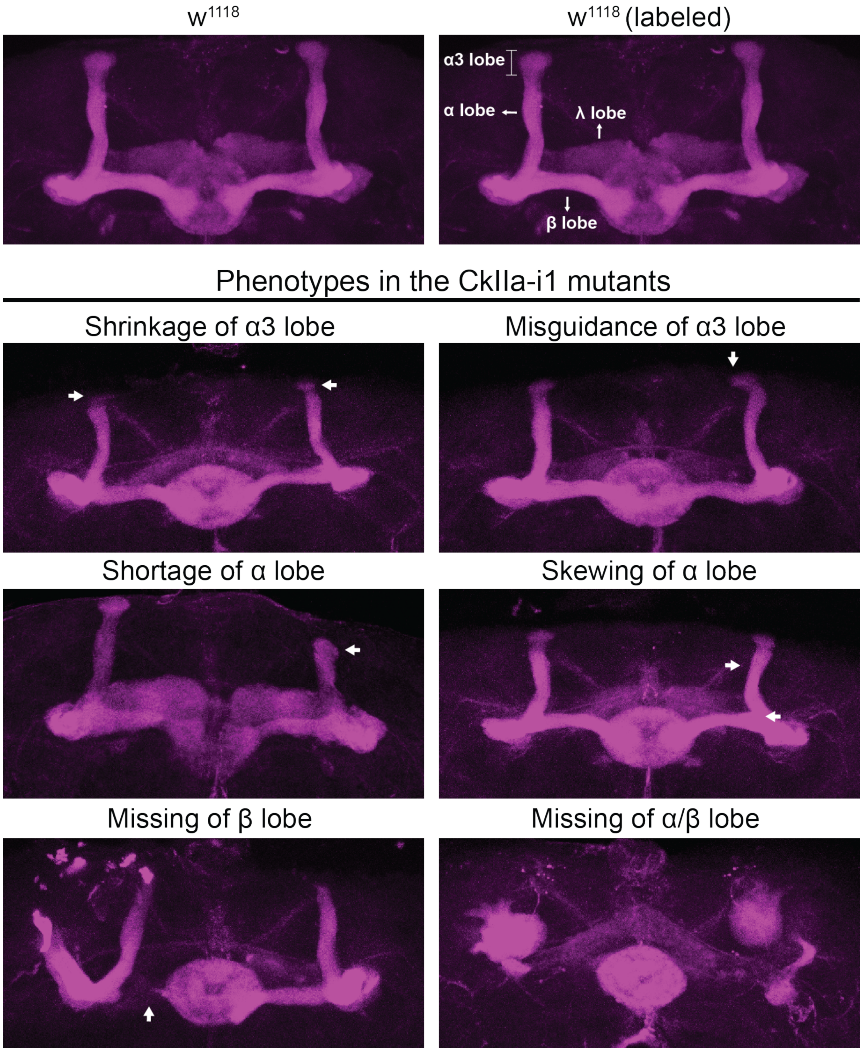

Figure 4.16. Morphological changes observed in the lobes of mushroom bodies in the mutant lines.

Quantification of the observed phenotypes showed that the most frequently observed phenotype is the shrinkage of the alpha 3 (α3) lobe (46%), followed by misguidance of the α3 lobe (24%) and skewing of the α lobe (24%) (see Table 4.3.). The listed phenotypes were also observed in the control flies and are listed in Table 4.3. However, their frequencies were lower than in CkIIα-i1^{M20}. Missing β lobes and α/β lobes was observed only in one of the brains of the CkIIα-i1^{M20} males. The severe shortage of a lobe is illustrated in Figure 4.16 and was observed in one brain each in both sexes of CkIIα-i1^{M20}. However, as I suspected a general decrease in the length of the α lobes, their length was measured and analyzed.

Table 4.3. Frequency of the observed phenotypes in both sexes of CkIIα-i1^{M20} lines.

Phenotypes	***CkII*α*-i1*$^{\mathbf{M20}}$**			***w*^{1118}**		
	Male	**Female**	**Total**	**Male**	**Female**	**Total**
Misguidance of α3 lobe	24%	25%	**24%**	10%	0%	**8%**
Shrinkage of α3 lobe	58%	19%	**46%**	4%	9%	**5%**
Skewing of α lobe	31%	6%	**24%**	8%	9%	**9%**

In order to compare the length of the α lobes, their lengths were measured and normalized to the width between the heels of the α lobes (Figure 4.17.A). As the number of the samples among the groups were not equal and the mean of the samples were not normally distributed, I utilized Welch's t-test between the groups and p values were annotated in the Figure 4.17.B. The analyses showed that while the length of α lobes was significantly shortened in CkIIα-i1^{M20} males, the length of α lobes was not changed in CkIIα-i1^{M20} females.

To conclude, morphological changes in α lobes of the CkIIα-i1^{M20} larvae were not observed. Several morphological changes were detected in the α and α3 lobes of the CkIIα-i1^{M20} adults, whereas no phenotype was observed in CkIIα-i1^{M16} males and females. While phenotypes were observed in both sexes of CkIIα-i1^{M20} their penetrance was higher in males than in females. Therefore, it is possible to suggest that CkIIα-i1 could have a role in development and maintenance of a lobes of MB in adult flies.

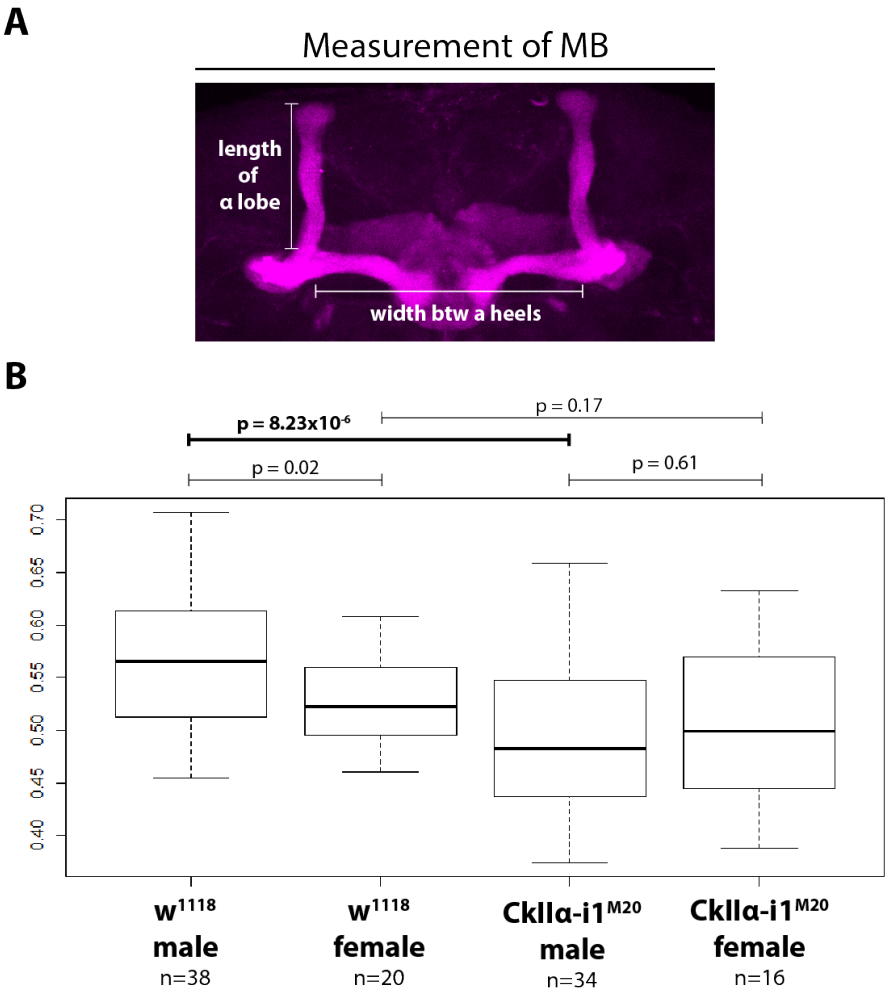

Figure 4.17. Measured lobes of MB and box plot of analysis of α lobe length of CkIIα-i1^{M20} line. A. Measured lobes of MB and B. Statistical analysis of α lobe length of CkIIα-i1M20 in both sexes.

4.4. Functional Role of MB-Specific Ectopic Over-Expression of CkIIα-i1 in MB

In the pursuit of identifying the function of a gene, different approaches aiming the disruption of a gene or its RNA product could be utilized as previously discussed in the result 4.2 and 4.3. In addition, gain-of-function experiments could also help to identify the function of a gene by providing the examination of possible phenotypes resulting from the ectopic overexpression of a gene.

Thus, MB-specific overexpression of CkIIα-i1 was performed by UAS-CkIIα-i1-HA line which was generated by cloning of the ORF of CkIIα-i1 under UAS control (FlyORF #F001872; Bischof *et al.*, 2013). The generated line expressed a canonical transcript of the CDS of CkIIα-i1 with a C terminal-fused HA tag that was used to stain CkIIα-i1. The UAS-CkIIα-i1-HA line and w^{1118} line as a control, were crossed with OK107-Gal4, UAS-mCD8::GFP which was previously utilized in knockdown of CkIIα-i1 (see result 4.3). Both control and experimental flies were heterozygous for all of the constructs. Their brains were dissected and stained with anti-GFP and anti-FasII antibodies. While OK107-Gal4 line drives the expression of mCD8-GFP in α/α', β and γ lobes, labelling of FasII covers α, β and γ lobes in MB. A total of 14 female and 10 male brains from CkIIα-i1-HA and 25 female and 31 male brains from the wild-type w^{1118} flies were imaged by confocal microscopy (Figure 4.18.).

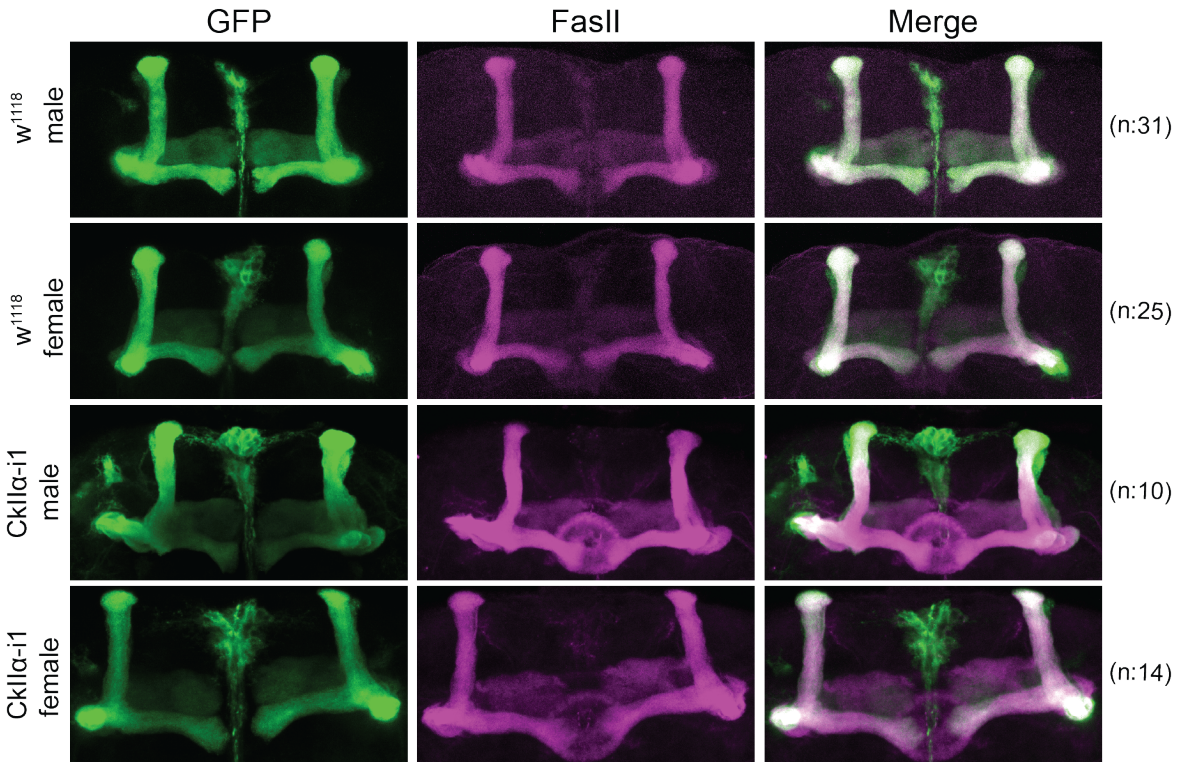

Figure 4.18. MB-specific overexpression of CkIIα-i1. Immunohistochemistry against in OK-107-Gal4>UAS-CkIIα-i1 expressing fly brains from both sexes.

I could not observe any phenotype that had been described in the loss-of-function experiments. Ectopic overexpression should result in other phenotypes. Therefore, I analyzed the images for other abnormalities in the MB, however, no changes between control and experimental brains could be observed.

4.5. Generation of ZBTB11-Expressing Flies and Validation of ZBTB11 Expression in *Drosophila*

To address the functional similarity/conservation of ZBTB11 and CkIIα-i1 in *Drosophila*, I generated fly lines expressing the wild-type form and two previously defined variants of the ZBTB11 gene (p.H729Y and p.H880Q) (Fattahi *et al.*, 2018) under control of the UAS promoter. Since there is no specific antibody to detect ZBTB11 in immunohistochemistry experiments, ZBTB11 was tagged with a hemagglutinin (HA) tag. Newly generated fly lines were crossed to actin-Gal4 flies in order to express ZBTB11 ubiquitously and its expression was analyzed using Western blotting. Then, ZBTB11 variants were expressed under the control of CkIIα-i1-Gal4 and their localization was analyzed in the *Drosophila* adult brain using immunohistochemistry.

4.5.1. Generation of Transgenic ZBTB11-Expressing Fly Lines

The wild-type and two variants of Zbtb11 were cloned into pUASg-HA.attB destination vector using Gateway® cloning strategy (Invitrogen™). First, the gene was amplified using primers UAS-zbtb11F3 and UAS-zbtb11R3 that contain attB sequences (Figure 4.19.A., BP cloning) and the PCR products were recombined into the donor vector pDONR207. The cloning was verified using the restriction enzyme *BglII* (Figure 4.19.C). Then the insert was transferred to the destination vector pUASg-HA.attB (LR cloning) and verified by analytical digestion using the restriction enzyme *BglII* (Figure 4.19.D).

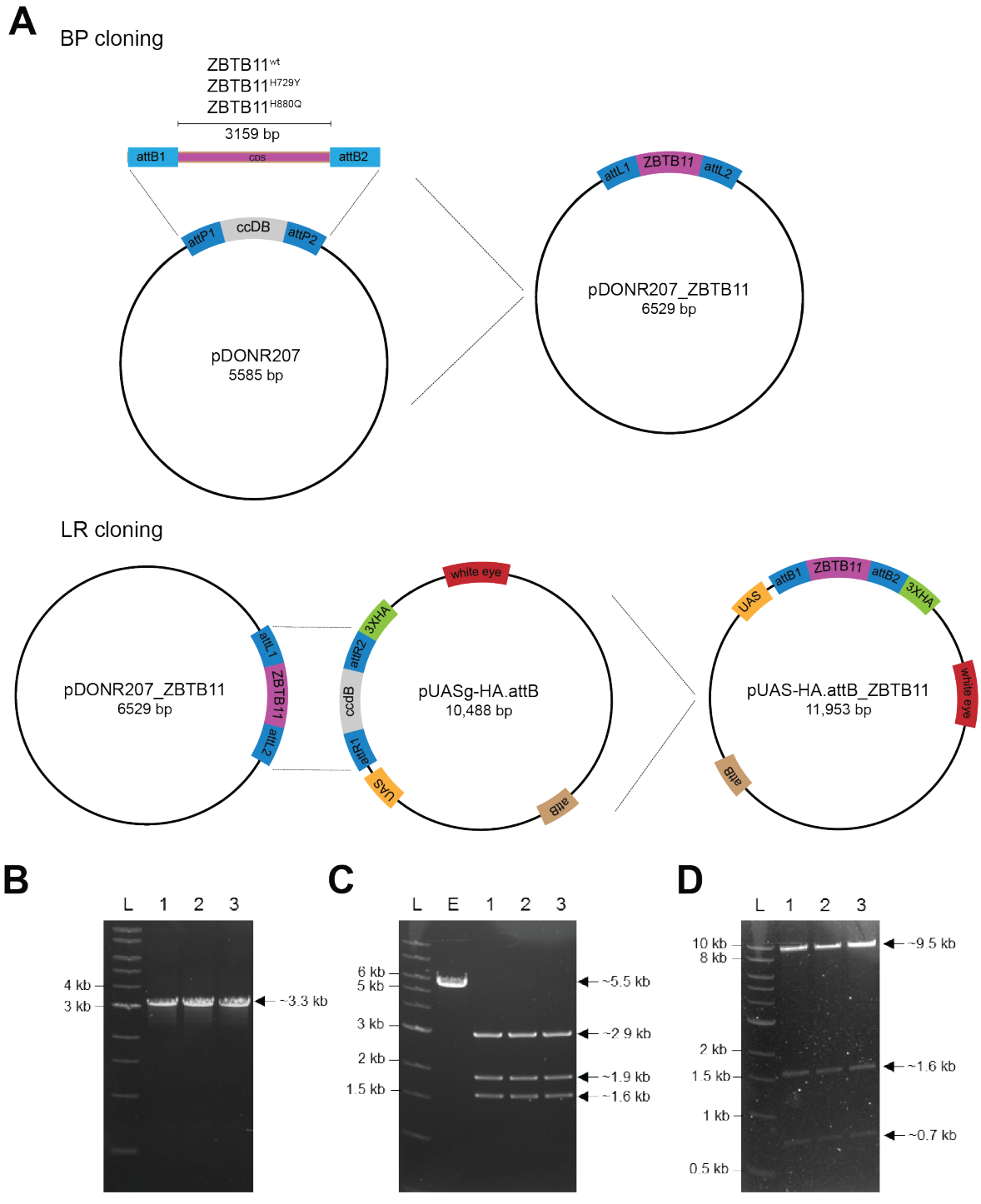

Figure 4.19. Cloning of ZBTB11 constructs. A. Representative scheme of Zbtb11 constructs by Gateway cloning. Electropherograms of B. attB-adjacent Zbtb11 fragments, C. pDONR_ZBTB11 plasmids, D. pUAS-ZBTB11-HA.attB plasmids.

Coding sequences (CDS) of wild-type and variant forms of Zbtb11 were previously cloned into pcDNA^{TM} DEST53 vector (Fattahi *et al*, 2018). These vectors were used as templates for amplification of CDSs of Zbtb11. A pair of primers UAS-zbtb11F3 and UAS-zbtb11R3 was designed to amplify Zbtb11 coding sequences by adding site-specific attB1 and attB2 recombination sites, which were flanking both sites of the template fragments. The attB sites provide site-directional recombination from the templates to the donor vector (Table 3. 5).

The PCR products (Fig 4.19.B) were purified from an agarose gel and incubated together with pDONR207 vector carrying attP1 and attP2 sites and BP clonase according to the manufacturer's instructions (Figure 4.19.A., BP cloning). The reaction products were transformed into E. coli DH5α competent cells. The plasmids were isolated from single transformants and digested with BglII restriction enzyme to analyze whether the Zbtb11 sequences were inserted in pDONR207. The restriction products of pDONR_ZBTB11_wt, pDONR_ZBTB11_H729Y and pDONR_ZBTB11_H880Q were analyzed by agarose gel electrophoresis (Figure 4.19.C) and the inserts were verified by Sanger sequencing. The primers that were utilized for sequencing are listed in Table 3.5.

As a second step of Gateway cloning, an LR reaction was performed for site-specific recombination of CDSs of Zbtb11 from the donor plasmids (pDONR_ZBTB11_wt, pDONR_ZBTB11_H729Y and pDONR_ZBTB11_H880Q) to the destination vector pUASg-HA.attB (Figure 4.19.A, LR cloning). pUASg-HA.attB is designed to express the coding sequence fused with a 3XHA tag in its 3'-terminus under control of the UAS promoter (Bischof *et al.*, 2013). In addition, it includes a site-specific integration site (attB), which can be used to integrate the vector into the fly genome that have the corresponding landing sites (attP) using phiC31-mediated integration (attB-attP-phiC31 integrase). Thus, pDONR_ZBTB11 plasmids and pUASg-HA.attB vector were incubated with LR clonase enzyme and the reaction products were transformed into E. coli DH5α competent cells. For each cloning the plasmids from two single transformants were isolated and digested with the restriction enzyme BglII to analyze whether the Zbtb11 constructs were recombined into the

pUASg-HA.attB vector. The restriction products of the three plasmids which were named pUASg-HA.attB_ZBTB11_wt, pUASg-HA.attB_ZBTB11_H729Y and pUASg-HA.attB_ZBTB11_H880Q were analyzed by agarose gel electrophoresis (Figure 4.19.D). The colonies were verified by Sanger sequencing at Macrogen company using sequencing primers listed in Table 3. 5.

After verification by sequencing, the plasmids were isolated in large scale with a midi-prep kit and sent to the GenetiVision company for injection. Each construct was injected into 250 fly embryos of a white-eyed fly strain. The pUASg-HA.attB_ZBTB11 plasmid carries the white gene as a marker for selection in *Drosophila*. Thus, the integration of the vector was detected by the presence of the red eye color provided by the white gene. Three independent red-eyed fly lines from each of UAS-ZBTB11-HA_wt, UAS-ZBTB11-HA_H729Y and UAS-ZBTB11-HA_H880Q flies were selected for further experiments. The lines were named as UAS-ZBTB11-HA_wt-1, wt-2, wt-3, UAS-ZBTB11-HA_H729Y_3, H729Y_5, H729Y_6, and UAS-ZBTB11-HA_H880Q_1, H880Q_2, H880Q_3.

4.5.2. *in vitro* and *in vivo* Characterization of ZBTB11 in *Drosophila*

Protein expression and tagging of ZBTB11 was analyzed *in vitro* by Western blotting. Transgenic UAS-ZBTB11-HA flies were used to express ZBTB11 ubiquitously in flies. Two lines corresponding to wild-type ZBTB11 and three lines corresponding to each of two mutant variants of ZBTB11 were analyzed.

UAS-ZBTB11-HA flies were crossed with the actin-Gal4 (BL 4414) fly line, which provides ubiquitous expression of ZBTB11. F1 progenies carried heterozygous actin-Gal4 and UAS-ZBTB11 constructs. The heads of six F1 adult flies were homogenized and lysed. The concentrations of total protein in the lysate of samples were equilibrated by dilution with the Laemmli buffer. 20 μg of the total protein were loaded on and resolved in an 8% acrylamide gel. After appropriate running time, the proteins were transferred to a PVDF membrane in order to detect ZBTB11 with anti-HA antibody. First, the membrane was stained with Ponceau S dye and imaged to com-

pare the amount of total protein in the samples transferred to the membrane (Figure 4.20.A). Second, the membrane was blocked and stained with HA antibody to observe the expression of ZBTB11 (Figure 4.20.B). While the lysate of wild-type Canton-S flies (N) was used as a negative control, the lysate of the previously generated endogenously HA-tagged Uzip flies was used as a positive control (P). The band corresponding to Uzip-HA (65 and 80 kDa) was not detected in the positive control probably due to the low level of expression of Uzip-HA. However, the $\sim$ 125 kDa bands corresponding to the wild type and mutant ZBTB11 were present in the lanes of the experimental samples. According to this result, wild-type and the two variants of ZBTB11 were expressed in flies in correct size.

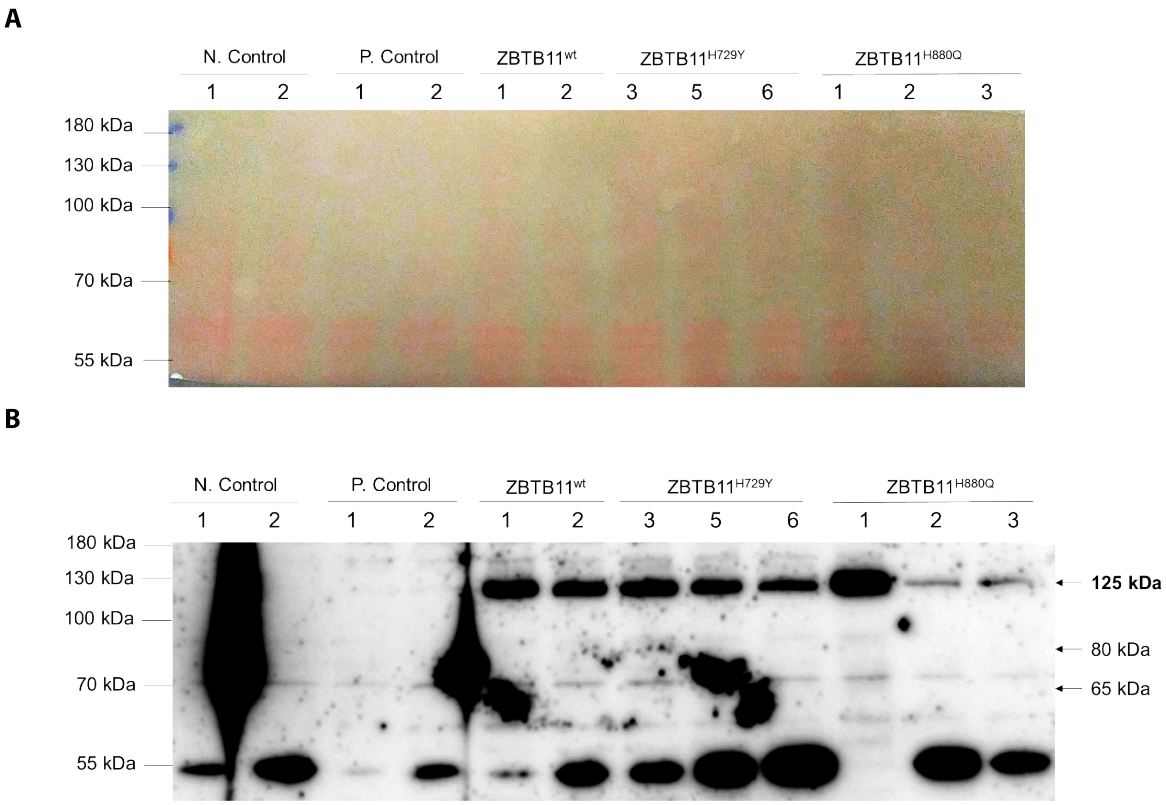

Figure 4.20. Analysis of ZBTB11-expressing flies. A. Total protein staining of the samples with Ponceau S. B. Western blotting against HA to label wildtype and variants of ZBTB11 expression in actin-Gal4>UAS-ZBTB11 expressing fly brains.

Later, I addressed the subcellular localization of ZBTB11 in CkIIα-i1-Gal4 expressing cells. Localization experiments of ZBTB11::GFP in HEK293 cells showed the localization of ZBTB11 to the nucleolus (Fattahi *et al.*, 2018).

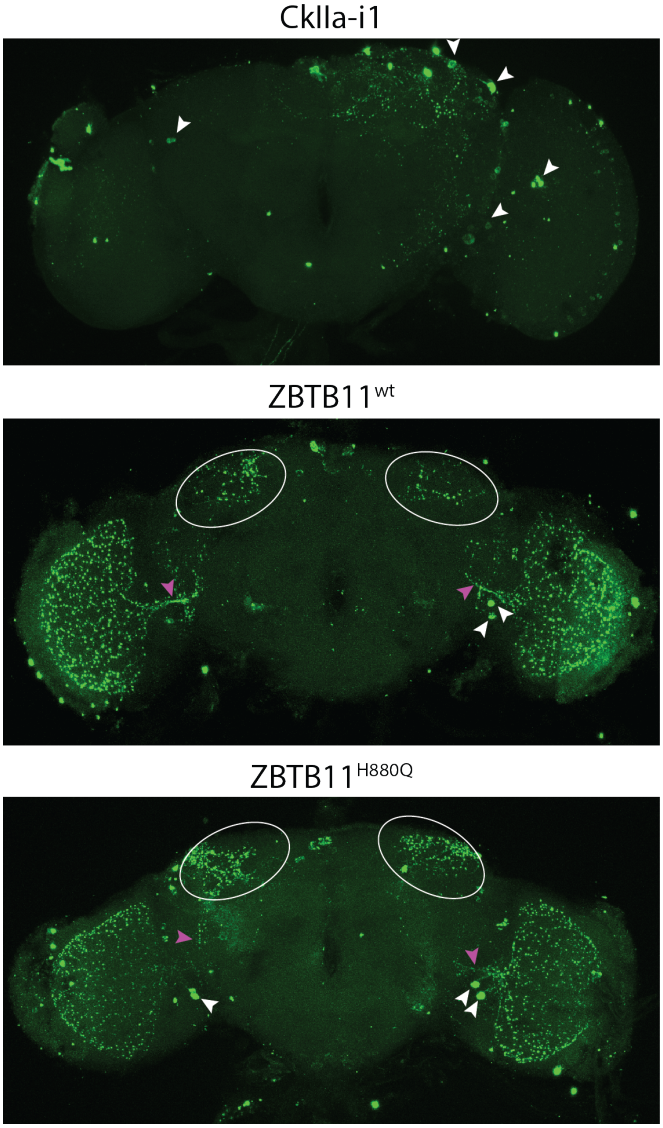

Figure 4.21. Analysis of CkIIα-i1 and ZBTB11 localization in the fly brain. Immunohistochemistry against HA (green), in CkIIα-i1 -Gal4>UAS-CkIIα-i1-HA and UAS-ZBTB11-HA^{wt} and UAS-ZBTB11-HA^{H880Q} expressing fly brains.

CkIIα-i1-Gal4 expressing cells were previously investigated in this study and their cell bodies and axonal projections were identified (see Figure 4.4). CkIIα-i1-Gal4 expression was observed in sLNVs, which have relatively long axons that are projected to dorsal cells. This gives the opportunity to observe subcellular localization. In addition, the Gal4/UAS system allows the overexpression of any coding sequence downstream of the UAS promoter. Thus, I over-expressed CkIIα-i1-HA using the UAS-CkIIα-i1-HA line and its human ortholog ZBTB11-HA in CkIIα-i1-Gal4 expressing cells to compare their subcellular localization with previously established membrane and nuclear staining of CkIIα-i1-Gal4 expressing cells.

Towards this aim, UAS-CkIIα-i1-HA, UAS-ZBTB11-HA$^{\text{wt-1}}$ and UAS-ZBTB11-HA$^{\text{H880Q-1}}$ flies were crossed with CkIIα-i1-Gal4 (Pr-2) flies and their F1 progeny, which carried heterozygous Gal4 and UAS constructs was analyzed. The F1 progeny flies were separated according to their sexes and their brains were subjected to immunohistochemical staining with anti-HA antibody (Figure 4.21.). 15 brains from UAS-CkIIα-i1-HA, 10 brains from UAS-ZBTB11-HA$^{\text{wt-1}}$, 9 brains from UAS-ZBTB11-HA$^{\text{H880Q-1}}$ were immuno-stained and the expression patterns of CkIIα-i1 and ZBTB11 proteins were analyzed. The analysis showed that while CkIIα-i1 was localized mostly in cell bodies, both wild type and H880Q forms of ZBTB11 were localized both to the cell bodies and the neurites. The cell bodies are indicated with white arrow-heads, the neurites are indicated with magenta arrow-heads, and the region corresponding to Kenyon cells is indicated with ellipse circles in Figure 4.21.

5. DISCUSSION

5.1. Expression and Localization of CkIIα-i1

5.1.1. Regulatory Elements of CkIIα-i1 and fwe Genes

The CREs, which were cloned in Gal4 constructs included an intergenic region, which was between CkIIα-i1 and flower (*fwe*) genes expressed in opposite direction of the strands. While CkIIα-i1 is expressed from the sense strand, fwe is expressed from the antisense strand. Therefore, the intergenic region could include regulatory sites of both genes as illustrated in Figure 4.1. In addition, it was shown that regulatory elements can regulate transcription both unidirectionally and bidirectionally (Rennie *et al.*, 2018). Therefore, characterization of the expression pattern of the Gal4 lines needs to be verified by analyzing endogenous expression. To exclude the fact that the cloned region contains Fwe regulatory sites the known expression pattern of Fwe was compared with the expression pattern of the CkIIα-i1-Gal4. In larvae eye-antennae imaginal disc, Fwe localizes ubiquitously to the cytoskeleton of all eight photoreceptor cells and was shown to co-localize with F-actin staining (Rhiner *et al.*, 2010). However, the nuclear expression of CkIIα-i1-Gal4 specifically localizes to two neighboring photoreceptor cells (data not shown). Consequently, at least in the imaginal disc, the observed expression can be suggested not to belong to Fwe.

In addition, initiation of transcription is tightly regulated by accessibility of transcription factor, enhancer or open chromatin structure (Hu and Tee, 2017). Even though the cloned CREs share the same nucleotides with endogenous CREs, their accessibility for interaction with regulatory elements is not predictable, and thus could result in observing expression pattern of both few and CkIIα-i1. Therefore, in order to prove that the expression pattern observed with the Gal4 lines reflects endogenous CkIIα-i1 expression, an in situ hybridization experiment could be performed.

5.1.2. Comparison of Expression Pattern of CkIIα-i1 Gal4 and BAC Lines

The expression pattern of CkIIα-i1-Gal4 line and the BAC line were investigated to identify localization of CkIIα-i1 activity in the adult fly brain. Thus, the expression patterns of the Gal4 lines and the BAC line were compared. Even though, it was shown that transcription of a gene does not ensure translation of the corresponding protein, since they are regulated by distinct mechanisms, most of the genes are expected to be transcribed and then translated into protein under physiological condition (Sonenberg and Hinnebusch, 2009). The presence of CkIIα-i1 around MB and in the clock cells both in the Gal4 line and the BAC line support the hypothesis that CkIIα-i1 has a role in MB and clock cells. In addition, the co-staining in the BAC line around the MB was observed in a net-like structure covering the MB and it was claimed that it could correspond to the structures belonging to two possible cell groups. The first one could be MB-interacting neurons such as dopaminergic PAM neurons (Mao, 2009) and the second one could be glial cells, which regulate both axonal maturation and homoeostasis of the MB (Hakim *et al.*, 2014). In the co-staining of CkIIα-i1-Gal4 line and FasII, I could only observe the cell bodies of 1-2 cells located just above the MB α lobe. However, unfortunately, it was not possible to observe their full cellular extensions using UAS-mCD8::GFP. Thus, analysis of axonal and dendritic arborization of CkIIα-i1-Gal4 using axonal (tau-GFP) and dendritic (Denmark) reporters could help to determine the identity of CkIIα-i1-expressing cells.

In addition, nuclear co-staining of CkIIα-i1-Gal4 and the Kenyon cell marker Dachshund should be verified because Dachshund stains not only Kenyon cells but also other groups such as insulin producing cells (IPCs) that are positionally close to Kenyon cells (Okamoto *et al.*, 2012). Verification can be performed by co-staining of CkIIα-i1-Gal4 with Kenyon cell and IPC specific markers. Expression of CkIIα-i1 within a/B subgroup of Kenyon cells was explained in the section of investigation of scRNAseq analysis. By nuclear staining of CkIIα-i1-Gal4 with Dachshund staining it could not be identified whether CkIIα-i1 is expressed in IPCs. However, by analyzing CkIIα-i1-Gal4 expression with membrane-associated reporter GFP, CkIIα-i1-expressing IPCs were morphologically identified. However, it is necessary to verify

the expression of CkIIα-i1-expressing IPCs by co-staining with IPCs-specific reporter lines. IPCs have a role in innate immunity, stress response, energy balance and homoeostasis and mood-associated social behavior like aggression (Luo *et al.*, 2014). They have a developmental and functional role similar to the hypothalamus, which is the hormone and homoeostasis center in mammals (Wang *et al.*, 2007). Similarly, mammalian ZBTB family proteins show high expression in the hypothalamus (Cheng *et al.*, 2020) and they are highly implicated in the regulation of lymphoid differentiation (Cheng *et al.*, 2021). In addition, a function for ZBTB11 in energy homeostasis was recently shown to be related to mitochondrial homeostasis (Wilson *et al.*, 2020). Therefore, the functional similarity between CkIIα-i1 and ZBTB11 in energy metabolism and the role of CkIIα-i1 in IPCs should be further investigated.

5.1.3. Expression Pattern and Cellular Identities of CkIIα-i1 in both Gal4 and BAC Line Regarding Co-Staining for Pacemaker Cells

Expression and localization of CkIIα-i1 in circadian cells was observed in both the CkIIα-i1-Gal4 and the BAC line. CkIIα, a serine-threonine kinase that phosphorylates CkIIα-i1 is expressed in the same circadian cells (Lin *et al.*, 2002). The nuclear translocation of Clock, a central circadian clock protein, is regulated by CkIIα and another CkIIα-i1 interactor protein Widerborst (Wdb) (Andreazza *et al.*, 2015). Thus, I hypothesize that the nuclear localization of CkIIα-i1 may be regulated by CkIIα and Wdb similar to Clock. To investigate this hypothesis, the role of CkIIα-i1 in the molecular clock mechanism and circadian rhythm can be tested in different Zeitgebers by co-staining of CkIIα-i1 with CkIIα, Wdb, and Clock antibodies and by analyzing the locomotor activity of CkIIα-i1 KO mutants.

5.1.4. *trans*-Tango

trans-Tango is a post-synaptic tracing system that allows to label both Gal4-expressing cells and their post-synaptic partners with different fluorescent tags to mark their expression in the nervous system (Talay *et al.*, 2017). In our study, *trans*-Tango was used to identify post-synaptic partners of CkIIα-i1-expressing cells. FasII staining was additionally used to determine the existence of post-synaptic partners in the MB. Even though no colocalization of cells post-synaptic to CkIIα-i1-expressing cells and FasII was observed, several sub-compartments of the fan-shaped body were labeled. The fan-shaped body is another important brain structure that can be used modeling of ID, since it regulates motor behavior by processing sensory input with the help of spatial memory in addition to its role in arousal and sleep (Coll-Tané *et al.*, 2019). Therefore, identification of the fan-shaped body as a possible post-synaptic partner, might implicate a possible role of CkIIα-i1 in fan-shaped body.

In the *trans*-Tango experiments, it appears that dendritic and axonal extension of most of the pre-synaptic and post-synaptic neurons could not be observed and thus their synaptic interaction could not be examined explicitly. It has been suggested that in order to improve the expression signal in axons and dendrites, aging of the flies for 20 days in 18^{o}C before dissection might increase the efficiency of the *trans*-Tango system (Coll-Tané *et al.*, 2019). This experiment could be performed as recommended to make sure all post-synaptic partners have been identified.

5.1.5. Endogenous Tagging of Ckiiα-I1 by CRISPR/Cas

Endogenous modification of a gene-of-interest by the CRISPR/Cas system is a highly utilized method in the field. However, the success rate of HDR for the intended modification is variable depending on the efficiency of the gRNA, accessibility of intended loci (Bosch *et al.*, 2020). Increasing the efficiency of endogenous modification by CRISPR/Cas is a hot topic in *Drosophila* research. Different techniques can be utilized to increase the efficiency of the intended C-terminus tagging of CkIIα-i1. For instance, utilizing short homology sequences around 200 bp rather than 1 kb was shown to in-

crease the success rate from 50% to 75% for 10 genes (Kanca *et al.*, 2019). In addition, targeting different positions within the gene of interest such as the first intron could be another option for endogenous tagging. It was shown that tagging of a protein at the N- or C-terminus could disturb its function and decrease the efficiency of the intended modification, while internal tagging (such as tagging in intron) was shown to increase viability and number of modification events (Serebrenik *et al.*, 2019).

5.2. Characterization of Function of Misexpression and Overexpression of CkIIα-i1 in MB Morphology

5.2.1. Knockdown and Knock-out of CkIIα-i1

In order to reveal the function of CkIIα-i1, I utilized two loss-of-function approaches, RNAi-mediated knockdown and CRISPR/Cas-mediated knock-out of CkIIα-i1. First, knockdown of CkIIα-i1 was performed by two different shRNAs constructs: UAS-CkIIα-i1^{53025} and UAS-CkIIα-i1^{60102}. The efficiency of knockdown by the UAS-CkIIα-i1^{60102} construct was tested by qRT-PCR (Fattahi *et al.*, 2018) and it was shown that the RNA level of CkIIα-i1 was decreased significantly ($p<0.005$). However, quantitative analysis for UAS-CkIIα-i1^{53025} should also be performed to estimate the efficiency of the shRNA since RNAi-mediated knockdown has variable efficiency depending on different parameters such as sufficiency of the expression of shRNA vector, level of mRNA expression of downregulated gene and accessibility of Dicer2, which cleaves the mRNA mediated by shRNA (Kim *et al.*, 2006). Both CkIIα-i1 targeting shRNA construct are cloned in VALIUM20 vector which was optimized for reducing leaky expression from the promoter and increase the expression levels of shRNA (Qiao *et al.*, 2018), thereby increasing the efficiency and precision of the knockdown event without additional expression of Dicer2 nucleases (Qiao *et al.*, 2018). Therefore, I decided to perform, first, the knockdown of CkIIα-i1 in two separate transgenic shRNA-expressing lines and compare their efficiency by evaluating the alteration of MB morphology. The common phenotypes of UAS-CkIIα-i1-shRNA after crossing with MB-specific Gal4 line were the shrinkage of a3 lobe with 44% and 37% reduction, respectively. The penetrance for the shrinkage of a3 lobe was higher for UAS-CkIIα-i1^{53025} and the additional

phenotype for the α' lobe was observed in UAS-CkIIα-i1^{53025}. However, the phenotype observed in the a' lobe was not observed in knockdown by UAS-CkIIα-i1^{60102} or in the KO mutants, which may indicate an off-target activity of shRNA. Therefore, in further knockdown experiments for CkIIα-i1 the UAS-CkIIα-i1^{60102} flies should be utilized. In addition, in order to repeat the knockdown experiment in Fattahi *et al.*, 2018, MB-specific knockdown of CkIIα-i1 was performed with the same experimental procedure. Previously, total fluorescent intensity of the MB areas was analyzed to test the loss-of-function effect of CkIIα-i1. However, morphological changes have not been addressed. Therefore, I decided to analyze and compare the effect of both knockdown and knock-out of CkIIα-i1 on the morphology of the MB. In the CkIIα-i1 KO flies, I observed morphological changes only in the CkIIα-i1^{M20} line. Even though, there were additional phenotypes such as misguidance of α3 lobe, skewing and shortage of α lobe in CkIIα-i1^{M20} line, all of these phenotypes could depend on the same mechanisms such as projection of α lobe axons. Therefore, the variety of the phenotypes observed in CkIIα-i1^{M20} line can be interpreted as relatively higher penetration of mutation than in knockdown flies and could result from two different reasons. The first one is that while knockdown of CkIIα-i1 was specific to the MB, knockout of CkIIα-i1 occurred in the whole body. This might indicate a non-cell autonomous effect of CkIIα-i1 in the MB rather than resulting from its expression in Kenyon cells. Other cell groups such as CkIIα-i1-expressing glial cells could cause the malfunctioning of axonal projection of the α lobe. The second one is that RNAi-knockdown could not be as efficient as genomic mutation. It could result in a decrease of the observed phenotype frequency. A similar phenotype, which is misguidance and severe shrinkage of a3 lobes was observed in ID- and speech disorder-related FoxP mutant flies (Castells-Nobau *et al.*, 2019). However, further functional analysis in necessary to reveal the function of CkIIα-i1 in a3 lobe of MB.

In addition, absence of the described phenotypes in the CkIIα-i1^{M16} line could be explained by the expression of the functional domain of CkIIα-i1 by an alternative start codon in the second exon since the mutation in CkIIα-i1^{M16} line is located in the first exon and the predicted functional domains of CkIIα-i1 are located in the second exon. However, due to the absence of the specific antibody for CkIIα-i1 this could

not be further addressed. Alternatively, both of the mutant lines could and should be analyzed for expression of different exons by RT-qPCR.

5.2.2. Ectopic Overexpression

MB-specific overexpression of CkIIα-i1 did not result in phenotypic changes in the MB, while both knockdown and knockout of CkIIα-i1 demonstrated a promising phenotype in the α lobes. It was shown that overexpression of transcription factors (TF) can alter their function since they can have a role as enhancer and/or suppressor of their downstream genes and overexpression of the TF can boost or decrease the expression of the downstream genes (Prelich, 2012). As previously described, interaction partners of the CkIIα-i1 protein were functionally clustered in the regulation of the neuroblast and progenitor fate (see Introduction 1.4). Therefore, CkIIα-i1 may have a role in regulation of expression of developmental genes as an enhancer or suppressor. Although misexpression of CkIIα-i1 could result in malfunctioning of downstream target genes, if the expression of downstream target genes of CkIIα-i1 was not dose-dependent it might not result in any phenotype . In addition, similar to my result, if the function of CkIIα-i1 is controlled by other mechanisms such as dimerization with another concomitant TF, overexpression of CkIIα-i1 might not be seen in the phenotype (Zolotarev *et al.*, 2016).

5.3. Generation of ZBTB11-Expressing Flies and Validation of ZBTB11 Expression in Fly

In order to reveal the orthology between ZBTB11 and CkIIα-i1, ZBTB11- expressing transgenic flies were generated. subcellular localization of ZBTB11 and CkIIα-i1 was analyzed in CkIIα-i1-expressing cells by crossing CkIIα-i1-Gal4 with UAS-CkIIα-i1-HA, UAS-ZBTB11-HA^{wt} and UAS-ZBTB11-HA^{H880Q} flies. CkIIα-i1 was localized mostly in the cell bodies. Although nuclear localization of ZBTB11 in human HEK293 cells was shown (Fattahi *et al.*, 2018), both wt and variant of ZBTB11 were localized to cell bodies and axons. Subcellular localization of a protein could be dynamic depending on its function in different cell types and external conditions (Qi and

Boateng, 2006; Bervoets *et al.*, 2019). Therefore, nuclear localization of ZBTB11 in HEK293 cells could not display neural subcellular localization of ZBTB11 and, physiologically, it can be localized in the cell body and axonal part of neurons in the fly brain. On the other hand, subcellular localization is directed by alternative isoform choice and post-transcriptional modifications (Bauer *et al.*, 2015). However, ZBTB11 was expressed by the same constructs of ZBTB11 variants in both studies. Thus, alternative isoform choice is not a likely reason of altered localization. If regulatory proteins which are responsible for post-transcriptional modification of ZBTB11 were absent in the fly, ZBTB11 could be mislocalized in CkIIα-i1-expressing cells. In addition, if UAS controlled ZBTB11 expression was enhanced compared to physiological level protein production, it could result in the aggregation of ZBTB11 in altered subcellular compartments.

5.4. Suggestion for Future Research

In the thesis, I have characterized the function of CkIIα-i1 in MB and expression pattern of CkIIα-i1 in MB and clock cells. In addition, I have generated and validated ZBTB11-expressing fly lines. This study aimed to contribute to the identification of a possible orthology between CkIIα-i1 and ZBTB11 by consideration of ID pathology and deficiency in learning and memory. This study could address whether MB can be utilized as a model to analyze function of CkIIα-i1 and ZBTB11 and included the generation and validation of necessary fly lines to study the orthology. However, further experiments need to be performed to reveal the possible orthology between CkIIα-i1 and ZBTB11.

It would be a good start to analyze rescue of α3 lobe shrinkage of MB in CkIIα-i1 mutants by transgenically expressing CkIIα-i1 in the CkIIα-i1^{M20} mutant via genomic rescue constructs such as BAC clone "CH322-72N9" (see result 4.1.5). Afterwards, to investigate possible functional orthology between ZBTB11 and CkIIα-i1 in MB morphology, humanized (cross-species) flies can be generated. To do this, human ZBTB11 gene variants can be expressed in the CkIIα-i1^{M20} mutant background using UAS-ZBTB11 wt and variant lines that were generated in this study (Yamaguchi *et*

al., 2018). If wild-type ZBTB11 rescues the α3 lobe shrinkage of the MB that was observed in the mutant, we would suggest an orthology between ZBTB11 and CkIIα-i1. Also, ZBTB11 variants would be analyzed for their function in MB morphology. We would expect to observe no rescue in expression of ZBTB11 variants in the CkIIα-i1 KO background if mutations disturb the function of ZBTB11.

Analysis of MB morphology gives an indirect answer of the function of investigated protein in learning and memory because, thanks to functional plasticity of nervous system, structural abnormality in MB does not always result in any problem in learning (Sugie *et al.*, 2018). Therefore, the effect of CkIIα-i1 loss of function and its rescue by CkIIα-i1 and wt and mutant ZBTB11 expression should be analyzed by behavioral assays which address learning capacities.

Learning begins with the detection of external stimuli via different sensory systems and is acquired as a knowledge, and the response to presented stimuli can be modified according to the type of learning. In ID patients, it was shown that learning capacities could be affected in different levels such as non-associative and associative learning which can be studied by different paradigms (Coll-Tané *et al.*, 2019). For instance, courtship learning assay was established in 1979 by Siegel and Hall to analyze associative learning and memory of male flies (Siegel and Hall, 1979). It aims to detect learning deficiencies of male flies which were rejected by previously mated female flies. Courtship is a straight-forward and complex behavior which is composed of six main acts such as following (male orients its body toward the interested female and follows the targeted female), tapping (male touches the female abdomen by one of its forelegs), singing (male vibrates one of its wings to attract female by its "song"), licking (male licks female's genitalia), copulation (male curls its abdomen toward female and penetrates and ejaculates) (Hall, 1994). In trained males, which previously experienced the rejection by pre-mated females, sexual attraction towards pre-mated female decreases because they can learn and memorize to reduce courtship duration and comparison of courtship duration reveals learning and memory capacity of naïve and trained males (Kamyshev *et al.*, 1999; Koemans *et al.*, 2017). In all of the courtship acts, the decision of males and females to continue to the next steps of copulation are reinforced by

visual, olfactory and mechanosensory stimuli that come from both environment and opposite sex (Dickson, 2008). Therefore, any functional problem in their sensory systems such as visual, mechanosensory, olfactory, and gustatory and/or in their response mechanisms such as intermediate motor neurons, neuromuscular junctions or abnormal muscle function should be distinguished in data from their learning capacity defects by analyzing their functions separately. The optic lobe is necessary for receiving visual input and control visual processing in learning (Guo *et al.*, 2013). In this study, it was shown that expression of CkIIα-i1 localizes to the optic lobe and post-synaptic neurons of CkIIα-i1 were observed in the fan-shaped body. Visual input like the picture of an appealing female for a male fly is sufficient to initiate sexual arousal without any olfactory or gustatory reinforcers (Hindmarsh *et al.*, 2021). So, defects in the visual system caused by loss-of-function of CkIIα-i1 could prevent sexual attraction of the male, which would also decrease the learning index. In trans-Tango experiments post-synaptic neurons of CkIIα-i1 expressing cells localized in the fan-shaped body. Those neurons could be post-synaptic to optic lobe neurons which express CkIIα-i1 and they could control visual learning (Pan *et al.*, 2009). Therefore, visual ability and visual memory of CkIIα-i1 mutant should be analyzed before investigating its learning and memory capacity. To sum up, courtship learning paradigm could be a well-suited learning assay to address learning and memory deficiencies in CkIIα-i1 mutant flies. However, as explained, their sensory and motor nervous system have to be analyzed as well.

REFERENCES

Abbasi-Moheb L., S. Mertel, M. Gonsior, L. Nouri-Vahid, K. Kahrizi, S. Cirak, D. Wieczorek, M.M. Motazacker, S. Esmaeeli-Nieh, K. Cremer, R. Weißmann, A. Tzschach, M. Garshasbi, S.S. Abedini, H. Najmabadi, H.H. Ropers, S.J. Sigrist, A.W. Kuss, 2012, "Mutations in NSUN2 Cause Autosomal-Recessive Intellectual Disability.", *The American Society of Human Genetics*, 90, no. 5, pp. 847-855.

Al-Anzi, B., and K. Zinn, 2018, "Identification and Characterization of Mushroom Body Neurons That Regulate Fat Storage in Drosophila.", *Neural Development*, 13, no. 1, p. 18.

Altschul, S.F., W. Gish, W. Miller, E.W. Myers, and D.J. Lipman, 1990, "Basic Local Alignment Search Tool.", *Journal of Molecular Biology*, 215, pp. 403-410.

Andreazza S., S. Bouleau, B. Martin, A. Lamouroux, P. Ponien, C. Papin, E. Chélot, E. Jacquet, F. Rouyer, 2015, "Daytime CLOCK Dephosphorylation Is Controlled by STRIPAK Complexes in Drosophila.", *Cell Report*, 11, no. 8, pp. 1266-1279.

American Psychiatric Association (APA), 2013, *Diagnostic and Statistical Manual of Mental Disorders*, 5th edition, DC: Author, Arlington.

Arnett AB, S. Trinh, R.A. Bernier, 2019, "The State of Research on The Genetics of Autism Spectrum Disorder: Methodological, Clinical and Conceptual Progress." *Current Opinion in Psychology*, 27, pp. 1-5.

Aso Y., D. Hattori, Y. Yu, R.M. Johnston, N.A. Iyer, T.T. Ngo, H. Dionne, L.F. Abbott, R. Axel, H. Tanimoto, G.M. Rubin, 2014, "The Neuronal Architecture of the Mushroom Body Provides a Logic for Associative Learning.", *Elife*, 3.

Aspromonte MC, M. Bellini, A. Gasparini, M. Carraro, E. Bettella, R. Polli, F. Cesca, S. Bigoni, S. Boni, O. Carlet, S. Negrin, I. Mammi, D. Milani, A. Peron, S. Sartori, I. Toldo, F. Soli, L. Turolla, F. Stanzial, F. Benedicenti, C. Marino-Buslje, S.C.E. Tosatto, A. Murgia, E. Leonardi, 2019, "Characterization of Intellectual Disability and Autism Comorbidity Through Gene Panel Sequencing.", *Human Mutation*, 40, no. 9, pp. 1346–1363.

Baio, J., L., Wiggins, D. L. Christensen, M. J. Maenner, J. Daniels, Z. Warren, M. Kurzius-Spencer, W. Zahorodny, C. Robinson Rosenberg, T. White, M. S. Durkin, P. Imm, L. Nikolaou, M. Yeargin-Allsopp, L. C. Lee, R. Harrington, M. Lopez, R. T. Fitzgerald, A. Hewitt, S. Pettygrove, J.N. Constantino, A. Vehorn, J. Shenouda, J. Hall-Lande, K. Van Naarden Braun, N. F. Dowling, 2018, "Prevalence of Autism Spectrum Disorder Among Children Aged 8 Years - Autism and Developmental Disabilities Monitoring Network, 11 Sites, United States", 2014, *Morbidity And Mortality Weekly Report - Surveillance Summaries*, 67, no. 6, pp. 1–23.

Bassett, A. R., and J. L. Liu, 2014, "CRISPR/Cas9 and Genome Editing in Drosophila.", *Journal of Genetics and Genomics*, 41, no. 1, pp. 7–19.

Bate M., K. Broadie, 1995, "Wiring by Fly: The Neuromuscular System of the Drosophila Embryo.", *Neuron*, 15, no. 3, pp. 513-525.

Bauer, N. C., P. W. Doetsch, and A. H. Corbett, 2015, "Mechanisms Regulating Protein Localization.", *Traffic*, 16, no. 10, pp. 1039–1061.

Berendzen, K. W., K. Stüber, K. Harter, and D. Wanke, 2006, “Cis-Motifs Upstream of the Transcription and Translation Initiation Sites Are Effectively Revealed by Their Positional Disequilibrium in Eukaryote Genomes Using Frequency Distribution Curves.”, *BioMed Central Bioinformatics*, 7, no. 522.

Bervoets, S., N. Wei, M.-L. Erfurth, S. Yusein-Myashkova, B. Ermanoska, L. Mateiu, B. Asselbergh, D. Blocquel, P. Kakad, T. Penserga, F. P. Thomas, V. Guergueltcheva, I. Tournev, T. Godenschwege, A. Jordanova, and X.-L. Yang, 2019, “Transcriptional Dysregulation by a Nucleus-Localized Aminoacyl-tRNA Synthetase Associated with Charcot-Marie-Tooth Neuropathy.”, *Nature Communications*, 10, no. 1.

Besedovsky, L., T. Lange, and J. Born, 2012, “Sleep and Immune Function.”, *Pflugers Archive: European Journal of Physiology*, 463, no. 1, pp. 121–137.

Beumer, K. J., J. K. Trautman, A. Bozas, J. L. Liu, J. Rutter, J. G. Gall, and D. Carroll, 2008, “Efficient Gene Targeting in Drosophila by Direct Embryo Injection with Zinc-Finger Nucleases.”, *Proceedings of the National Academy of Sciences of the United States of America*, 105, no. 50, pp. 19821–19826.

Beumer, K. J., J. K. Trautman, K. Mukherjee, and D. Carroll, 2013, “Donor DNA Utilization During Gene Targeting with Zinc-Finger Nucleases.”, *G3 Genes, Genomes, Genetics*, 3, no. 4, pp. 657–664.

Bibikova M., M. Golic, K.G. Golic, D. Carroll, 2002, “Targeted Chromosomal Cleavage and Mutagenesis in Drosophila Using Zinc-Finger Nucleases.”, *Genetics*, 161, no. 3, pp. 1169-1175.

Bier E., 2005, "Drosophila, The Golden Bug, Emerges as A Tool for Human Genetics.", *Nature Reviews Genetics*, 6, pp. 9–23

Bitta, M., S. M. Kariuki, A. Abubakar, and C. Newton, 2017, "Burden of Neurodevelopmental Disorders in Low and Middle-Income Countries: A Systematic Review and Meta-Analysis.", *Wellcome Open Research*, 2, no. 121.

Bolduc, F. V., K. Bell, H. Cox, K. S. Broadie, and T. Tully, 2008, "Excess Protein Synthesis in Drosophila Fragile X Mutants Impairs Long-Term Memory.", *Nature Neuroscience*., 11, pp. 1143-1145.

Bosch, J. A., G. Birchak, and N. Perrimon, 2021, "Precise Genome Engineering in Drosophila Using Prime Editing", *Proceedings of the National Academy of Sciences of the United States of America*, 118, no. 1.

Brooks, M. J., H. Y. Chen, R. A. Kelley, A. K. Mondal, K. Nagashima, N. De Val, T. Li, V. Chaitankar, and A. Swaroop, 2019, "Improved Retinal Organoid Differentiation by Modulating Signaling Pathways Revealed by Comparative Transcriptome Analyses with Development In Vivo.", *Stem Cell Reports*, 13, no. 5, pp. 891–905.

Brown, H. L., K. R. Kaun, and B. A. Edgar, 2012 "The Small GTPase RHEB Affects Central Brain Neuronal Morphology and Memory Formation in *Drosophila*.", *Plos One*, 7, no. 9.

Castells-Nobau, A., I. Eidhof, M. Fenckova, D. B. Brenman-Suttner, J. M. Scheffer-de Gooyert, S. Christine, R. L. Schellevis, K. van der Laan, C. Quentin, L. van Ninhuijs, F. Hofmann, R. Ejsmont, S. E. Fisher, J. M. Kramer, S. J. Sigrist, A. F. Simon, and A. Schenck, 2019, "Conserved Regulation of Neurodevelopmental Processes and Behavior by FoxP in Drosophila.", *Plos One*, 14, no. 2.

Chaste P, K. Roeder, B. Devlin, 2017, "The Yin and Yang of Autism Genetics: How Rare De Novo and Common Variations Affect Liability.", *Annual Review of Genomics and Human Genetics,* 18, pp. 167-187.

Cheng, H., S. J. Pablico, J. Lee, J. S. Chang, and S. Yu, 2020, "Zinc Finger Transcription Factor ZBTB16 Coordinates the Response to Energy Deficit in The Mouse Hypothalamus.", *Frontiers in Neuroscience*, 14.

Cheng, Z. Y., T. T., He, X. M. Gao, Y. Zhao, and J. Wang, 2021, "ZBTB Transcription Factors: Key Regulators of the Development, Differentiation and Effector Function of T Cells.", *Frontiers in Immunology*, 12, no. 7, pp. 132-194.

Chiurazzi, P., A. K. Kiani, J. Miertus, S. Paolacci, S. Barati, E. Manara, L. Stuppia, F. Gurrieri, and M. Bertelli, 2020, "Genetic Analysis of Intellectual Disability and Autism.", *Acta bio-medica: Atenei Parmensis*, 91, no. 13-S.

Chubak, M. C., K. C. Nixon, M. H. Stone, N. Raun, S. L. Rice, M. Sarikahya, S. G. Jones, T. A. Lyons, T. E. Jakub, R. L. Mainland, M. J. Knip, T. N. Edwards, and J. M. Kramer, 2019, "Individual Components of the SWI/SNF Chromatin Remodelling Complex Have Distinct Roles in Memory Neurons of the *Drosophila* Mushroom Body.", *Disease Models and Mechanisms*, 12, no. 3.

Coll-Tané, M., A. Krebbers, A. Castells-Nobau, C. Zweier, and A. Schenck, 2019 "Intellectual Disability and Autism Spectrum Disorders 'On the Fly': Insights from Drosophila.", *Disease Models and Mechanisms*, 12, no. 5.

Czech, B., and Hannon, G. J., 2011, "Small RNA sorting: matchmaking for Argonautes.", *Nature Reviews Genetics*, 12, no. 1, pp. 19-31.

Davie, K., J. Janssens, D. Koldere, M. De Waegeneer, U. Pech, Ł. Kreft, S. Aibar, S. Makhzami, V. Christiaens, C. Bravo González-Blas, S. Poovathingal, G. Hulselmans, K. I. Spanier, T. Moerman, B. Vanspauwen, S. Geurs, T. Voet, J. Lammertyn, B. Thienpont, S. Liu, N. Konstantinides, M. Fiers, P. Verstreken, S. Aerts, 2018, "A Single-Cell Transcriptome Atlas of the Aging Drosophila Brain.", *Cell*, 174, no. 4, pp. 982–998.

Dickson, B. J., 2008, "Wired for sex: The neurobiology of drosophila mating decisions.", *Science*, pp. 904–909.

Dubnau J., L. Grady, T. Kitamoto, T. Tully, 2001, "Disruption of Neurotransmission in *Drosophila* Mushroom Body Blocks Retrieval but Not Acquisition of Memory.", *Nature*, 411, no. 6836, pp. 476-480.

Dubowy, C., and A. Sehgal, 2017, "Circadian Rhythms and Sleep in *Drosophila melanogaster*.", *Genetics*, 205, no. 4, pp. 1373–1397,

Eid A., and M.M. Mahfouz, 2016, "Genome Editing: The Road Of CRISPR/Cas9 from Bench to Clinic.", *Experimental and Molecular Medicine*, 14, no. 48, p. 265.

Fahrbach S. E., 2006, “Structure of The Mushroom Bodies of the Insect Brain.”, *Annual Review of Entomology*, 51, pp. 209–232.

Fattahi, Z., T. I. Sheikh, L. Musante, M. Rasheed, I. I. Taskiran, R. Harripaul, H. Hu, S. Kazeminasab, M. R. Alam, M. Hosseini, F. Larti, Z. Ghaderi, A. Celik, M. Ayub, M. Ansar, M. Haddadi, T. F. Wienker, H. H. Ropers, K. Kahrizi, J. B. Vincent, H. Najmabadi, 2018, “Biallelic Missense Variants in ZBTB11 Can Cause Intellectual Disability in Humans.”, *Human Molecular Genetics*, 27, no. 18, pp. 3177–3188.

Fire A, S. Xu, M.K. Montgomery, S.A. Kostas, S.E. Driver, C.C. Mello, 1998, “Potent and specific genetic interference by double-stranded RNA in Caenorhabditis elegans.”, *Nature,* 391, no. 6669.

Gaine, M. E., 2021, *Altered Hippocampal Transcriptome Dynamics Following Sleep Deprivation.BioRxiv*,https://www.biorxiv.org/content/10.1101/2021.05.20.445021v1, 20/12/2021

Garipler, G., 2020, *The BTB Transcription Factors ZBTB11 and ZFP131 Maintain Pluripotency by Pausing POL II at Pro-differentiation Genes. BioRxiv,* https://www.biorxiv.org/content/10.1101/2020.11.23.391771v1, 24/11/2021

Gatto, C. L., and K. Broadie, 2009, “Temporal Requirements of the Fragile X Mental Retardation Protein in Modulating Circadian Clock Circuit Synaptic Architecture.”, *Frontiers in Neural Circuits,* 3, no. 8.

Gil-Ranedo, J., E. Gonzaga, K. J. Jaworek, C. Berger, T. Bossing, and C. S. Barros, 2019, “Stripak Members Orchestrate Hippo and Insulin Receptor Signaling to Promote Neural Stem Cell Reactivation.”, *Cell Reports*, 27, no. 10.

Giot L, J. S., Bader, C. Brouwer, A. Chaudhuri, B. Kuang, Y. Li, Y.L. Hao, C.E. Ooi, B. Godwin, E. Vitols, G. Vijayadamodar, P. Pochart, H. Machineni, M. Welsh, Y. Kong, B. Zerhusen, R. Malcolm, Z. Varrone, A. Collis, M. Minto, S. Burgess, L. McDaniel, E. Stimpson, F. Spriggs, J. Williams, K. Neurath, N. Ioime, M. Agee, E. Voss, K. Furtak, R. Renzulli, N. Aanensen, S. Carrolla, E. Bickelhaupt, Y. Lazovatsky, A. DaSilva, J. Zhong, C.A. Stanyon, R.L. Finley, Jr, K.P. White, M. Braverman, T. Jarvie, S. Gold, M. Leach, J. Knight, R.A. Shimkets, M.P. McKenna, J. Chant, J.M. Rothberg, 2003, "A Protein Interaction Map of *Drosophila* Melanogaster.", *Science,* 302, no. 5651, pp. 1727-1736.

Glanzman, D. L., 2011, "Olfactory Habituation: Fresh Insights from Flies.", *Proceedings of the National Academy of Sciences of the United States of America,* 108, pp. 14711-14712.

Gratz S.J., A.M. Cummings, J.N. Nguyen, D.C. Hamm, L.K. Donohue, M.M. Harrison, J. Wildonger, K.M. O'Connor-Giles, 2013, "Genome Engineering of Drosophila with the CRISPR RNA-Guided Cas9 Nuclease.", *Genetics*, 194, no. 4, pp. 1029-35.

Guo, A., H. Lu, K. Zhang, Q. Ren, Y.-N. Chiang Wong, 2013, "Visual Learning and Decision Making in Drosophila Melanogaster.", *Invertebrate Learning and Memory*, pp. 378–394.

Guo, H. F., J. Tong, F. Hannan, L. Luo, Y. Zhong, 2000, "A Neurofibromatosis-1-Regulated Pathway is Required for Learning in *Drosophila*.", *Nature*, 403, no. 6772, pp. 895–898.

Guy, J., J. Gan, J. Selfridge, S. Cobb, A. Bird, 2007, "Reversal of Neurological Defects in A Mouse Model of Rett Syndrome.", *Science*, 315, no. 5815, pp. 1143–1147.

Hakim, Y., S. P. Yaniv, and O. Schuldiner, 2014, "Astrocytes Play a Key Role in *Drosophila* Mushroom Body Axon Pruning.", *Plos One*, 9, no. 1, pp. 861-878.

Hall J.C., 1994, "The mating of a fly.", *Science*, pp. 1702-14.

Hamdan, F. F., H. Daoud, D. Rochefort, A. Piton, J. Gauthier, M. Langlois, G. Foomani, S. Dobrzeniecka, M. O. Krebs, R. Joober, R. G. Lafrenière, J. C. Lacaille, L. Mottron, P. Drapeau, M. H. Beauchamp, M. S. Phillips, E. Fombonne, G. A. Rouleau, and J. L. Michaud, 2010, "De Novo Mutations in FOXP1 in Cases with Intellectual Disability, Autism, And Language Impairment.", *American Journal of Human Genetics*, 87, no. 5, pp. 671–678.

Haywood A.F., B.E. Staveley, 2004, "Parkin Counteracts Symptoms in A Drosophila Model of Parkinson's Disease.", *BioMed Central Neuroscience*, 5, p. 14.

Heisenberg M., 1998, "What Do the Mushroom Bodies Do for The Insect Brain? An Introduction.", *Learning and Memory, 5*, no. 1-2, pp. 1–10.

Hentze, M.W., and A.E. Kulozik, 1999, "A Perfect Message: RNA Surveillance and Nonsense-Mediated Decay.", *Cell*, no. 96, pp. 307–310.

Heringa, J., 1999, "Two Strategies for Sequence Comparison: Profile-Preprocessed and Secondary Structure-Induced Multiple Alignment.", *Computers and Chemistry*, 23, pp. 3-4

Hindmarsh Sten T, R. Li, A. Otopalik, V. Ruta, 2021, "Sexual Arousal Gates Visual Processing During Drosophila Courtship.", *Nature*, pp. 549-553.

Hu, Z., and W.W. Tee, 2017, “Enhancers and Chromatin Structures: Regulatory Hubs in Gene Expression and Diseases.”, *Bioscience Reports*, 37, no. 2.

Huai, C., G. Li, R. Yao, Y. Zhang, M. Cao, L. Kong, C. Jia, H. Yuan, H. Chen, D. Lu and Q. Huang, 2017, "Structural Insights into DNA Cleavage Activation of CRISPR-Cas9 System", *Nature Communications*, Vol. 8, No. 1, pp. 1–9.

Iqbal Z., G. Vandeweyer, M. van der Voet, A.M. Waryah, M.Y. Zahoor, J.A. Besseling, L.T. Roca, A.T. Vulto-van Silfhout, B. Nijhof, J.M. Kramer, N. Van der Aa, M. Ansar, H. Peeters, C. Helsmoortel, C. Gilissen, L.E. Vissers, J.A. Veltman, A.P. de Brouwer, R. Frank Kooy, S. Riazuddin, A. Schenck, H. van Bokhoven, L. Rooms, 2013, “Homozygous and Heterozygous Disruptions of ANK3: at the Crossroads of Neurodevelopmental and Psychiatric Disorders.”, *Human Molecular Genetic*, 22, no. 10, pp. 1960-70.

Iseli, C., G. Ambrosini, P. Bucher, C. V. Jongeneel, 2007, “Indexing Strategies for Rapid Searches of Short Words in Genome Sequences.”, *Plos One*, 2, no. 6, p. 579

Ito K., W. Awano, K. Suzuki, Y. Hiromi, D. Yamamoto, 1997, “The Drosophila Mushroom Body Is a Quadruple Structure of Clonal Units Each of Which Contains a Virtually Identical Set of Neurones and Glial Cells”, *Development,* 124, pp. 761–771.

Jennings, B. H., 2011, “*Drosophila* – A Versatile Model in Biology & Medicine.”, *Materials Today*, 14, no. 5, pp. 190–195.

Ji, S. J., and S. R. Jaffrey, 2014, “Axonal Transcription Factors: Novel Regulators of Growth Cone-To-Nucleus Signaling.”, *Developmental Neurobiology*, 74, no. 3, pp. 245–258.

Jinek M., K. Chylinski, I. Fonfara, M. Hauer, J.A. Doudna, E. Charpentier, 2012, "A Programmable Dual-RNA-Guided DNA Endonuclease in Adaptive Bacterial Immunity.", *Science*, 337, no. 6096, pp. 816-821.

Joiner, W. J., A. Crocker, B. H. White, and A. Sehgal, 2006, "Sleep in Drosophila is Regulated by Adult Mushroom Bodies.", *Nature*, 441, pp. 757-760.

Kalive, M., R. L. Trott, and A. P. Bidwai, 2001, "A Gene Located at 72a in *Drosophila* Melanogaster Encodes a Novel Zinc-Finger Protein That Interacts with Protein Kinase CK2.", *Molecular and Cellular Biochemistry*, pp. 99–105.

Kammenga, J. E., 2017, "The Background Puzzle: How Identical Mutations in The Same Gene Lead to Different Disease Symptoms.", *The FEBS Journal*, 284, no. 20, pp. 3362–3373.

Kamyshev N.G., K.G. Iliadi, J.V. Bragina, 1999, "Drosophila conditioned courtship: two ways of testing memory.", *Learning and Memory,* pp. 1-20.

Kanca, O., J. Zirin, J. Garcia-Marques, S. M. Knight, D. Yang-Zhou, G. Amador, H. Chung, Z. Zuo, L. Ma, Y. He, W.W. Lin, Y. Fang, M. Ge, S. Yamamoto, K. L. Schulze, Y. Hu, A. C. Spradling, S. E. Mohr, N. Perrimon, and H. J. Bellen, 2019, "An Efficient CRISPR-Based Strategy to Insert Small and Large Fragments of DNA Using Short Homology Arms.", *ELife*, 8.

Keightley, M. C., D. P. Carradice, J. E. Layton, L. Pase, J. Y. Bertrand, J. G. Wittig, A. Dakic, A. P., Badrock, N. J. Cole, D. Traver, S. L. Nutt, J. McCoey, A. M. Buckle, J. K. Heath, and G. J. Lieschke, 2017, "The Pu.1 Target Gene Zbtb11 Regulates Neutrophil Development Through Its Integrase-Like HHCC Zinc Finger.", *Nature Communications*, 8.

Kepa, A., L. Martinez Medina, S. Erk, D. P. Srivastava, A. Fernandes, R. Toro, S. Levi, B. Ruggeri, C. Fernandes, F. Degenhardt, 2017, "Associations of The Intellectual Disability Gene MYT1L with Helix-Loop-Helix Gene Expression, Hippocampus Volume and Hippocampus Activation During Memory Retrieval.", *Neuropsychopharmacology*, 42, pp. 2516-2526.

Kim, S., J. Kim, S. Park, J.J., Park, and S. Lee, 2021, "*Drosophila* Graf Regulates Mushroom Body β-Axon Extension and Olfactory Long-Term Memory.", *Molecular Brain*, 14, no. 1.

Koemans, T. S., C. Oppitz, R. Donders, H. van Bokhoven, A. Schenck, K. Keleman, J. M. Kramer, 2017, "Drosophila Courtship Conditioning as a Measure of Learning and Memory.", *Journal of visualized experiments: Jove*.

Kramer, J. M., K. Kochinke, M. A. Oortveld, H. Marks, D. Kramer, E. K. de Jong, Z. Asztalos, J. T. Westwood, H. G. Stunnenberg, M. B. Sokolowski, K. Keleman, H. Zhou, H. van Bokhoven, and A. Schenck, 2011, "Epigenetic Regulation of Learning and Memory by *Drosophila* EHMT/G9a.", *Plos Biology*, 9, no. 1.

Kudron, M.M., A. Victorsen, L. Gevirtzman, L.W. Hillier, W.W. Fisher, D. Vafeados, M. Kirkey, A.S. Hammonds, J. Gersch, H. Ammouri, M.L. Wall, J. Moran, D. Steffen, M. Szynkarek, S. Seabrook-Sturgis, N. Jameel, M. Kadaba, J. Patton, R. Terrell, M. Corson, T.J. Durham, S. Park, S. Samanta, M. Han, J. Xu, K.K. Yan, S.E. Celniker, K.P. White, L. Ma, M. Gerstein, V. Reinke, R.H. Waterston, 2018, "The ModERN Resource: Genome-Wide Binding Profiles for Hundreds of *Drosophila* and *Caenorhabditis elegans* Transcription Factors.", *Genetics*, 3, no. 3, pp. 937-949.

Kuert PA, V. Hartenstein, B.C. Bello, J.K. Lovick, H. Reichert, 2014, "Neuroblast Lineage Identification and Lineage-Specific Hox Gene Action During Postembryonic Development of The Subesophageal Ganglion in The *Drosophila* Central Brain.", *Developmental Biology*, 390, no.2, pp. 105-115.

Kulkarni, M. M., M. Booker, S. J. Silver, A. Friedman, P. Hong, N. Perrimon, B. Mathey-Prevot, 2006), "Evidence of Off-Target Effects Associated with Long DsRNAs in Drosophila Melanogaster Cell-Based Assays.", *Nature Methods*, pp. 833–838.

La Malfa G., S. Lassi, M. Bertelli, R. Salvini, and G. F. Placidi, 2004, "Autism and Intellectual Disability: A Study of Prevalence on A Sample of The Italian Population.", *Journal of Intellectual Disability Research.*, no. 3, pp. 262–267.

Lanore, F., V. F. Labrousse, Z. Szabo, E. Normand, C. Blanchet, and C. Mulle, 2012, "Deficits in Morphofunctional Maturation of Hippocampal Mossy Fiber Synapses in A Mouse Model of Intellectual Disability.", *Journal of Neuroscience*, 32, pp. 17882-17893.

Larkin A, S.J. Marygold, G. Antonazzo, H. Attrill, G. dos Santos, P.V. Garapati, J.L. Goodman, L.S. Gramates, G. Millburn, V.B. Strelets, C.J. Tabone, J. Thurmond and the FlyBase Consortium, 2021, "Flybase: Updates to The *Drosophila* Melanogaster Knowledge Base", *Nucleic Acids Research,* pp. 899–907.

Le Fevre A. K., S. Taylor, N. H. Malek, D. Horn, C. W. Carr, O. A. Abdul-Rahman, S. O'Donnell, T. Burgess, M. Shaw, J. Gecz, N. Bain, K. Fagan, M. F. Hunter, 2013, "FOXP1 Mutations Cause Intellectual Disability and A Recognizable Phenotype.", *American Journal of Medical Genetics*, pp. 3166–3175.

Lee T., A. Lee, L. Luo, 1999, "Development of The Drosophila Mushroom Bodies: Sequential Generation of Three Distinct Types of Neurons from A Neuroblast", *Development* pp. 4065–4076.

Lee, H., D.-Y. Cho, C. Whitworth, R. Eisman, M. Phelps, J. Roote, T. Kaufman, K. Cook, S. Russell, T. Przytycka, B. Oliver, 2016, "Effects of Gene Dose, Chromatin, And Network Topology on Expression in Drosophila Melanogaster.", *Plos Genetics,* 12, no.9.

Lee, T., A. Lee, L. Luo, 1999, Development of the "Drosophila Mushroom Bodies: Sequential Generation of Three Distinct Types of Neurons from A Neuroblast.", *Development*, pp. 4065-4076.

Lee, Y. S., D. Ehninger, M. Zhou, J. Y. Oh, M. Kang, C. Kwak, H. H. Ryu, D. Butz, T. Araki, Y. Cai, J. Balaji, Y. Sano, C. I. Nam, H. K. Kim, B. K. Kaang, C. Burger, B. G. Neel, A. J. Silva, 2014, "Mechanism and Treatment for Learning and Memory Deficits in Mouse Models of Noonan Syndrome.", *Nature Neuroscience*, 12, pp. 1736–1743.

Lee, Y.-S., D. Ehninger, M. Zhou, J.-Y. Oh, M. Kang, C. Kwak, H.-H. Ryu, D. Butz, T. Araki, Y. Cai, J. Balaji, Y. Sano, C. I. Nam, H. K. Kim, B.-K. Kaang, C. Burger, B. G. Neel, A. J. Silva, 2014, "Mechanism and Treatment for Learning and Memory Deficits in Mouse Models of Noonan Syndrome.", *Nature Neuroscience*. pp. 1736-1743.

Li, H., Janssens, J., De Waegeneer, M., Kolluru, S. S., Davie, K., Gardeux, V., Saelens, W., David, F., Brbić, M., Leskovec, J., McLaughlin, C. N., Xie, Q., Jones, R. C., Brueckner, K., Shim, J., Tattikota, S. G., Schnorrer, F., Rust, K., Nystul, T. G., S. Aerts, 2021, *Fly Cell Atlas: A Single-Cell Transcriptomic Atlas of The Adult Fruit Fly. Biorxiv,* https:// www. Biorxiv .org /content/ 10. 1101 /2021 .07 .04 .4 510 50 v1, 27/10/2021

Liu Q, S. Liu, L. Kodama, M.R. Driscoll, M.N. Wu, 2012, "Two Dopaminergic Neurons Signal to The Dorsal Fan-Shaped Body to Promote Wakefulness in Drosophila.", *Current Biology*, 11, pp. 2114-23.

Maaskant, M., E. van de Wouw, R. van Wijck, H. M. Evenhuis, M. Echteld, 2013, "Circadian Sleep-Wake Rhythm of Older Adults with Intellectual Disabilities." *Research in Developmental Disabilities*, pp. 1144–1151.

Mao, Z., 2009, "Eight Different Types of Dopaminergic Neurons Innervate the Drosophila Mushroom Body Neuropil: Anatomical and Physiological Heterogeneity.", *Frontiers in Neural Circuits*, 3, no. 5.

Mariano, V., T. Achsel, C. Bagni, A. K. Kanellopoulos, 2020, "Modelling Learning and Memory in *Drosophila* to Understand Intellectual Disabilities.", *Neuroscience*, pp. 12–30.

Markstein M, C. Pitsouli, C. Villalta, S.E. Celniker, N. Perrimon, 2008, "Exploiting Position Effects and The Gypsy Retrovirus Insulator to Engineer Precisely Expressed Transgenes.", *Nature Genetics.*, 4, pp. 476-83.

Marsh J.L., J. Pallos, L.M. Thompson, 2003, "Fly Models of Huntington's Disease.", *Human Molecular Genetics*, 12, no. 2, pp. 187-193.

Masek, P. and K. Scott, 2010, "Limited Taste Discrimination in Drosophila.", *Proceedings of the National Academy of Sciences of the United States of America*, 107, pp. 14833-14838.

McBride, S. M., C. H. Choi, Y. Wang, D. Liebelt, E. Braunstein, D. Ferreiro, A. Sehgal, K. K. Siwicki, T. C. Dockendorff, H. T. Nguyen, T. V. McDonald, T. A. Jongens, 2005, "Pharmacological Rescue of Synaptic Plasticity, Courtship Behavior, And Mushroom Body Defects in A *Drosophila* Model of Fragile X Syndrome." *Neuron*, pp. 753–764.

Mi H., D. Ebert, A. Muruganujan, C. Mills, L.P. Albou, T. Mushayamaha, P.D. Thomas, 2021, "PANTHER Version 16: A Revised Family Classification, Tree-Based Classification Tool, Enhancer Regions and Extensive API.", *Nucleic Acids Research*, 49, pp. 394-403.

Michel, C. I., 2004, "Defective Neuronal Development in The Mushroom Bodies of *Drosophila* Fragile X Mental Retardation 1 Mutants.", *Journal of Neuroscience*, pp. 5798–5809.

Morris-Rosendahl, D. J., and Crocq, M. A., 2020, "Neurodevelopmental Disorders-The History and Future of a Diagnostic Concept.", *Dialogues in Clinical Neuroscience*, pp. 65–72.

Moser H. W., 2004, “Genetic Causes of Mental Retardation.”, *Annals of the New York Academy of Sciences*, pp. 44–48.

Ni, J. Q., R. Zhou, B. Czech, L. P. Liu, L. Holderbaum, D. Yang-Zhou, N. Perrimon, 2011, “A Genome-Scale shRNA Resource for Transgenic RNAi In Drosophila.” *Nature Methods*, pp. 405-407.

Ohishi, A., Y. Masunaga, S. Iijima, K. Yamoto, F. Kato, M. Fukami, H. Saitsu, T. Ogata, 2020, “De Novo ZBTB7A Variant in A Patient with Macrocephaly, Intellectual Disability, And Sleep Apnea: Implications for The Phenotypic Development in 19p13.3 Microdeletions.”, *Journal of Human Genetics*, pp. 181–186.

Okamoto, N., Y. Nishimori, T. Nishimura, 2012, “Conserved Role for The Dachshund Protein with Drosophila PAX6 Homolog Eyeless in Insulin Expression.” *Proceedings of the National Academy of Sciences of the United States of America*, pp. 2406–2411.

Pan, Y., Y. Zhou, C. Guo, H. Gong, Z. Gong, L. Liu, 2009, “Differential Roles of the Fan-Shaped Body and the Ellipsoid Body in Drosophila Visual Pattern Memory.”, *Learning and Memory*, pp. 289–295.

Panda, S., J. B. Hogenesch, S. A. Kay, 2002, “Circadian Rhythms from Flies to Human.” *Nature*, pp. 329–335.

Panier, S., and S. J. Boulton, 2013, “Double-Strand Break Repair: 53BP1 Comes into Focus.”, *Nature Reviews Molecular Cell Biology*, 15, no. 1, pp. 7–18.

Port, F., H.-M. Chen, T. Lee, S. L. Bullock, 2014, “Optimized CRISPR/CAS Tools for Efficient Germline and Somatic Genome Engineering in Drosophila.”, *Proceedings of the National Academy of Sciences of the United States of America*, 111, no. 29, pp. 2967-2976.

Prelich, G., 2012, “Gene Overexpression: Uses, Mechanisms, And Interpretation.”, *Genetics*, pp. 841–854.

Qi, L., and Boateng, S. Y., 2006, “The Circadian Protein Clock Localizes to The Sarcomeric Z-Disk and Is a Sensor of Myofilament Cross-Bridge Activity in Cardiac Myocytes.”, *Biochemical and Biophysical Research Communications*, pp. 1054–1059.

Qiao, H.-H., F. Wang, R.-G. Xu, J. Sun, R. Zhu, D. Mao, X. Ren, X. Wang, Y. Jia, P. Peng, D. Shen, L.-P. Liu, Z. Chang, G. Wang, S. Li, J.-Y. Ji, Q., Liu, J.-Q. Ni, 2018, “An Efficient and Multiple Target Transgenic RNAI Technique with Low Toxicity in Drosophila.” *Nature Communications*, 9, no. 4160.

Rennie, S., M. Dalby, M. Lloret-Llinares, S. Bakoulis, C. Dalager Vaagensø, T. Heick Jensen, R. Andersson, 2018, “Transcription Start Site Analysis Reveals Widespread Divergent Transcription in D. Melanogaster and Core Promoter-Encoded Enhancer Activities.”, *Nucleic Acids Research*, pp. 5455–5469.

Rhiner, C., J. M. López-Gay, D. Soldini, S. Casas-Tinto, F. A. Martín, L. Lombardía, E. Moreno, 2010, “Flower Forms an Extracellular Code That Reveals the Fitness of a Cell to Its Neighbors in Drosophila.”, *Developmental Cell*, pp. 985–998.

Sakai, T., S. Inami, S. Sato, T. Kitamoto, 2012, “Fan-Shaped Body Neurons Are Involved in Period-Dependent Regulation of Long-Term Courtship Memory in Drosophila.”, *Learning and Memory*, pp. 571–574.

Sanders, S. J., M. T. Murtha, A. R. Gupta, J. D. Murdoch, M. J. Raubeson, A. J. Willsey, A. G. Ercan-Sencicek, R. D. DiLullo, N. J. Carriero, M. W. State, 2012, “De Novo Mutations Revealed by Whole-Exome Sequencing Are Strongly Associated with Autism.”, *Nature*, pp. 237–241.

Serebrenik, Y. V., S. E. Sansbury, S. S. Kumar, J. Henao-Mejia, O. Shalem, 2019, “Efficient and Flexible Tagging of Endogenous Genes by Homology-Independent Intron Targeting.”, *Genome Research*, pp. 1322–1328.

Sheeba, V., M. Kaneko, V. K. Sharma, T. C. Holmes, 2008, “The Drosophila Circadian Pacemaker Circuit: Pas De Deux or Tarantella?”, *Critical Reviews in Biochemistry and Molecular Biology*, pp. 37–61.

Siegel R.W., Hall J.C., 1979, “Conditioned Responses in Courtship Behavior of Normal and Mutant Drosophila.”, *Proceedings of the National Academy of Sciences of the United States of America,* 76, no. 7, pp. 3430-3434.

Siggs, O. M., and Beutler, B., 2012, “The BTB-ZF Transcription Factors. Cell Cycle”, *Cell Cycle*, pp. 3358–3369.

Sonenberg, N., and Hinnebusch, A. G., 2009, “Regulation of Translation Initiation in Eukaryotes: Mechanisms and Biological Targets.”, *Cell*, pp. 731–745.

Spradling A.C., G.M. Rubin, 1982, “Transposition of Cloned P Elements into Drosophila Germ Line Chromosomes.”, *Science*, 218, no. 4570, pp. 341-347.

Sugie, A., G. Marchetti, G. Tavosanis, 2018, “Structural Aspects of Plasticity in The Nervous System of Drosophila.”, *Neural Development*, 13, no. 1.

Talay M, E.B. Richman, N.J. Snell, G.G. Hartmann, J.D. Fisher, A. Sorkaç, J.F. Santoyo, C. Chou-Freed, N. Nair, M. Johnson, J.R. Szymanski, G. Barnea, 2017, “Transsynaptic Mapping of Second-Order Taste Neurons in Flies by *trans*-Tango.”, *Neuron*, pp. 783-795.

Taxman, D. J., C. B. Moore, E. H., Guthrie, M. T. H. Huang, 2010, “Short Hairpin RNA (shRNA): Design, Delivery, And Assessment of Gene Knockdown. In RNA Therapeutics”, *Humana Press*, pp. 139-156.

Tian, Y., Z. C. Zhang, and J. Han, 2017, “Drosophila Studies on Autism Spectrum Disorders.”, *Neuroscience Bulletin*, 33, no. 6, pp. 737–746.

Tonchev, A. B., T. C. Tuoc, E. H. Rosenthal, M. Studer, A. Stoykova, 2016, “Zbtb20 Modulates the Sequential Generation of Neuronal Layers in Developing Cortex.” *Molecular Brain*, 9, no. 1.

van Bokhoven H., 2011, “Genetic and Epigenetic Networks in Intellectual Disabilities”, *Annual Review of Genetics*, 45, pp. 81-104.

van Bon B.W., M.A. Oortveld, L.G. Nijtmans, M. Fenckova, B. Nijhof, J. Besseling, M. Vos, J.M. Kramer, N. de Leeuw, A. Castells-Nobau, L. Asztalos, E. Viragh, M. Ruiter, F, Hofmann, L. Eshuis, L. Collavin, M.A. Huynen, Z. Asztalos, P. Verstreken, 2013, "Rodenburg RJ, Smeitink JA, De Vries BB, Schenck A. "CEP89 Is Required for Mitochondrial Metabolism and Neuronal Function in Man and Fly.", *Human Molecular Genetics*, 22, no. 15, pp. 3138-3151.

van der Voet, M., B. Nijhof, M. A. W. Oortveld, A. Schenck, 2014, "Drosophila Models of Early Onset Cognitive Disorders and Their Clinical Applications.", *Neuroscience and Biobehavioral Reviews*, 46, pp. 326-342.

van Karnebeek, C. D., and Stockler, S., 2012, "Treatable Inborn Errors of Metabolism Causing Intellectual Disability: A Systematic Literature Review.", *Molecular Genetics and Metabolism*, pp. 368–381.

Vogt, K., C. Schnaitmann, K. V. Dylla, S. Knapek, Y. Aso, G. M. Rubin, and H. Tanimoto, 2014, "Shared Mushroom Body Circuits Underlie Visual and Olfactory Memories in Drosophila.", *ELife*, 3.

Wang, H., H. Yang, C. S. Shivalila, M. M. Dawlaty, A. W. Cheng, F. Zhang, and R. Jaenisch, 2013, "One-Step Generation of Mice Carrying Mutations in Multiple Genes By CRISPR/Cas-Mediated Genome Engineering.", *Cell*, 153, no. 4, pp. 910–918.

Wang, S., N. Tulina, D. L. Carlin, E. J. Rulifson, 2007, "The Origin of Islet-Like Cells in Drosophila Identifies Parallels to The Vertebrate Endocrine Axis.", *Proceedings of the National Academy of Sciences of the United States of America*, pp. 19873–19878.

Wei, J.-Y., S.-Y. Chu, Y.-C. Huang, P.-C. Chung, H.-H Yu, 2022, "*Drosophila* Septin Interacting Protein 1 Regulates Neurogenesis in The Early Developing Larval Brain.", *Scientific Reports*, 12, no. 292.

Wiedenheft B., S.H. Sternberg, J.A. Doudna, 2012, "RNA-Guided Genetic Silencing Systems in Bacteria and Archaea.", *Nature*, 482, no. 7385, pp. 331-338.

Wilson, B.C., L. Boehme, A. Annibali, 2020, "Intellectual Disability-Associated Factor Zbtb11 Cooperates With NRF-2/GABP To Control Mitochondrial Function.", *Nature Communications*, 11, no. 5469.

Yamaguchi, M., 2018, "Humanized Flies and Resources for Cross-Species Study. In *Drosophila* Models for Human Diseases.", *Springer*, 1076, no. 277-288.

Yang M.Y., J.D. Armstrong, I. Vilinsky, N.J. Strausfeld, K. Kaiser, 1995, "Subdivision of The Drosophila Mushroom Bodies by Enhancer-Trap Expression Patterns.", *Neuron*, 15, no. 1, pp. 45-54.

Yu H. H., T. Lee, 2007, "Neuronal Temporal Identity in Post-Embryonic Drosophila Brain.", *Trends Neuroscience*, 30, no. 10, pp. 520-526

Zhu S., A.S. Chiang, T. Lee, 2003, "Development of The Drosophila Mushroom Bodies: Elaboration, Remodeling and Spatial Organization of Dendrites in The Calyx.", *Development*, 130, pp. 2603–2610.

Zhu, C., G. Chen, Y. Zhao, X. M. Gao, J. Wang, 2018, "Regulation of the Development and Function of B Cells by ZBTB Transcription Factors.", *Frontiers in Immunology*, 9.

Zhu, K. Y., and Palli, S. R., 2020, “Mechanisms, Applications, And Challenges of Insect RNA Interference.”, *Annual Review of Entomology*, pp. 293-311.

Zolotarev, N. A., O. G. Maksimenko, P. G. Georgiev, A. N. Bonchuk, 2016, “ZAD-Domain Is Essential for Nuclear Localization of Insulator Proteins in Drosophila melanogaster.” *Acta Naturae*, pp. 97–102.